



SAPIENZA
UNIVERSITÀ DI ROMA

PhD course in Biochemistry
XXXVI Cycle (Academic year 2020-2023)

**Sex-dependent Brain-specific Alterations of
Insulin Signalling Uncover Early Molecular
Mechanisms Leading to Cognitive Decline**

PhD Student

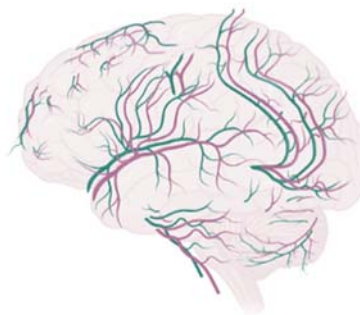
Simona Lanzillotta

Tutor

Prof. Eugenio Barone

PhD Coordinator

Prof. Maria Luisa Mangoni



*Ai Miei Genitori,
A Mio Fratello,
A Mia Sorella.*

INDEX

1. INTRODUCTION	9
1.1. Alzheimer’s Disease	9
1.2. Risk factors and metabolic disorders-related to AD	14
1.3. Brain Insulin Resistance: a major risk factor for AD	15
1.3.1. Role of Insulin in peripheral tissues and Central Nervous System (CNS) .15	
1.3.2. The molecular mechanisms of brain Insulin Resistance (bIR)	19
1.3.3. Brain Insulin resistance and development of Alzheimer’s disease neuropathology	24
1.4. Biliverdin reductase-A: a pleiotropic protein regulating insulin signalling ...	28
1.4.1. BVR-A: structure and function	28
1.4.2. BVR-A and Insulin Signalling pathway	29
2. AIM OF THE WORK	34
3. MATERIALS AND METHODS	36
3.1. Animals and housing	36
3.2. Dietary Treatments	36
3.3. Experimental setup	38
3.4. Morphometric analyses	39
3.5. Behavioural tests	39
3.6. Intraperitoneal Glucose tolerance test (IPGTT)	41
3.7. Intranasal Insulin treatment (INI)	41
3.8. Tissues and Plasma preparation	41
3.9. Western blot	42
3.10. Slot blot	44
3.11. BVR-A ELISA assay	45
3.12. PanY IRS1 ELISA assay	46
3.13. INSULIN ELISA assay	46
3.14. Bioplex assay	46
3.15. Statistical analysis	47
4. RESULTS	48
4.1 HFD leads to peripheral glucose dysmetabolism both in male and female mice ..	48

4.2	HFD leads to reduced BVR-A protein levels both in female and male mice ..	51
4.3	Loss of BVR-A impairs brain insulin signalling in the frontal cortex of female mice fed with HFD.....	53
4.4	Loss of BVR-A impairs brain insulin signalling in the frontal cortex of male mice fed with HFD.....	61
4.5	Brain insulin signalling shows mild alterations in the hippocampus of female mice fed with HFD.....	67
4.6	Loss of BVR-A impairs brain insulin signalling in the hippocampus of male mice fed with HFD.....	72
4.7	Loss of BVR-A in the liver alters insulin signalling and worse glucose metabolism in female mice fed with HFD	78
4.8	Sex-associated differences in cognitive tasks after HFD can be observed and are associated with the impairment of brain insulin signalling.....	82
4.9	HFD is not associated with increased oxidative stress levels in both male and female mice	85
5.	DISCUSSION AND CONCLUSION	87
6.	REFERENCES	97
7.	APPENDIX	109
	Appendix A	109
	Appendix B	110

List of Abbreviations:

3-NT: 3-nitrotyrosine

AAP: gene on chromosome 21

AD: Alzheimer disease

AICD: : Amyloid intracellular C-terminal fragments

AKT: PKB or protein kinase B

AP-1: Activator protein 1

aPKC ζ : atypical protein kinase C- ζ

APOE: ApolipoproteinE

APP: Amyloid precursor protein

ATF-2: activating transcription factor-2

AUC: area under curve

A β : amyloid b (A β)-peptide

BACE1: β -site amyloid precursor protein-cleaving enzyme 1

BBB: Blood brain barrier

BCIP: 5-bromo-4-chloro-3-indolyl phosphate

BHA: butylated hydroxy anisole

bIR: brain Insulin resistance

BMI: Body mass index

BVR: Biliverdin reductase

BVR-A: Biliverdin reductase -A

bZip: leucine zipper

cAMP: catabolite activator protein / CAP

CNS: Central Nervous System

CREB: cAMP response element-binding protein

DI: discrimination index

DNP: dinitrophenylhydrazine

Elk1: ETS Transcription Factor

ERK1/2: Signal-regulated kinases 1/2

FOXO: inhibition of the forkhead transcription factor

GLUT3: glucose transporter type 3

GLUT4: glucose transporter type 4

Grb-2: growth factor receptor-bound protein-2

GSH: glutathione

GSK3 β : glycogen synthase kinase 3 β

GTT: glucose tolerance test

HFD: high fat diet

HNE: 4-hydroxy-2-nonenal

HO: Heme oxygenase

IGF: Insulin-like growth factor

IL-1 β : interleukin 1 family of cytokines

INI: Intranasal insulin

iNOS: inducible nitric oxide synthase

IR: Insulin receptor

IRS: Insulin receptor substrate

ITI: Inter-trial interval

JNK: c-Jun N-terminal kinases

LTD: long-term depression

LTP: long-term potentiation

MAPK: Mitogen-activated protein kinases

MCI: mild cognitive impairment

mTOR: mammalian target of rapamycin

NAC: N-acetyl-cysteine

NBT: nitroblue tetrazolium

NFT: neurofibrillary tangle

NIA-AA: National Institute on Aging–Alzheimer’s Association

NOR: novel object recognition

OS: Oxidative stress

P70S6K: Ribosomal protein S6 kinase beta-1

PC: protein carbonyls

PDPK1: phosphoinositide-dependent kinase 1

PH: pleckstrin homologue

PI: preference index

PI3K: Fosfoinositide 3-chinasi

PIP3: phosphatidylinositol (3,4,5)-triphosphate

PPAR: peroxisome proliferator activated receptor alpha

PSEN1/2: Presenilin 1/2

PTB: phosphotyrosine-binding

PTEN: phosphatase and tensin homolog

RER: rough endoplasmic reticulum

RNS: reactive nitrogen species

ROS: Reactive oxygen species

S6K1: ribosomal protein S6 kinase beta-1

SD: Standard diet

SH2: Src homology 2

Shc: homology collagen

T2D: type 2 diabetes

T2DM: type 2 diabetes mellitus

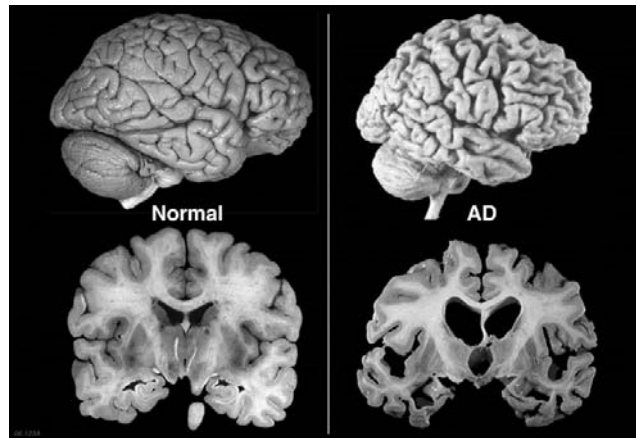
TNF-a: Tumor necrosis factor α

T-PER: Tissue Protein Extraction Reagent

1. INTRODUCTION

1.1. Alzheimer's Disease

Alzheimer's disease (AD) was identified more than 100 years ago by Alois Alzheimer, who described for the first time the degenerative lesions of the eponymous disease by examining at autopsy the brain of one of his 51-year-old demented patients, Auguste D. [1].



integrity between control subjects (left) and subjects with Alzheimer's disease (right).

AD is the most common type of dementia and can be defined as a slowly progressive neurodegenerative disease characterized by neurotic plaques and neurofibrillary tangles as a result of amyloid-beta peptide's ($A\beta$) accumulation, positive features, in the most affected area of the brain [1]. According to the amyloid hypothesis of AD, the overproduction of $A\beta$ is a consequence of the disruption of homeostatic processes that regulate the proteolytic cleavage of the amyloid precursor protein (APP) [2]. The β amyloid peptide is cleaved from APP by the action of proteases named α , β (BACE1), and γ -secretase. Interestingly, APP can be cleaved by either α or β -secretase and the fragments formed by them are named C-terminal 83 and 99,

respectively. The C99 fragment, in turn, is cut by the γ -secretase enzyme that promotes both the formation of an intracellular C-terminal peptide residue (AICD) and the release of the N-terminal fragment, represented by the A β peptides (A β 1-40 and A β 1-42). Elevation in levels of A β 42 leads to aggregation of amyloid that causes neuronal toxicity. A β 42 favours the formation of aggregated fibrillary amyloid protein over normal APP degradation [3].

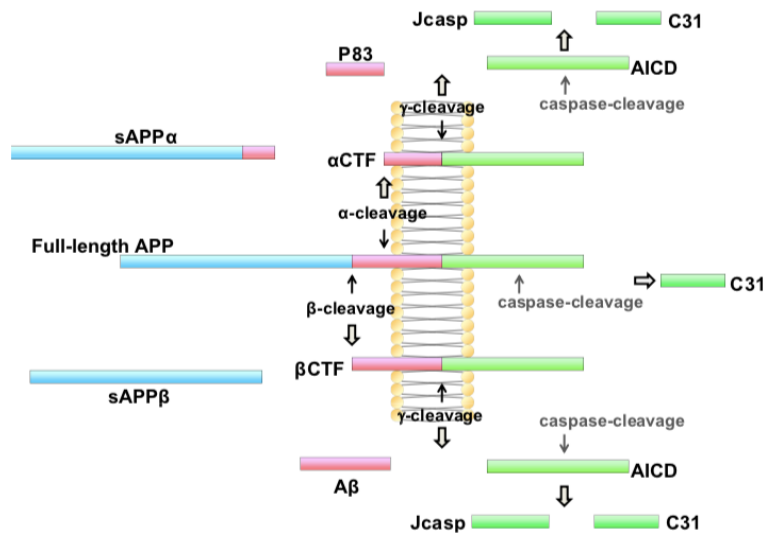


FIGURE 1. Schematic representation of processing of the APP protein.

Neurofibrillary tangles (NFTs) are fibrillary intracytoplasmic structures in neurons formed by a protein called Tau. The primary function of the Tau protein is to stabilize axonal microtubules. In AD, due to aggregation of extracellular A β , there is hyperphosphorylation of Tau, which then causes the formation of Tau aggregates. Tau aggregates form twisted paired helical filaments known as NFTs. They occur first in the hippocampus and then may be seen throughout the cerebral cortex [4].

The neuropathological changes of AD brain include, also, negative features that are characterized by large atrophy due to a neural, neuropil, and synaptic loss. Besides, other factors can cause neurodegeneration such as neuroinflammation, oxidative stress, and injury of cholinergic neurons [5, 6]. Each of these lesions is present in a characteristic pattern in AD, which provides some clues about the relationship between the lesions and disease progression and symptoms [7] Typically, the symptoms of the disease begin with mild memory difficulties and evolve towards cognitive impairment, dysfunctions in complex daily activities, and several other aspects of cognition [8].

From genetic basis, AD can be inherited as an autosomal dominant disorder with nearly complete penetrance [9] The autosomal dominant form of the disease is linked to mutations in 3 genes: APP gene on chromosome 21, Presenilin1 (PSEN1) on chromosome 14, and Presenilin 2 (PSEN2) on chromosome 1 [9]. APP mutations may lead to increased generation and aggregation of A β -peptides. PSEN1 and PSEN2 mutations lead to aggregation of A β by interfering with the processing of γ -secretase. Mutations in these 3 genes account for about 5 % to 10 % of all the cases and about the majority of early-onset AD [9].

Another gene involve in AD is Apolipoprotein E (APOE), encodes a polymorphic glycoprotein expressed in liver, brain, macrophages, and monocytes. APOE participates in transport of cholesterol and other lipids and is involved in neuronal growth, repair response to tissue injury, nerve regeneration, immunoregulation, and activation of lipolytic enzymes. The APOE gene contains three major allelic variants at a single gene locus (ϵ 2, ϵ 3, and ϵ 4), encoding for different isoforms (ApoE2, ApoE3, and ApoE4)

[10]. The APOE ϵ 4 allele increases risk in familial and sporadic early-onset and late-onset AD, but it is not sufficient to cause disease [11] [12].

AD has been considered a multifactorial disease associated with several risk factors such as increasing age, genetic factors, vascular diseases, obesity

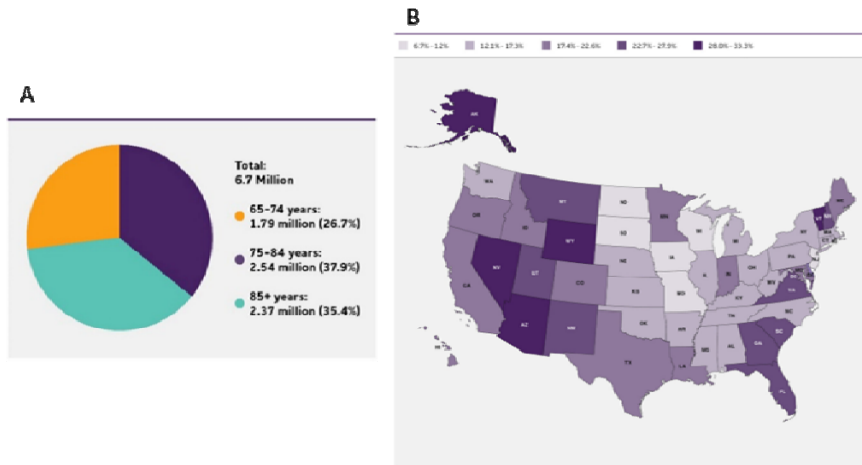


FIGURE 2. (A) Number and ages of people 65 or older with Alzheimer's dementia, 2023. Percentages do not total 100 due to rounding; (B). Projected increases between 2018 and 2040 in Alzheimer's dementia prevalence by state.

and diabetes [13]. The vast majority of people who develop Alzheimer's dementia are age 65 or older [13]. Age is the greatest of these risk factors. Indeed, the percentage of people with Alzheimer's dementia increases dramatically with age. 26,7% of people age 65 to 74, 37,9% of people age 75 to 84, and 35,4% of people age 85 or older have Alzheimer's dementia [14]. The most recent data indicate that, by 2050, the prevalence of dementia will double in Europe and triple worldwide [15]. The group of older adults who will be at risk for Alzheimer's in the coming years will be socially, culturally and economically different from previous groups of older U.S. adults [14]. For example, between 2018 and 2040, projections for older adults show increases in the American Indian population of 75%, in the Black population

of 88%, in the Asian population of 113% and in the Hispanic population of 175% [16].

The National Institute on Aging–Alzheimer’s Association (NIA–AA) revised the clinical criteria for the diagnosis of mild cognitive impairment (MCI) and the different stages of dementia due to AD [17, 18]: (1) *Pre-clinical* or the *pre-symptomatic* stage, which is characterized by mild memory loss and early pathological changes in cortex and hippocampus, with no functional impairment in the daily activities and absence of clinical signs and symptoms of AD [2, 19] The *mild* or *early* stage of AD, where several symptoms start to appear in patients, such as a trouble in the daily life of the patient with a loss of concentration and memory, disorientation of place and time, a change in the mood, and a development of depression [20, 21]. (3) *Moderate AD* stage, in which the disease spreads to cerebral cortex areas that results in an increased memory loss with trouble recognizing family and friends, a loss of impulse control, and difficulty in reading, writing, and speaking [20]. (4) *Severe AD* or *late-stage*, which involves the spread of the disease to the entire cortex area with a severe accumulation of neurotic plaques and neurofibrillary tangles, resulting in a progressive functional and cognitive impairment where the patients cannot recognize their family at all and may become bedridden with difficulties in swallowing and urination, and eventually leading to the patient’s death due to these complications [2, 22].

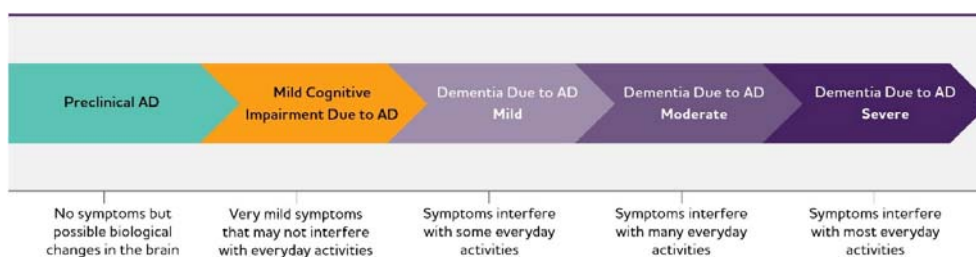


FIGURE 3. Alzheimer's disease continuum. Although these arrows are of equal size, the components of the AD continuum are not equal in duration. FIGURE 4. Comparison of brain

1.2. Risk factors and metabolic disorders-related to AD

The accumulation of the neuropathological hallmarks start around the early stage of AD, and there are a number of risk factors that lead to cognitive decline. The main factors are [23]:

- Age;
- Genes;
- Gender;
- Family history;
- Brain abnormalities;
- Physical inactivity;
- Smoking;
- Excessive alcohol consumption;
- Air pollution;
- Head injury;
- Infrequent social contact;
- Less education;
- Depression;
- Hypertension;
- Insulin resistance;
- Obesity;
- Diabetes.

Among several risk factors, insulin resistance and the onset of metabolic diseases like obesity, diabetes, they represent strong risk factors for development of AD. The mechanisms underlying these relationships are complex and not totally understood, but they often involve vascular factors,

inflammation, oxidative stress, and the impact of these metabolic disorders on the brain's structure and function.

Several studies, including those from our research group [24, 25], have shed light on the complex connections between these conditions and cognitive decline, particularly AD, which is the most common cause of dementia. In fact, glucose is a critical nutrient for the brain, and it is the primary source of energy for brain cells. The brain's high energy demands are due to its continuous and essential functions, including thinking, processing information, and regulating various body functions. Research has shown that in AD, there is a reduction in glucose utilization in various brain regions such as hippocampus. This phenomenon is often named to as *brain hypometabolism*.

1.3. Brain Insulin Resistance: a major risk factor for AD

1.3.1. Role of Insulin in peripheral tissues and Central Nervous System (CNS)

Insulin is an endocrine peptide hormone with 51 amino acids and composed of an α (21 amino acids) and a β (30 amino acids) chain linked together as a dimer by disulfide bridges [26] along with a third intrachain disulfide bridge in the α chain (Fig. 5) [27, 28]. Insulin secreted principally by pancreatic β -cells and is well known for its role in glucose homeostasis, cell growth, and metabolism. Insulin secretion is tightly regulated to maintain blood glucose levels within a narrow physiological range. Insufficient secretion of insulin contributes to the chronic *hyperglycemia* characteristic of diabetes [27].

Insulin production is regulated both at the transcriptional and translation level and one of the main nutrients involved in the regulation of gene expression that encodes insulin is glucose [29].

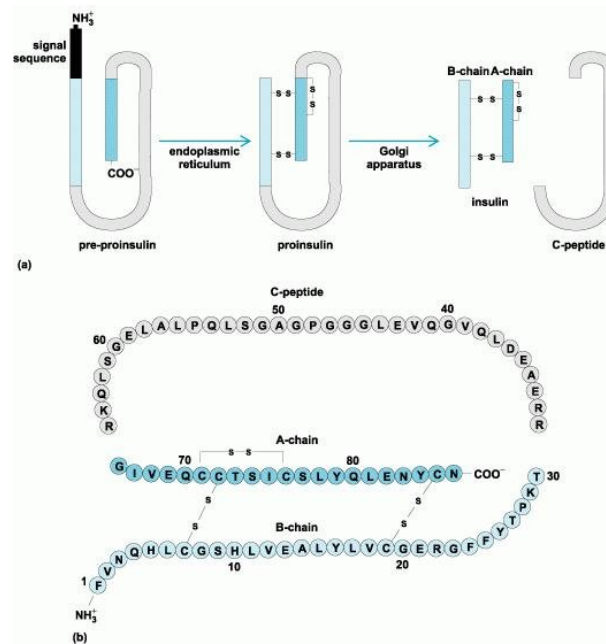


FIGURE 5. Biosynthesis of insulin

From a molecular point of view, humans have a single insulin gene, *INS* located on chromosome 11, the transcription of which is controlled largely by upstream enhancer elements that bind key transcription factors [30]. Insulin is translated initially as a *preproinsulin*, which is then processed to *proinsulin* in the rough endoplasmic reticulum (RER) upon cleavage of its signal sequence by a signal peptidase (Fig. 5). In the RER, proinsulin is folded and stabilized in its 3D proinsulin configuration, linking the semi helical A domain and helical B domain via the formation of three disulfide bonds. After transit to the Golgi apparatus, the properly folded proinsulin is sorted into still-immature secretory granules where it is processed via the

prohormone convertases PC1/3 and PC2, which cleave the *C-peptide*. Subsequently, carboxypeptidase E removes C-terminal basic amino acids from the resulting peptide chains, yielding *mature insulin* consisting of A- and B-peptide chains linked by disulfide bonds (Fig. 5) [31].

In normal physiology, the actions of insulin on peripheral tissues are different. The major tissues targeted by insulin's effects on metabolism include: muscle, where insulin promotes glucose uptake and protein synthesis; adipose tissue, where insulin promotes glucose and fatty acid uptake and inhibits lipolysis; the liver, where insulin promotes glucose utilization, suppresses glucose production, and promotes triglyceride synthesis (Fig. 6) [32]. In addition, insulin promotes the conversion of glucose into glycogen, modulating the storage of excess metabolic energy [33].

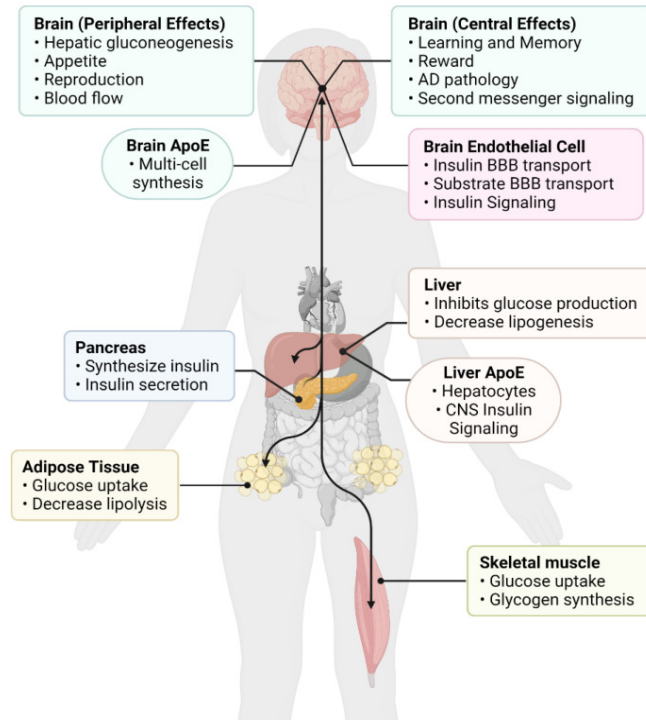


FIGURE 6. Insulin actions in the brain and peripheral tissues

Insulin also has a multifaceted role in the central nervous system (CNS). Initially, the brain was considered insulin insensitive because glucose uptake in this organ is unaffected by insulin [34, 35]. However, growing evidence suggested that insulin can increase glucose uptake in the spinal cord tissues and some brain regions [36, 37]. Insulin readily crosses the blood–brain barrier (BBB) via a receptor-mediated transport process, and the rate of transport can be modulated by several conditions, such as obesity and inflammation [38].

In addition to glucose metabolism and the energy balance in the brain, insulin is reported to control other vital physiological functions, such as neuronal plasticity, memory processing, and cognition [39, 40].

Recently, the role of insulin in brain ageing has received increasing attention, along with the possibility that dysregulation of its functions may contribute to neurodegenerative disease in late life [41].

1.3.2. The molecular mechanisms of brain Insulin Resistance (bIR)

The activation of the insulin signal is triggered by the binding of insulin to its insulin receptor (IR, belonging to a family of tyrosine kinase receptors) on the plasma membrane of target cells, leading to the recruitment/phosphorylation of downstream proteins, that primarily including insulin receptor substrate (IRS), phosphatidylinositol 3-kinase (PI3K, a lipid kinase), and AKT (also known as PKB or protein kinase B) isoforms, that are largely conserved among insulin target tissues and that initiate the insulin response [32, 42]. IR is expressed at the cellular surface, in $\alpha 2\beta 2$ configuration. The α subunit contains the ligand binding sites, usually located at a cysteine-rich domain on the extracellular region (Fig. 7) [43, 44]. The β subunits of IR include a large cytoplasmic region with tyrosine kinase activity (Fig. 7). The IR has a modular structure encoded by a gene (located on chromosome 19) with 22 exons and 21 introns [45]. The short exon 11 that encodes a 12-amino acid sequence is alternatively spliced, resulting in two receptor isoforms (A and B) that differ slightly in affinity for insulin [46, 47].

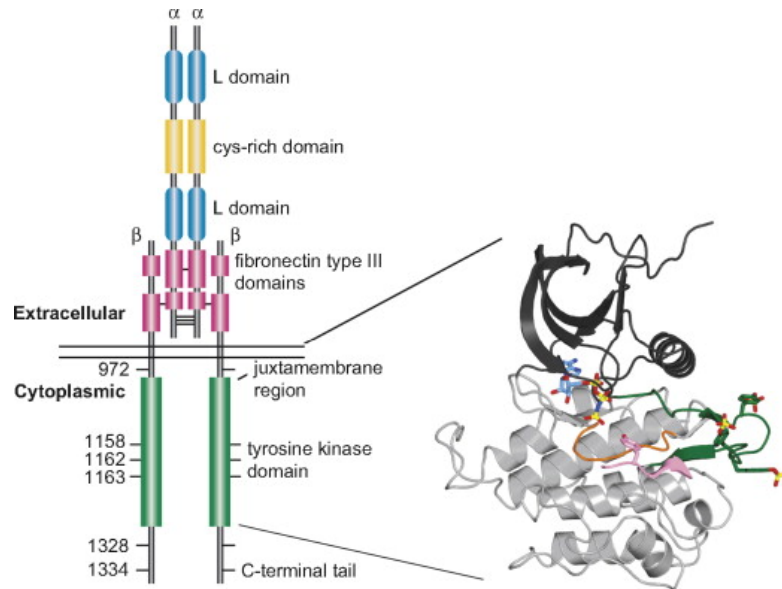


FIGURE 7. Insulin receptor structure

The B isoform binds insulin-like growth factors I and II (IGF-I and IGF-II) with at least 100 times lower affinity than insulin, while the A isoform has significantly higher affinity than the B isoform for IGF-I and especially IGF-II [48] and may play a role in tumorigenesis.

In the presence of insulin, IR phosphorylates IRS proteins that are linked to the activation of two main signalling pathways: the *PI3K–AKT/ PKB pathway*, which is responsible for most of the metabolic actions of insulin, and the *Ras–mitogen-activated protein kinase (MAPK) pathway*, which regulates expression of some genes and cooperates with the PI3K pathway to control cell growth and differentiation (Fig. 8) [49]. Once insulin is bound to the extracellular α -subunit of IR, it induces the dimerization of the intracellular β - subunit. The α -subunit also promotes autophosphorylation of tyrosine residues (Tyr¹¹⁵⁸, Try¹¹⁶², and Tyr¹¹⁶³) on the β -subunit by activation

of intrinsic tyrosine kinases (Fig. 8) [50]. The auto-phosphorylated β -subunit then phosphorylates tyrosine residues on IRS. There are six IRS isoforms (IRS1–6), IRS1 and IRS2 are thought to mediate most of the metabolic effects of IR activation. IRS proteins have NH₂-terminal pleckstrin homology (PH) and phosphotyrosine-binding domains (PTB) that target them to activated IR, and their long COOH-terminal tails are replete with tyrosine and serine/threonine phosphorylation sites [51]. After binding of the IRS PTB domain to IR pTyr⁹⁷², IR phosphorylates multiple IRS tyrosine residues, which in turn recruit downstream signalling effectors to propagate and amplify the insulin response [52]. Once IRS1 is activated it promotes the activation of PI3K. PI3K consists of a p110 catalytic subunit and a p85 regulatory subunit, which catalyses the generation of the lipid product phosphatidylinositol (3,4,5)-triphosphate (PIP₃) (Fig. 8). This results in phosphoinositide dependent kinase 1 (PDK1) mediated activation of the kinase AKT (Fig. 8) [53].

AKT mediates a variety of cellular processes by phosphorylating proteins involved in: (i) *inhibition of the forkhead transcription factor (FOXO) family* which inhibits nuclear translocation and transcriptional activity of promoters that encode pro-apoptotic signalling molecules; (ii) *inhibition of glycogen synthase kinase 3 β (GSK-3 β)* and promotes glycogen synthesis; (iii) *activation of mechanistic target of Rapamycin (mTOR)*, a protein complex regulating somatic growth and protein synthesis (Fig. 8). In this way, insulin stimulates the translocation of GLUT 4 from the intracellular space to the plasma membrane, increasing glycolytic metabolism (Fig. 8) [54]. Stimulation of this pathway preserves mitochondrial membrane integrity [55] and inhibits the production of free radicals that damage mitochondrial DNA and pro-apoptosis mechanisms [56].

As mentioned above, the second main insulin signalling pathway is insulin–IR–IRS–Raf/Ras/MAPK. This pathway is activated by the growth factor receptor-bound protein-2 (Grb-2) binding to Tyr-phosphorylated Src homology collagen (Shc) or IRS via its Src homology 2 (SH2) domain. The MAPK signalling pathway includes extracellular signal regulated kinases 1 and 2 (ERK1 and ERK2), p38 and c-Jun-N-terminal kinases (JNKs). This pathway controls various transcription factors and elements such as CREB, and the protooncogenes [57]. It also regulates the transcription, translation and post-translational modification of various proteins. This signal is involved in the expression of genes associated with glucose metabolism, GLUT 3 biosynthesis and induction of mitosis in cells [58] (Fig. 8).

In contrast to tyrosine phosphorylation, IR and IRS proteins also undergo serine phosphorylation that is generally associated with reduced insulin action [58] (Fig. 8). The inhibitory sites are clustered near the PTB domain. These sites are also located in the C-terminal tail of IRS1 where they negatively regulate the interaction between IRS1 and PI3K. Insulin can promote IRS1 Ser (Ser³⁰⁷, Ser³¹², Ser⁶³⁶) phosphorylation through a pathway involving PI3K/AKT/mTORC1/S6K1. This phosphorylation is also stimulated by free fatty acids via activation of JNK1 or mTORC1 [59]. JNK activation induces IRS1 phosphorylation at S³⁰⁷ and desensitizes insulin action in liver and other tissues, providing a mechanism for *insulin resistance* [60].

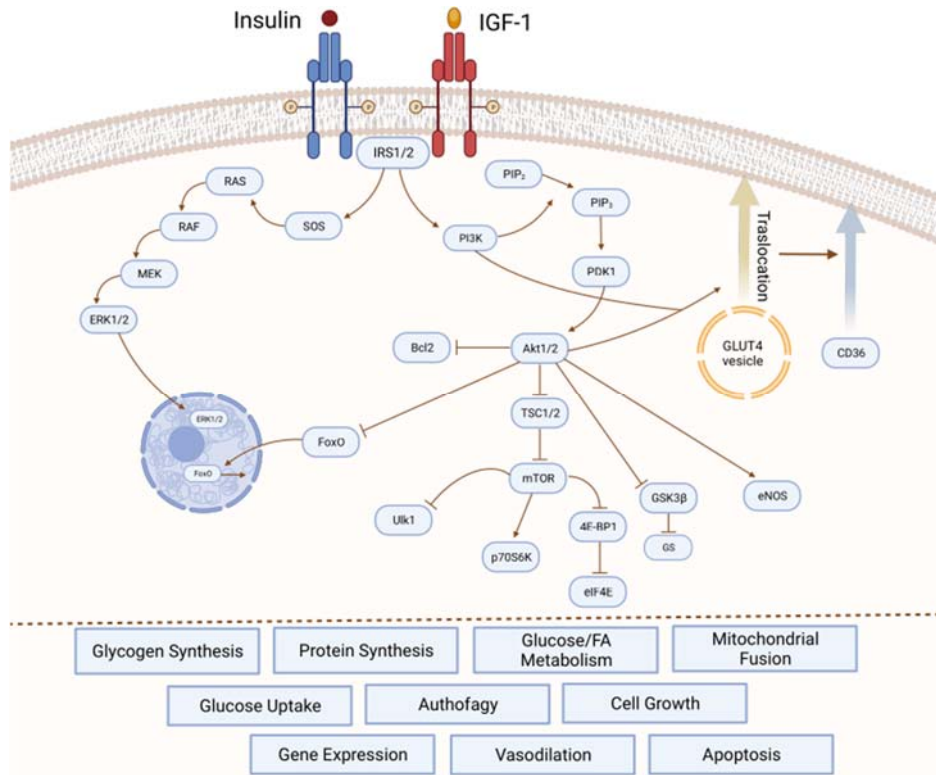


FIGURE 8. Schematic representation of insulin signalling pathway

Insulin resistance is defined as a failure of target tissues to mount a normal response to insulin [61]. Insulin resistance is a shared hallmark feature of obesity, type 2 diabetes (T2D), and neuropathological processes underlying cognitive aging and dementia.

Detection of insulin in the brain reveals that the brain is a target organ for insulin. Indeed, insulin plays several functions in the CNS ranging from regulation of protein synthesis and cytoskeletal protein expression, to neurite outgrowth, migration, and differentiation, and synapse formation [62]. All these functions participate in cognitive processes, including attention, executive functioning, learning, and memory [62]. Insulin also has the ability

to provide neuroprotection, acting mainly against apoptosis, amyloid- β ($A\beta$) toxicity, oxidative stress and ischemia [63]. Several studies suggested that disturbances in brain insulin action are not only observed in obesity and T2D, but also in brain aging and dementia. It has therefore been proposed that decreases in the sensitivity of central nervous pathways to insulin, i.e., *brain insulin resistance* (bIR), constitute a potential link between metabolic and cognitive dysfunctions [64, 65].

1.3.3. Brain Insulin resistance and development of Alzheimer's disease neuropathology

Brain insulin resistance (bIR) can be defined as the failure of brain cells to respond to insulin. Lack of response to insulin may be due to various causes, including downregulation of insulin receptors, the inability of IR to bind insulin or an impairment of the insulin cascade [66]. Insulin signalling is well characterized at the peripheral level and the same pathways are preserved in the CNS [67]. From the molecular point of view, bIR is characterized by:

- Reduction of IR levels due to increased receptor internalisation and/or reduced gene expression [68];
- Reduction of insulin binding to its receptor due to receptor desensitization, which, following a conformational change, has a lower affinity for insulin binding [69];
- Increased inhibition of IRS mediated by phosphorylation of specific serine residues (Ser 312, Ser616 e Ser636) [70];
- Reduction of PI3K [71] and PDK-1 [72] levels .

At the cellular level, this dysfunction might appear as an impairment of neuroplasticity and neurotransmitter release in neurons, or an alteration in

insulin response such as decreased expression of neuronal glucose uptake (GLUT4) and inflammatory responses. Indeed, metabolic stress and neuroinflammation are key hallmarks in AD pathology [73, 74]. Moreover, insulin regulates the metabolism of APP, which in turn modulates the balance between the anabolism and catabolism of A β . Low levels of insulin, or the lack of its action, may increase NFT formation and result in oxidative damage to cells. In addition, low insulin levels result in elevated A β levels and form amyloid plaques in the brain [75].

Also, the Tau protein may play a role in the dysregulation of insulin signalling and pathogenic alterations in the brain [76]. Indeed, it has been identified as the main component of neurofibrillary tangles in the brain of patients with AD [61]. The activity of Tau protein is modulated by phosphorylation, and the molecule itself contains more than 85 potential phosphorylated or phosphorylable serine, threonine and tyrosine sites [77]. In addition, both the expression of the Tau gene and the phosphorylation of Tau protein itself are regulated by insulin and IGF stimulation [78]. Furthermore, impaired insulin or IGF-1 signalling may enhance Tau phosphorylation by inhibition of PI3-K/AKT and increased GSK3-activation [78]; inhibition of insulin/IGF-1 signalling which negatively regulates GSK3- β . Interestingly, GSK3- β can also be activated by oxidative stress, which is a consequence of insulin resistance.

Several studies have shown the importance of oxidative stress (OS) in the pathogenesis of neurodegenerative diseases, diabetes and other disorders [79]. With regard to the insulin signalling, the interplay between oxidants like hydrogen peroxide (H₂O₂) and antioxidants such as butylated hydroxy anisole (BHA) or N-acetyl-cysteine (NAC) can influence this pathway [80]. There is a redox priming step in the IR activation process. This step involves

the regulation of the redox (oxidation-reduction), and it appears to play a role in modulating IR autophosphorylation and activation.

A subsequent study found that the role of H₂O₂ is not restricted to the redox priming of IR, but also includes inhibition of protein tyrosine phosphatase PTP1B, which inactivates the IR by dephosphorylating A-loop phosphotyrosine [81]. This suggesting that the H₂O₂ signal is a critical requirement for the activation of the IR in neurons [82].

In addition to the mechanisms outlined above, age-associated increased OS levels along with reduced glutathione (GSH) levels were reported in both human [83] and animals, insulin resistance and T2DM mice showed increased OS markers and reduced GSH levels in the brain [84, 85] [86], thus suggesting a close link among OS, development of brain insulin resistance, and cognitive dysfunction. As individuals age, reactive oxygen species (ROS) are integrated, to some extent, in the aging brain, disrupting redox-related communication and leading to cellular alterations, such as senescence and cell death, due to the inability to maintain redox homeostasis [80].

Oxidative stress is defined as an imbalance in the levels of oxidant (ROS)/ reactive nitrogen species (RNS)) and antioxidant defence systems [87] . This increase in the ROS/RNS may further lead to the damage of biomolecules leading to loss of function and consequently to cell death, one of major characteristic observed in AD brain [87].

Proteins can be oxidized by direct ROS attack, by secondary oxidation products such as reactive aldehydes (malondialdehyde and 4-hydroxynonenal [HNE]), formed as final by-products of lipid peroxidation that bind to proteins via Michael addition, or by glycooxidation reactions [88, 89] [90]. Protein carbonyls (PC) levels are one of the most abundant indices of protein oxidation that may result in the loss of function of the affected protein [91,

92]. Furthermore, the reaction of $\cdot\text{O}_2^-$ with the free radical nitric oxide ($\cdot\text{NO}$) produces peroxynitrite, a powerful pro-oxidant molecule. Proteins can undergo nitration in the presence of peroxynitrite and CO_2 by modification of tyrosine residues to produce 3-nitrotyrosine (3-NT) [93]. Protein nitration, as well as carbonylation, inactivate proteins or enzymes by altering their protein structure. ROS are unavoidable byproducts during electron transport of aerobic respiration in the mitochondria [94].

Mitochondria are the central coordinators of energy metabolism and are sources and targets of ROS, their impairment may represent a downstream event of T2DM and/or AD-associated abnormal brain insulin and glucose metabolism [95, 96]. Indeed, an increase OS leads to the inhibition of cellular energy production and to the reduction of both insulin secretion and sensitivity [97, 98]. In turn, defective insulin signalling makes neurons energy-deficient and more vulnerable to oxidizing insults, which could promote structural and functional alterations of mitochondria [99, 100]. Basing on these assumptions, defects mitochondria machinery include: reduced Complex I, III, IV and ATPase levels [101]. In conclusion, the accumulation of OS markers alterations of insulin signalling and mitochondrial machinery contribute to the impairment of brain energy metabolism, ultimately resulting in neuronal damage.

From prior studies, another molecular mechanism responsible for the onset of bIR is the impairment of the biliverdin reductase-A (BVR-A) activity.

1.4. Biliverdin reductase-A: a pleiotropic protein regulating insulin signalling

1.4.1. BVR-A: structure and function

In 1965, Singleton JW described for the first time the biliverdin reductase (BVR) protein from guinea pig liver [102]. Later, Maines MD and colleagues purified and characterized BVR from rat liver [103], and in 1993 they described human BVR [104]. BVR has two isoforms with a different molecular weight: A and B. BVR-B is prevalent during fetal development, whereas BVR-A is ubiquitously expressed in adult tissues [105, 106].

From a structural point of view, BVR-A is a monomeric protein that consists of two major regions, the catalytic and the regulatory/DNA interaction domains [107]. The N terminus, the catalytic domain (Rossmann fold), contains a binding motif for nicotinamide adenine dinucleotide phosphate [NADP(H)] and nicotinamide adenine dinucleotide [NAD(H)] cofactors, which are used at different pH optima: 6.7 and 8.7, respectively [107]. The C-terminal domain of BVR-A consists of a large, six-stranded β -sheet that hosts the bulk of key signalling sequences: the leucine zipper (bZip) motif, adenine dinucleotide-binding motif, serine/threonine kinase domain, SH2 domains, and Zn/metal-binding motif [108, 109].

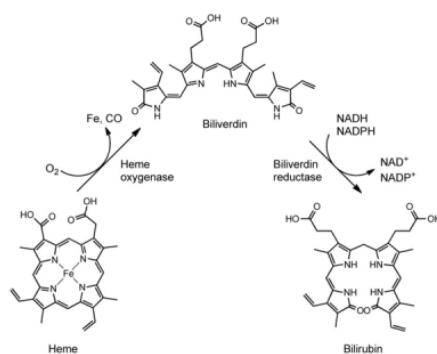


FIGURE 9. Chemical form of biliverdin and bilirubin

From a functional point of view, BVR-A was traditionally known as the reductase that catalyses the last step in the heme-degradation pathway, driving, in a powerful redox cycle, the conversion of biliverdin, a product of heme oxygenase (HO) activity, to bilirubin, the major physiological antioxidant [110, 111] (Fig. 9). Intriguingly, BVR-A also participates in cell signalling through several distinct tracks, and the range and diversity of its functions is unmatched by any enzyme characterized to date [106, 112] [113, 114].

In particular, BVR-A has been demonstrated to be also endowed with a dual-specificity serine/threonine/tyrosine (Ser/Thr/Tyr) kinase activity [115, 116], directly involved in the regulation of the complex insulin signalling pathway at different levels, influencing many metabolic processes, such as glucose uptake, regulation of lipid and protein metabolism, cell proliferation, differentiation, and death [117] [118, 119] (Fig. 9). Last but not least, being a bZip DNA binding protein, BVR-A can also act as a transcription factor for activator protein 1 (AP-1) and cyclic adenosine monophosphate (cAMP)-regulated genes, modulating, among others, activating transcription factor-2 (ATF-2) and HO-1 expression, key components of the inflammatory and stress-responsive system [120, 121].

1.4.2. BVR-A and Insulin Signalling pathway

As mentioned previously, the activation of insulin signalling promotes multiple effects. Among them Biliverdin reductase-A (BVR-A) has an important role in the modulation of this pathway [122]. The coupling between IR and IRS1 is crucial for the induction of the intracellular cascade. Like IRS-1, BVR-A is a direct target of IR [117], which phosphorylates both

BVR-A and IRS-1 on specific Tyr residues, thus resulting in their activation [117] (Fig. 10). IRS-1 mediates the activation of the PI3K/protein kinase B (Akt), which favours the translocation of GLUT4 to the plasma membrane to mediate glucose uptake [107].

In parallel, as part of a regulatory loop, BVR-A works by phosphorylating IRS-1 on Ser residues, i.e., Ser307 acting as inhibitory site, to avoid an excessive activation of IRS-1 in response to insulin [117]. In that way, BVR-A may be considered an upstream regulator of the whole insulin pathway [107]. Furthermore, downstream from IRS-1, BVR-A functions as scaffold protein, favouring: (i) PDK1-mediated activation of Akt [103]; (ii) the PDK1-mediated activation of the atypical protein kinase C- ζ (aPKC ζ) [38,53], known to regulate GLUT-4 translocation, and (iii) the Akt-mediated inhibition of GSK-3 [123] (Fig. 10). Finally, BVR-A encompasses specific motifs in its sequence by which it modulates IR kinase activity either positively or negatively [118], and consequently regulates the degradation of the peroxisome proliferator activated receptor alpha (PPAR) (Fig. 10). The MAPK signalling is also influenced by BVR-A [104]. In particular, BVR-A is a nuclear transporter of the MAPK kinase (MEK)-activated ERK1/2. Hence, it takes part in the activation of the ETS Transcription Factor (Elk1), the transcription factor for oxidative-stress-responsive genes, i.e., HO-1 and inducible nitric oxide synthase (iNOS) [124, 125].

Considering the multidimensional input of BVR-A in the different insulin signalling pathways and the breadth of cell functions that can be potentially influenced, it is not surprising that in recent years researchers have focused on studying the role of this protein in the mechanisms of insulin resistance that underlie cognitive and metabolic deterioration in metabolic and neurodegenerative disorders [107].

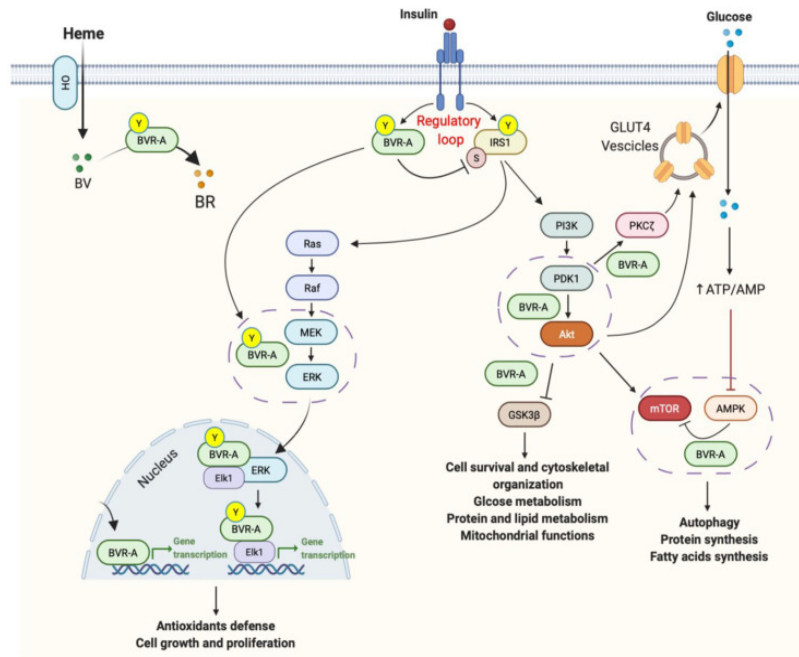


FIGURE 10. Known sites of BVR-A interaction in the insulin signalling pathway

1.5 Gender-associated differences in the onset of bIR and AD

In the last few years, addressing gender and sex differences has emerged as a priority topic in several medical areas and research [126]. Sex has a significant impact on the pathogenesis of metabolic disorders, such as T2DM. Research has shown that females tend to have higher insulin sensitivity than

males, this means that their cells are more responsive to insulin [127]. The higher insulin sensitivity in females can act as a protective factor against the development of insulin resistance. Therefore, both clinical and experimental studies suggest that sexual hormones, due to gender-dependent differences, may affect the IS pathway and as consequence bIR occurs, that as mentioned above, bIR is a condition that characterized the early stage of AD pathology. More specifically, endogenous oestrogens stimulate insulin synthesis and secretion and exert protective effects on islets from females, preserving beta cell function and preventing apoptosis induced by metabolic injuries, such as oxidative stress and lipotoxicity [128].

A sex difference in the prevalence of AD has been noted, while sex differences in the cerebral pathology and relevant molecular mechanisms are not well clarified [129]. Women have a higher propensity of developing AD compared to men [130, 131], a higher risk of mild cognitive impairment [132]. In support of these findings, greater age-related, non-neurodegenerative impairments of spatial learning and memory have been observed in female rats [133] and mice [134, 135] when compared to age-matched males. Furthermore, females demonstrate age-related changes in metabolic processes in the brain earlier than males [136].

Epidemiological studies show an increased risk of AD with the age-related loss of sex steroid hormones. In women, estrogens are produced from cholesterol primarily in the ovaries and placenta, although small but significant amounts can be produced by non-reproductive organs, such as the liver, heart, skin, and brain [137]. Estrogens are known to have protective effect on the brain, and loss of estrogens during menopause could, in part, lead to the deficits seen in brain metabolism in AD [138]. Testosterone levels tend to decline gradually in men as they age, while the decline in estrogen

levels in postmenopausal women is more sharp. This difference in hormone decline may indeed contribute to the higher prevalence of AD in women compared to men.

The brain regional effect of estrogens have also been confirmed by recent studies which further highlighted the potent effects of estrogens on neuronal morphology and plasticity in hippocampus [139, 140] [141, 142] [143]. Another important neuroprotective role of estrogens in AD is supported by the observation that estrogens can reduce A β levels, or prevent them from rising, in the presence of pathological triggers [144].

Although sex differences have been reported in AD patients, there is still a lack of systematic pathological evidence from assessing A β plaques, phosphorylated Tau, and neuroinflammation in the same AD animals [129]. Few studies on rodent models show females have a higher A β burden as well as greater neuronal and synaptic degeneration than males; and the levels of pro-inflammatory cytokines such as IL-1 β and TNF- α in the brain of female mice are all higher than those in males [145].

Historically, many preclinical studies, including those involving animal models, favoured the use of male animals. This practice was based on the assumption that females, due to hormonal fluctuations, might introduce variability into experiments, but today focusing on sex differences and divergences in gene expression is essential for advancing our understanding of biology, sex differences in health and disease.

2. AIM OF THE WORK

This research project aims to investigate the role of BVR-A dysfunction as a key molecular event contributing to bIR development, and its relevance to AD neuropathology. To achieve this goal, we will: (i) determine the sequence of the molecular events underlying bIR development; and (ii) decipher the role of BVR-A in these processes.

Phosphorylation of IRS1 in the brain, which can negatively impact on IS activation, occurs through several mechanisms that are similar to those observed in systemic insulin resistance. This finding may have implications for understanding the role of insulin resistance in neurological conditions and diseases. The IS pathway contains several regulatory points, which represent critical nodes [49]. We focused most of our research on BVR-A especially in AD, and recent pioneering studies of our group proposed BVR-A as a physiological regulator needed (i) to maintain the correct activation of IRS1 in response to IR and (ii) to favour the correct transduction of the IS downstream from IRS1. We suggest a potential relationship between the loss of BVR-A activity, early changes in the IS pathway and the development of IR. This hypothesis would likely require further investigation and experimentation to confirm and to understand the underlying mechanisms. Furthermore, we previously reported that reduced BVR-A activation: (i) occurs in AD and MCI brain [146, 147]; (ii) is an early event leading to IRS1 hyper-activation and favouring GSK3 β -mediated Tau phosphorylation in 3xTg-AD mice brain [24, 148]; and (iii) impairs of long-term potentiation (LTP) in cortical neurons [148]. Finally, reduced BVR-A activity was observed in peripheral blood mononuclear cells collected from obese subjects at risk to develop systemic IR [25], thus suggesting this could be a mechanism conserved in different cell types.

In light of the above-cited lines of evidence, the purpose of this work is to understand what happens in a condition that is prior to the onset of IR. In particular, we were interested in evaluating: (i) how BVR-A levels change over time, as well as following the administration of a diet enriched in fats, and (ii) how what we observe then is subsequently reflected in a mouse model deficient for BVR-A.

3. MATERIALS AND METHODS

3.1. Animals and housing

The study was conducted on two mouse colonies: (i) C57Bl/6j is one of the most widely used and well-established inbred strains of laboratory mice in scientific research. C57Bl/6j mice are used in a developmental biology, diabetes and obesity, genetics, immunology, neurobiology, and sensorineural research; and (ii) BVR-A-deficient C57Bl/6j mice (BVR-A^{-/-}). These mice were already characterized [3] and are available at the Jackson laboratory (USA). Compared with C57Bl/6j mice, BVR-A^{-/-} mice appear normal in body weight and organ-to-body weight ratio without major alterations of liver or kidney functions [3]. C57Bl/6j mice were chosen because they develop systemic and brain IR (but not diabetes) without a pronounced development of obesity and adiposity. Parental generations were purchased from Jackson Laboratories (Bar Harbour, ME, USA). Mice were housed in clear Plexiglas cages (20 × 22 × 20 cm) under standard laboratory conditions with a temperature of 22 ± 2 °C and 70% humidity, a 12-h light/dark cycle.

All the experiments were performed in strict compliance with the Italian National Laws (DL 116/92), the European Communities Council Directives (86/609/EEC). Experimental protocol was approved by Italian Ministry of Health authorization n° 522/2020-PR. All efforts were made to minimize the number of animals used in the study and their suffering.

3.2. Dietary Treatments

A high-fat diet (HFD) is known to foster metabolic dysregulation and insulin resistance in the brain and such effects have been associated with the reduction of cognitive performances. Studies on mice fed with a HFD, which

mimicked a hypercaloric Western-style diet [149], thus leading to obesity and T2DM, demonstrated impaired performance in learning and memory tasks, alterations of synaptic integrity, altered CA1-related long-term depression (LTD) and LTP, and the development of AD pathological hallmarks [150, 151].

Nutritional requirements are listed below (Table 1).

TABLE 1. Diet composition

Ingredient (g/Kg)	Standard Diet (SD)	High Fat Diet (HFD)
Acid Casein 741	200	265.00
L-Cysteine	2.8	4
Maltodextrine-0032	33.2	160
Sucrose	300	90
Cellulose (Arbocel)	50	65.5
Soybean oil	24	30
Lard	19	220
Vitamin mix AIN-93-VX-PF2439	10	13
Mineral mix AIN-93G-MX-PF2348	45	48
Choline bitartrate	1.9	3
Calcium Phosphate disabic	13	3.4
Total Energy		
Kcal/g	3.5	6
Protein, %	18.5	23
Carbohydrate, %	60	38
Fat, %	3	34

3.3. Experimental setup

At 4 weeks of age, male and female C57Bl/6j mice, were split into four groups ($n=10$ mice/group). Groups were labelled according to their respective diets (standard chow or control diet (SD) and HFD) (Table 1), genotype and sex (male and female separately): $SD^{+/+}$, $HFD^{+/+}$, $SD^{-/-}$, $HFD^{-/-}$ (Table 2). Mice were housed five per cage with free access to water and controlled food intake. All diets were purchased from Mucedola srl, Italy. Two of the randomly selected cages were fed with SD, while to induce bIR the other two of the four groups were switched to HFD. The experiment was performed for different time points (1 and 8 weeks) (Figure 11). At each of the above time points mice will undergo a series of tests (listed below) aimed to evaluate morphological and metabolic parameters prior to sacrifice. At the end of diet, mice were sacrificed by decapitation; blood, brain and peripheral tissues were collected and then stored at -80°C until further analysis.

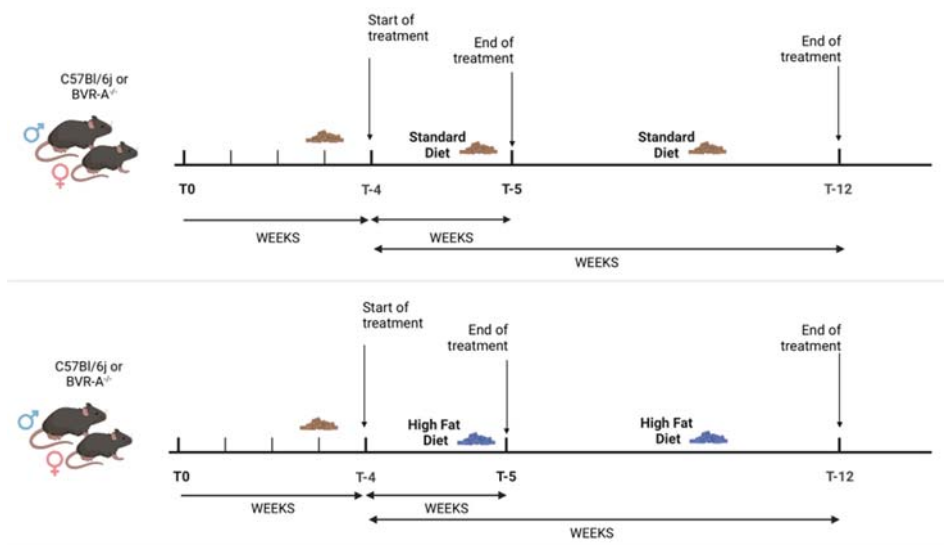


FIGURE 11. Mouse samples and experimental flow

3.4 Morphometric analyses

Individual weights and heights were taken on all mice at the beginning and at the end of diet. Body mass index (BMI) was calculated as the ratio between body weight and square surface area (g/m^2). Body surface area was derived from the DuBois equation:

$$\text{body surface (m}^2\text{)} = 0,007184 \times \text{weight (Kg}^{0,0425}\text{)} \times \text{height (cm}^{0,0725}\text{)} \text{ [152].}$$

3.5 Behavioural tests

Novel object recognition (NOR). The NOR task is used to evaluate cognition, particularly recognition memory, in rodent models of CNS disorders. All experimental male and female groups (SD^{+/+}, HFD^{+/+}, SD^{-/-}, HFD^{-/-} at 1 and 8 weeks) were involved in the test procedures. This test is based on the tendency of rodents to have an innate preference for novelty, a mouse that remembers the familiar object will spend more time exploring the novel object. The NOR is an efficient and flexible method for studying learning and memory in mice, such as consolidation or recall. The task procedure consists of three phases: habituation, familiarization, and test phase. In the habituation phase at 1st day, each animal is allowed 10 min to freely exploring the open-field arena (50 cm deep \times 30 cm widths \times 30 cm height) in the absence of objects. During the familiarization phase on the 2nd day, a single animal is placed in the open-field arena containing two identical objects (two balls), for 5 min. To prevent coercion to explore the objects, rodents are released against the centre of the opposite wall with its back to the objects. The experimental context is not drastically different during the familiarization and the test phase. In the test phase after 24 h, the animal is returned to the open-field arena with two objects, one is the familiar object

and the other is novel (ball + plastic brick) [153, 154]. The discrimination index and preference index percentage are recorded. Discrimination index (DI), allows discrimination between the novel (TN) and familiar (TF) objects [$DI = (TN - TF)/(TN + TF)$]. The preference index (PI) is a ratio of the amount of time spent exploring any one of the two objects in training phase (A, B) or the novel one in test phase (C) over the total time spent exploring both objects, i.e., A, B or $C/(A, B + C) \times 100$ (%) in the test phase. Therefore, a preference index above 50% indicates novel object preference, below 50% familiar object preference, and 50% no preference [154].

Y-maze test. The Y-maze test was carried out as described previously [155, 156]. Spatial memory and exploratory activity were measured using a Y-maze apparatus, where each arm is 40 cm long, 8 cm high, 15 cm wide at the bottom, and 10 cm wide at the top. The arms (A, B and C) are all placed at 120 degrees to each other and converge in an equilateral triangular central area that is 4 cm at its longest axis. Each mouse is placed individually into the apparatus and allowed to move freely through the maze during an 5-min session. The task procedure consists of two phases: (i) training session or session one, spatial reference memory can be tested by placing the test mouse into the Y-maze with one arm of the maze closed off during training; after a time interval (Inter-trial interval, ITI) that lasts 30-min, during which the mouse is removed from the maze, starts the (ii) testing session, the mouse is placed back into the maze with the blockage removed [157]. Alternation or Spontaneous alternation is defined as successive entries into the three arms, on overlapping triplet sets, and it is associated with the capacity of spatial short-term memory. The percent alternation is calculated as the ratio of actual to possible alternations (defined as the total number of arm entries minus 2) multiplied by 100.

3.6 Intraperitoneal Glucose tolerance test (IPGTT)

Animals were fasted for 6 hours and a glucose tolerance test (GTT) was performed using glucose (1,5g/kg bodyweight), which was administered by intraperitoneal injection. A blood sample was drawn from the tail veins of conscious mice for measurements of serum glucose using a glucometer and strips (CONTOUR®NEXT, Ascensia Diabetes Care Holdings AG, Basel, Switzerland). Glucose readings were taken at baseline (time = 0 min) and at 30, 60, 90 and 120 min after injection.

3.7 Intranasal Insulin treatment (INI)

For each group, it was included a sub-group of mice to test brain insulin sensitivity. Mice were intranasally treated with rapid insulin (Humalog 2U/mL 10µL/nostril, KwikPen, Eli Lilly Nederland B.V., A10AB04) [148, 158] ($n=3/\text{group}/\text{sex}$) or vehicle ($n=3/\text{group}/\text{sex}$) and then sacrificed after 30 min for biochemical analyses.

For both SD and HFD groups we had: vehicle ($n=3/\text{group}/\text{sex}$) and insulin-treated mice ($n=3/\text{group}/\text{sex}$) to use for the western blot (WB).

3.8 Tissues and Plasma preparation

Total protein were extracted from prefrontal-cortex, hippocampus and liver of C57Bl/6j and BVR-A^{-/-} mice. Samples were prepared in Tissue Protein Extraction Reagent (T-PER (1:200), 78510, Thermo Fisher Scientific, Waltham, MA, USA) and supplemented with phosphatase and protease inhibitor cocktail (1:100, Sigma-Aldrich, St. Louis, MO, USA). Then, samples were homogenized by 45 strokes of a Wheaton tissue homogenizer, sonicated, and centrifuged at 14,000 rpm for 30 min at 4 °C to remove debris. The supernatant was collected, and the total protein concentration was

determined by the BCA method according to manufacturer's instructions (Thermo Fisher Scientific, Waltham, MA, USA).

Blood samples were obtained from C57Bl/6j and BVR-A^{-/-} mice at the end of diet treatment. All blood draws and processing followed established protocols using standard procedures. Blood was collected in ethylenediaminetetraacetic acid (EDTA) polypropylene tubes, and was centrifuged at 3000×g for 15 minutes at 4°C. Afterward, plasma was isolated and centrifuged again at 3000×g for 15 minutes at 4°C to eliminate clots and aggregates. Plasma samples were stored at -80°C until analysis.

3.9 Western blot

Western blot was performed on prefrontal-cortex and hippocampus samples, 15 µg of proteins were resolved via SDS-PAGE using Criterion™ TGX Stain-Free™ precast gel (Bio-Rad Laboratories, Hercules, CA, USA) in a Criterion large format electrophoresis cell (Bio-Rad Laboratories, Hercules, CA, USA) in Tris/Glycine/SDS (TGS) Running Buffer (Bio-Rad Laboratories, Hercules, CA, USA). Immediately after electrophoresis, the gel was placed on a Chemi/UV/Stain-Free tray and then placed into a ChemiDoc MP imaging System (Bio-Rad Laboratories, Hercules, CA, USA) to collect total protein load image (as described below). Following electrophoresis and gel imaging, the proteins were transferred onto a nitrocellulose membrane by Trans-Blot Turbo Transfer System (Bio-Rad Laboratories, Hercules, CA, USA). The nitrocellulose membrane was blocked using 3% BSA (SERVA Electrophoresis GmbH, Heidelberg, Germany) in 1X Tris Buffer Saline (TBS) containing 0.01% Tween20 (Sigma-Aldrich, St. Louis, MO, USA) and incubated overnight at 4 °C with the primary antibodies listed in Table 3. The day after, all membranes were washed with 1X TBS containing 0.01%

Tween20 (Sigma-Aldrich, St. Louis, MO, USA) and incubated at room temperature for 1 h with secondary antibody conjugated with horseradish peroxidase: anti-rabbit (1:10,000; Bio-Rad Laboratories, Hercules, CA, USA) or anti-mouse (1:10,000; Bio-Rad Laboratories, Hercules, CA, USA). Membranes were developed with Clarity enhanced chemiluminescence (ECL) substrate (Bio-Rad Laboratories, Hercules, CA, USA) and then acquired with Chemi-Doc MP (Bio-Rad, Hercules, CA, USA) and analysed using Image Lab 6.1 software (Bio-Rad, Hercules, CA, USA) that allows the normalization of a specific protein signal by the mean of total proteins load. Total protein staining measures the aggregate protein signal (sum) in each lane and eliminates the error that can be introduced by a single internal control protein. Total protein staining is a reliable and widely applicable strategy for quantitative immunoblotting. It directly monitors and compares the amount of sample protein in each lane, rather than using an internal reference protein as a marker of sample concentration. This direct straightforward approach to protein quantification may increase the accuracy of normalization. Total load can be detected taking advantage of the Stain free technology (Bio-Rad, Hercules, CA, USA). In detail, stain-free imaging technology utilizes a proprietary trihalo compound to enhance natural protein fluorescence by covalently binding to tryptophan residues with a brief UV activation, the described procedure permits the normalization of a specific protein signal with total proteins load. All the blots were analysed using Image Lab software (Bio-Rad Laboratories, Hercules, CA, USA).

3.10 Slot blot

For the analysis of total protein carbonyls (PC) levels, 5 μ L of total protein extract samples were derivatized with 5 μ L of 10 mM 2,4-dinitrophenylhydrazine (DNPH, OxyBlot™ Protein Oxidation Detection Kit, Merck-Millipore, Darmstadt, Germany) in the presence of 5 μ L of 10% sodium dodecyl sulphate (SDS) for 20 min at room temperature. The samples were then neutralized with 7.5 μ L of neutralization solution (2 M Tris in 30% glycerol) and loaded onto a nitrocellulose membrane as described below.

For total 3-nitrotyrosine (3-NT) levels 5 μ L of cortical total protein extract samples, 5 μ L of 12% SDS, and 5 μ L of modified Laemmli buffer containing 0.125 M Tris base (pH 6.8), 4% (v/v) SDS, and 20% (v/v) glycerol were incubated for 20 min at room temperature and then loaded onto nitrocellulose membrane as described below.

Proteins (250 ng) were loaded in each well on a nitrocellulose membrane under vacuum using a slot blot apparatus. Membranes were blocked for 1 h with a solution of 3% (w/v) BSA in PBS containing 0.01% (w/v) sodium azide and 0.2% (v/v) Tween 20 and incubated respectively with primary antibody anti-carbonyl and anti-3-NT (details are listed in Table 3) 2 h at RT and overnight, respectively. Following primary antibody incubation, membranes were washed in TTBS three times at intervals of 5 min each and then incubated with anti-rabbit or mouse IgG alkaline phosphatase secondary antibodies (Sigma-Aldrich, St Louis, MO, USA) for 1 h at room temperature. Then, membranes were washed three times in TBS solution containing 0.01% Tween 20 for 5 min each and developed with Sigma fast tablets (5-bromo-4-chloro-3-indolyl phosphate/nitroblue tetrazolium substrate [BCIP/NBT substrate]). Membranes were dried and the images were acquired using the

ChemiDoc XP image system and analysed using Image Lab software (Bio-Rad Laboratories, Hercules, CA, USA).

TABLE 2. Antibodies used in the current work

Name	Code	Company	Dilution
3-NT	SAB5200009	Sigma-Aldrich	1:1000
Akt	9272S	Cell signalling	1:1000
BVR-A	ADI-OSA-450-E	Enzo	1:1000
GSK3b (C-terminal)	Ab93926	ABCAM	1:1000
mTOR	6H9B10	Biologend	1:1000
pAkt (Ser473)	4060S	Cell signalling	1:1000
pGSK3b (Ser9)	5558S	Cell signalling	1:1000
pmTOR (S2448)	5536S	Cell signalling	1:1000
Protein Carbonyl	S7150	Sigma-Aldrich	1:5000

3.11 BVR-A ELISA assay

BVR-A protein levels were evaluated in the prefrontal-cortex, hippocampus and in the liver samples of C57Bl/6j mice fed with SD or HFD for 1 and 8 weeks ($n=6/\text{group}/\text{sex}$) by ELISA kit (Cat#LS-F74186, LifeSpan BioSciences, Seattle, WA) according to the manufacturer's instructions. The amount of BVR-A was normalized for total proteins of samples loaded into the ELISA kit and expressed as ng/ μg proteins.

3.12 PanY IRS1 ELISA assay

PanY of IRS1 in prefrontal-cortex and hippocampus samples of C57Bl/6j and BVR-A^{-/-} mice fed with SD or HFD for 1 and 8 weeks ($n=6$ /group/sex) were evaluated by an ELISA kit (PathScan® Phospho-IRS-1 (panTyr) Sandwich, Cat#7133, Cell Signalling Technology, Danvers, USA) according to the manufacturer's instructions. The amount of IRS-1 tyrosine phosphorylation was detected at 450 nm.

3.13 INSULIN ELISA assay

Insulin levels were evaluated in plasma samples of C57Bl/6j and BVR-A^{-/-} mice fed with SD or HFD for 1 and 8 weeks ($n=5-6$ /group/sex) by an ELISA kit (Cat#EMINIS, Invitrogen by Thermo Fisher Scientific, Waltham, MA, USA) according to the manufacturer's instructions. The amount of insulin was expressed as $\mu\text{U/mL}$.

3.14 Bioplex assay

A magnetic bead-based immunoassay was used to measure levels of eight phosphoproteins and total target proteins pertaining to the insulin signalling pathway in prefrontal-cortex, hippocampus and liver samples. All mediators were assayed in multiplex using the Bio-Plex ProCell Signalling protein kinase B (Akt) Panel, 8-plex (Bio-Rad Laboratories, #LQ00006JK0K0RR) to measure levels of the following phosphorylated proteins: insulin receptor substrate- 1 at Ser636/636 (pIRS1Ser636/636), phosphatase and tensin homolog at Ser380 (Phosphatase and tensin homolog (pPTEN)Ser380), serine/threonine protein kinase Akt-1 at Ser 473 (pAktSer473), glycogen

synthase kinase- $3\alpha/\beta$ at Ser21/Ser9 (pGSK- $3\alpha/\beta$ Ser21/9), mTOR at Ser2448 (pmTORSer2448), p70 S6 kinase at Thr389 (p70 S6 Kinase (pP70S6K)Thr389), ribosomal protein S6 kinase beta-1 at Ser235/236 (pS6Ser235/Ser236), and the Bcl2- associated agonist of cell death at Ser136 (pBADSer136). Experiments were run on a Bio-Plex System with Luminex xMAP Technology (Bio-Rad Laboratories) and data were acquired on a Bio-Plex Manager Software 6.1 (Bio-Rad Laboratories) with instrument default settings. Median fluorescence intensities (MFI) corrected for the blank background were obtained for all analytes and results were calculated as the ratio between the MFI of phosphorylated targets and total proteins.

3.15 Statistical analysis

Data are expressed as mean \pm SEM per group. Statistical analyses were performed using: (i) one-way analyses of variance (ANOVA) with Bonferroni multiple comparison tests for the evaluation of the behavioural tests and biochemical data; (ii) Student t-test was used to evaluate differences observed in INI experiments; (iii) Multiple t test was used to measure differences observed in IPGT test. $p < 0.05$ was considered significantly different from the reference value. All statistical analysis was performed using GraphPad Prism 8.0 software.

4. RESULTS

4.1 HFD leads to peripheral glucose dysmetabolism both in male and female mice

Starting at 4 weeks of age, WT and BVR-A^{-/-} C57Bl/6j mice received either a SD or an HFD for 1 or 8 weeks (Figure 11). C57Bl/6j mice were chosen because they develop systemic and brain IR (but not diabetes) without a pronounced development of obesity and adiposity (which could represent confounding factors) once fed a HFD over 12 weeks, starting at 4 weeks of age [1].

Starting from the baseline (4 weeks of age, T0), both SD and HFD body weight significantly increased over time (all $p < 0.0001$) (Figure 12a and 12b). At the end of the first week dietary treatment with SD and HFD (T1W), female body weight significantly increased respect to T0. The weight gain continued to be progressively higher and at the end of 8 weeks of diet both in SD and HFD groups (Figure 12a). The growth of mice is not correlated to the genotype. The same trend was observed in male mice (Figure 12a).

SD and HFD promoted a comparable increase of BMI after 1 week both in female and male mice (Figure 12b and 13b), except for female SD^{-/-} mice that show no significant changes (Figure 12b and 13b). A similar trend was observed after 8 weeks of SD or HFD in both sexes and genotypes (Figure 12b and 13b). However, we noticed that female HFD^{-/-} mice show a significant increase of BMI when compared to SD^{-/-} counterpart after 8 weeks of diet (Figure 12b), suggesting that persistent loss of BVR-A might favour fat accumulation as previously reported [2, 3]. Fasting glycemia was modified by HFD after 8 weeks, being significantly increased in HFD^{+/+} female compared to SD^{+/+} female mice (Figure 12c) and in both HFD^{+/+} and HFD^{-/-} compared to the respective SD groups (Figure 12c). No differences

based on the genotype were observed. Glucose tolerance test (IPGTT) performed at the end of the diet reveals a consistent glucose intolerance both in female and male mice, although genotype-dependent effects were observed. Female HFD^{+/+} mice show a significant increase at T30 compared to SD^{+/+} after 1 week, while an overall worsening was observed when compared to HFD^{-/-} (Figure 12c). No differences between SD^{-/-} and HFD^{-/-} were observed (Figure 12c), suggesting that loss of BVR-A, might delay the development of insulin resistance in the short time. After 8 weeks of diet, a further worsening of glucose tolerance was observed in HFD^{+/+} with respect to SD^{+/+} female mice as demonstrated by higher glycemia levels at each of the time points of the IPGTT and higher AUC (Figure 12d and 13d). Female HFD^{-/-} develop glucose intolerance after 8 weeks, although this appears less pronounced when compared to male mice (Figure 12d and 13d). Rather, male mice seem to be more susceptible to develop glucose intolerance. Indeed, both HFD^{+/+} and HFD^{-/-} male mice develop glucose intolerance after 1 week, that persist after 8 weeks with no differences depending on the genotype or on the diet duration (Figure 13c and 13d). These results highlight sex- and genotype-dependent differences.

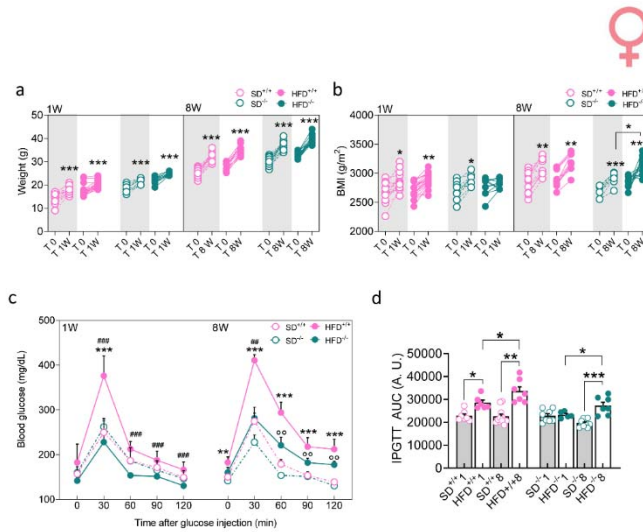


Figure 12. Morphometric and metabolic measurements performed in WT and BVR-A/-C57Bl/6j female mice fed with SD or HFD at T0 (4 weeks of age), T1W (after 1 week of diet) and T8W (at the end of each diet). (a) Body weight is expressed in grams; (b) Body mass index (BMI) is expressed as g/m²; (c) Intraperitoneal glucose tolerance test (IPGTT) after T1W and T8W of diets; (d) Area under curve. Data presented as mean \pm SEM. One-way ANOVA with Bonferroni test: * $p < 0.05$, ** $p < 0.001$, *** $p < 0.0001$. SD^{+/+}: WT mice fed with standard diet; HFD^{+/+}: WT mice fed with standard diet; SD^{-/-}: BVR-A knock-out mice fed with standard diet; HFD^{-/-}: BVR-A knock-out mice fed with standard diet.

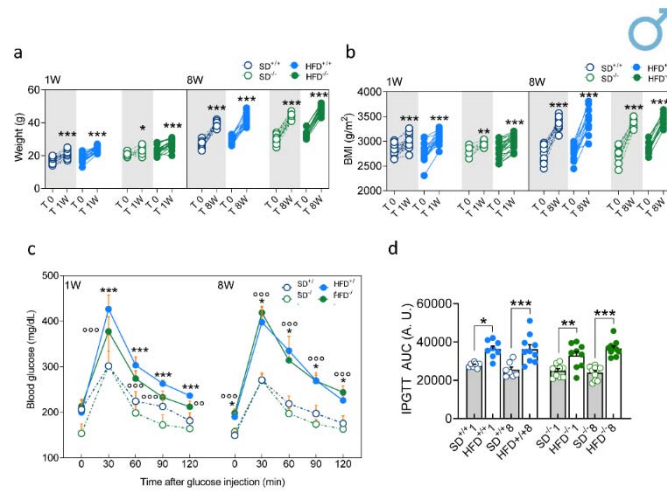


Figure 13. Morphometric and metabolic measurements performed in WT and BVR-A/-C57Bl/6j male mice fed with SD or HFD at T0 (4 weeks of age), T1W (after 1 week of diet) and T8W (at the end of

each diet). (a) Body weight is expressed in grams; (b) Body mass index (BMI) is expressed as g/m²; (c) Intraperitoneal glucose tolerance test (IPGTT) after T1W and T8W of diets; (d) Area under curve. Data presented as mean ± SEM. One-way ANOVA with Bonferroni test: * p < 0.05, **p < 0.001, ***p < 0.0001. SD^{+/+}: WT mice fed with standard diet; HFD^{+/+}: WT mice fed with standard diet; SD^{-/-}: BVR-A knock-out mice fed with standard diet; HFD^{-/-}: BVR-A knock-out mice fed with standard diet.

4.2 HFD leads to reduced BVR-A protein levels both in female and male mice

To unravel whether HFD and the development of peripheral insulin resistance had an impact in the brain, we first focused on BVR-A. We evaluated BVR-A protein levels by ELISA in two brain regions known to regulate learning and memory functions, i.e., frontal cortex and hippocampus. Moreover, to understand whether brain alterations parallel peripheral changes we looked at the liver, being this latter the main organ responsible for glucose homeostasis [159]. Our results, clearly show that mice under the HFD regimen are characterized by reduced BVR-A protein levels after 8 weeks. We observed that BVR-A levels are significantly reduced in the frontal cortex and in the liver of female mice after 8 weeks HFD (Figure 14a, c), while no significant changes in the hippocampus were observed (Figure 14b). Male mice show reduced BVR-A protein levels in the hippocampus and in the frontal cortex, while no significant changes in the liver were observed (Figure 14d, e, f). These results highlight for the first time that HFD, and likely insulin resistance, have an impact on BVR-A protein levels, and changes of BVR-A are already significant after a relatively short HFD regimen. We also highlight sex-dependent differences with male mice being more susceptible to develop brain alterations with respect to female at a young adult age.

Based on these observations, we aimed to explore whether loss of BVR-A was associated with alterations of brain insulin signalling. Since the reduction

of BVR-A levels was only evident in HFD-treated mice from 1 to 8 weeks, we decided to perform our further analyses by looking first at changes in HFD^{+/+} mice.

We then proceeded to:

- evaluate the variations observed in SD^{-/-} in comparison to SD^{+/+} mice. This allowed us to determine if the observed effects in HFD^{+/+} mice could be attributed solely to the loss of BVR-A;
- investigate the variations observed in HFD^{-/-} mice when compared to HFD^{+/+} mice. This helped us understand whether alterations in brain insulin signalling resulted from a combined effect of diet and genotype.

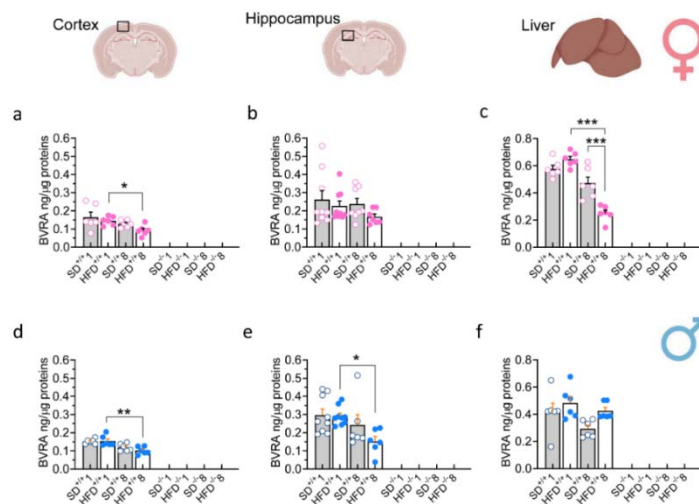


FIGURE 14. Dynamic changes of BVRA protein levels in CNS and in peripheral tissues in WT female and male mice fed with SD or HFD at the end of 1 week or 8 weeks of diets. (a and d) BVRA protein levels (ng/μg of proteins) evaluated in the prefrontal-cortex; (b and e) BVRA protein levels (ng/μg of proteins) evaluated in the hippocampus; (c and f) BVRA protein levels (ng/μg of proteins) evaluated in the liver. . Data presented as mean ± SEM. One-way ANOVA with Bonferroni test: * p < 0.05, **p < 0.001, ***p < 0.0001. SD^{+/+}: WT mice fed with standard diet; HFD^{+/+}: WT mice fed with standard diet; SD^{-/-}: BVR-A knock-out mice fed with standard diet; HFD^{-/-}: BVR-A knock-out mice fed with standard diet.

4.3 Loss of BVR-A impairs brain insulin signalling in the frontal cortex of female mice fed with HFD

Alterations of brain insulin signalling were evaluated by a multiplex approach that we [160] and others [161, 162] have successfully used in previous works, and that allows to measure the levels of multiple targets (pIRS1^{S636}, pPTEN^{S380}, pAkt^{S473}, pGSK3 β ^{S9}, pmTOR^{S2448}, pP70S6K^{T389}, pS6^{S235/S236}) at once. This analysis was implemented by evaluating pan-Y phosphorylation of IRS1 (panIRS1^Y) by ELISA. Furthermore, to test the activation of brain insulin signalling we treated mice with intranasal insulin (Humalog 2U/mL, 10 μ L/nostril) and we evaluated the activation state of few main targets downstream from IRS1 after 30'.

Our results show that female HFD^{+/+} mice are characterized by a significant increase of both pIRS1^{S636} and panIRS1^Y that finally result in no significant changes of IRS1 global activation [evaluated as ratio between the activation/inhibition phosphorylation sites, panY/S636], after 8 weeks of HFD (Figure 15c). In detail, lack of BVR-A is associated with reduced IRS1 inhibition (pIRS1^{S636} levels) in SD^{-/-}8 vs SD^{+/+}8 (Figure 15d). This is further corroborated by the observation that increased pIRS1^{S636} levels in HFD^{+/+} mice are completely prevented in HFD^{-/-} mice after 8 weeks of diet (Figure 15d). panIRS1^Y – a measure of IRS1 activation – increases with age in SD^{+/+} mice, with a similar trend observed in HFD^{+/+} mice, that reflects a lack of a significant effect due to HFD on this marker (Figure 15e). Rather, the increase of panIRS1^Y is prevented in both SD^{-/-} and HFD^{-/-} (Figure 15e). Overall, these changes result in no differences the pIRS1 Y/S ratio. Intriguingly, a trend toward an increased IRS1 activation (higher pIRS1 Y/S ratio) was observed in SD^{-/-} vs SD^{+/+} mice after 8 weeks of diet (Figure 15c), supporting the hypothesis that loss of BVR-A initially might favour IRS1

activation. This process seems to be driven by preventing IRS1 inhibition (S phosphorylation) rather than increased Y phosphorylation, since the effect observed on pIRS1^{S636} is greater than those observed with respect to panIRS1^Y. Indeed, we hypothesize that the increase of pIRS1^{S636} levels in the frontal cortex of HFD^{+/+} mice is partially buffered by the effect mediated by the loss of BVR-A. These observations agree with our hypothesis and our previous findings [24, 148] [25] suggesting that BVR-A has a regulatory role upstream in the pathway, whereby loss of BVR-A favour IRS1 activation by the mean of reduced inhibition.

Downstream from IRS1 we found reduced levels of PTEN under its inhibited form (pPTEN^{S380}) both in SD^{+/+} and HFD^{+/+} mice after 8 weeks of diet compared to 1 week (Figure 15f). A similar effect can be observed in SD^{-/-} mice after 1 week of diet, suggesting that loss of BVR-A might favour PTEN activation.

The PTEN protein is principally involved in the homeostatic maintenance of PI3K/AKT signalling [163]. Its typical function consists of the dephosphorylation of the lipid-signalling second messenger phosphatidylinositol-3,4,5-triphosphate (PIP3), a lipid product of the PI3K, to phosphatidylinositol-4,5-bisphosphate (PIP2), thereby directly antagonizing the PI3K function and blocking the activation of downstream signalling events, including AKT. Indeed, PIP3 is crucial for the recruitment and activation of PDK1 and AKT at the cell membrane, where PDK1 mediates AKT phosphorylation and activation [53].

Our results show that female HFD^{+/+} mice are characterized by a significant increase of AKT active form (pAKT^{S473}) after 8 weeks of diet (Figure 15g). Conversely, loss of BVR-A is associated with reduced pAKT^{S473} in SD^{-/-}8 vs SD^{+/+}8 mice and prevents the increase of pAKT^{S473} in

HFD^{-/-} mice (Figure 15g). As previously reported, BVR-A works as scaffold protein contributing to the formation of the PDK1/BVR-A/AKT complex that is crucial to promote the PDK1-mediated activation of AKT in response to insulin [164]. Considering that AKT protein is a hub on which converge many intracellular signalling pathways, it is conceivable to propose that the increased pAKT^{S473} levels in HFD^{+/+} mice can result from a different mechanism. However, this hypothesis does not exclude the possibility that the observed reduction of BVR-A in HFD^{+/+} frontal cortex might have a role, because, as discussed above for IRS1, reduced BVR-A might buffer the increase of pAKT^{S473} observed in HFD^{+/+} mice after 8 weeks of diet. We also noticed that despite the observed trend for IRS1 to be more activated in SD^{-/-} mice with respect to SD^{+/+}, a significant decrease for pAKT^{S473} was observed, strengthening the key role for BVR-A in favouring AKT activation. Moreover, despite the observed increased PTEN activation (less pPTEN^{S380} levels) in both SD^{+/+} and HFD^{+/+} mice, that means reduced PIP3 synthesis, and that would result in reduced AKT activation, we observed lower pAKT^{S473} levels only in SD^{-/-} and HFD^{-/-} mice further supporting the concept that increased pAKT^{S473} levels in HFD^{+/+} mice are driven by a mechanism different from insulin /growth factors signalling.

Among targets of Akt kinase activity we evaluated the glycogen synthase kinase 3 beta (GSK-3 β) and the mammalian target of rapamycin (mTOR). Under physiological conditions, Akt-mediated inhibition of GSK-3 β represents a neuro-protective and pro-survival mechanism rapidly activated in response to insulin [165, 166], while Akt-mediated activation of mTOR is of importance in regulating cellular growth and metabolism as well as degradative systems (i.e., autophagy) [167]. Notwithstanding with that,

sustained GSK-3 β inhibition and/or mTOR activation are detrimental for neurons [167, 168].

Our results show that pGSK3 β ^{S9} levels are not different in HFD^{+/+} mice when comparing 8 weeks vs 1 week (Figure 15h). This result is consistent with the role for BVR-A favouring AKT-mediated inhibition of GSK3 β [123]. Indeed, despite increased AKT activation, loss of BVR-A impairs GSK3 β ^{S9} phosphorylation (Figure 15h). Surprisingly, a consistent increase of pGSK3 β ^{S9} levels in SD^{-/-} vs SD^{+/+} mice was observed (Figure 15h), and deserves further investigations.

Regarding mTOR, we observed elevated pmTOR^{S2448} levels in HFD^{+/+} mice after 8 weeks of diet (Figure 15i). Increased mTOR activation might be due to AKT, that shows a similar pattern of increase. Lack of BVR-A promotes different effects on mTOR. We found a significant increase of pmTOR^{S2448} levels in SD^{-/-} vs SD^{+/+} mice after 1 week of diet, while a reduction was observed when persistent loss of BVR-A occurs [SD^{-/-} vs SD^{+/+} and HFD^{-/-} vs HFD^{+/+} mice after 8 weeks, Figure 15i). Therefore, the increased pmTOR^{S2448} levels in HFD^{+/+} might be an early response to HFD driven by reduced BVR-A protein levels. In addition, mTOR hyperactivation could lead to GSK3 β ^{S9} phosphorylation [169, 170] in SD^{-/-} mice (Figure 15i).

To further evaluate mTOR activation we looked at p70S6 kinase protein phosphorylated at the T389 (pP70S6K^{T389}). Phosphorylation of Thr389 is mediated by mTOR and is stimulated by growth factors such as insulin, and most closely correlates with p70 kinase activity in vivo [171, 172]. We found no changes of pP70S6K^{T389} in HFD^{+/+} mice. A significant reduction can be observed in HFD^{-/-} vs HFD^{+/+} mice after 1 week of diet (Figure 15j). This observation would suggest that lack of BVR-A preclude mTOR-mediated

P70S6K phosphorylation. In fact, despite increased levels of pmTOR^{S2448} observed both in HFD^{+/+} mice after 8 weeks and in SD^{-/-} mice after 1 week of diet, no changes for pP70S6K^{T389} were observed (Figure 15j).

Finally, downstream from P70S6K we evaluated S6 protein phosphorylated at S235/S236 (pS6^{S235/S236}), that are well-known targets P70S6K [173]. Surprisingly, we found that pS6^{S235/S236} levels are increased in HFD^{+/+} after 8 weeks of diet, despite non changes in pP70S6K^{T389} (Figure 15k). Lack of BVR-A is associated with reduced pS6^{S235/S236} in SD^{-/-} vs SD^{+/+} (Figure 15k). This is further corroborated by the observation that increased pS6^{S235/S236} are prevented in HFD^{-/-} mice after 8 weeks of diet (Figure 15k). Hence, our data suggest a negative role for BVR-A, particularly, for a persistent loss of BVR-A, since the most significant results can be observed after 8 weeks of diet either in the SD or HFD groups (Table 3). This is consonant, with the data collected about mTOR and pP70S6K^{T389}, providing evidence that persistent loss of BVR-A shut-down the mTOR/pP70S6K/S6 pathway. Therefore, the observed increase of pS6^{S235/S236} in HFD^{+/+} mice after 8 weeks might be driven by other mechanisms known to promote S6 phosphorylation on the same sites independently of mTOR, e.g., ERK1/2, PKA, RSK, PKC, PKG, and DAPK [174]. The measures obtained in the frontal cortex suggest that loss of BVR-A is associated with alterations of insulin signalling in the frontal cortex, that are consistent with the [122, 146].

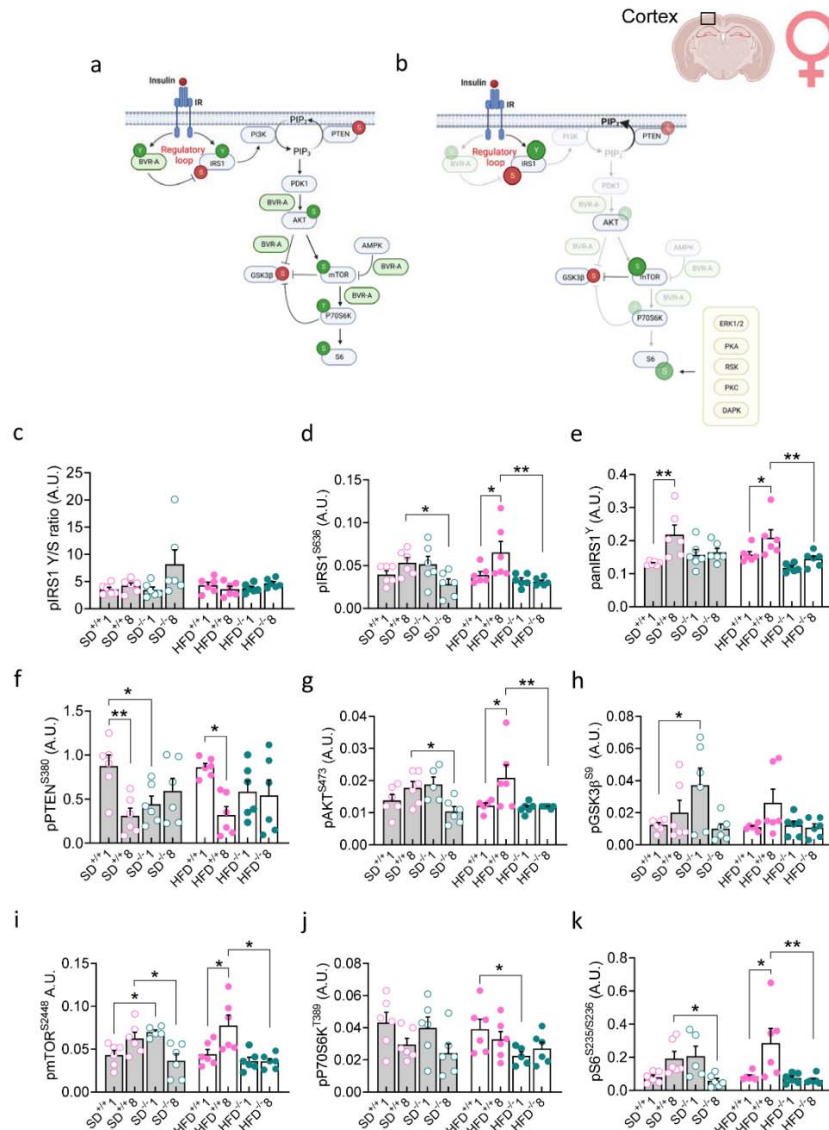


FIGURE 15. Evaluation of the levels of multiple targets of the insulin cascade in female C57Bl/6j and BVR-A^{-/-} mice. (a) Schematic representation of the insulin signalling under physiological conditions, and (b) in the absence of BVR-A protein. Arrows: activation; lines: inhibition; green circles: phosphorylation sites associated with protein activation; red circles: inhibitory phosphorylation sites. (c-k) Levels of proteins of the insulin signalling evaluated in frontal cortex isolated from C57Bl/6j and BVR-A^{-/-} mice fed with standard (SD) and high fat diets (HFD). Data presented as mean ± SEM. One-way ANOVA with Bonferroni test: * p < 0.05, **p < 0.001. SD^{+/+}: WT mice fed with standard diet; HFD^{+/+}: WT mice fed with standard diet; SD^{-/-}: BVR-A knock-out mice fed with standard diet; HFD^{-/-}: BVR-A knock-out mice fed with standard diet.

TABLE 3. Summary representation of dynamic changes of proteins involved in the insulin pathway. Arrows: ↑ indicates an increase, ↓ indicates a decrease. ≠ indicates no changes. Highlighted in red changes observed in WT mice fed with HFD. Highlighted in green similar changes observed in BVR-A^{-/-} mice, to support lack of BVR-A-mediated alterations.

			Age effect	Early Loss	Persistent Loss	Early Loss + diet	Persistent Loss + diet
		HFD ^{+/+} 8	SD ^{+/+} 8	SD ^{-/-} 1	SD ^{-/-} 8	HFD ^{-/-} 1	HFD ^{-/-} 8
inhibited	pIRS1 ^{S636}	↑	≠	≠	↓	≠	↓
activated	panIRS1 ^Y	↑	↑	≠	≠	≠	↓
	IRS1 Y/S	≠	≠	≠	↑	≠	≠
inhibited	pPTEN ^{S380}	↓	↓	↓	≠	≠	≠
activated	pAKT ^{S473}	↑	≠	≠	↓	≠	↓
inhibited	pGSK3β ^{S9}	≠	≠	↑	≠	≠	≠
activated	pmTOR ^{S2448}	↑	≠	↑	↓	≠	↓
activated	pP70S6K ^{T389}	≠	≠	≠	≠	↓	≠
activated	pS6 ^{S235/S236}	↑	≠	≠	↓	≠	↓

To prove that insulin signalling activation is altered we treated mice with intranasal insulin and we tested the insulin-mediated activation of AKT, GSK3β, and mTOR.

We found that intranasal insulin administration did not promote an increased activation of AKT, nor of GSK3β, nor of mTOR in the frontal cortex of SD^{+/+} mice. No significant changes were observed in SD^{-/-}, HFD^{+/+}, or HFD^{-/-} mice after 1 week of diet (Figures 16c,d and e). Lack of changes might be related to the developmental stage of the brain [175, 176]. Rather, administration of insulin in SD^{+/+} mice after 8 weeks of diet leads to a significant increase of AKT activation along with a reduction of GSK3β inhibition and an increase of mTOR activation (Figures 16f and 16g). Intriguingly, AKT activation is completely prevented in HFD^{+/+} mice after 8 weeks of diet, and it is associated with reduced GSK3β inhibition and no

changes in mTOR activation (Figure 16h). Similar results can be observed in SD^{-/-} mice, supporting our hypothesis that lack of BVR-A impairs insulin signalling activation. In addition, we observed an overactivation of AKT and mTOR in HFD^{-/-} mice, that seems to be an abnormal response.

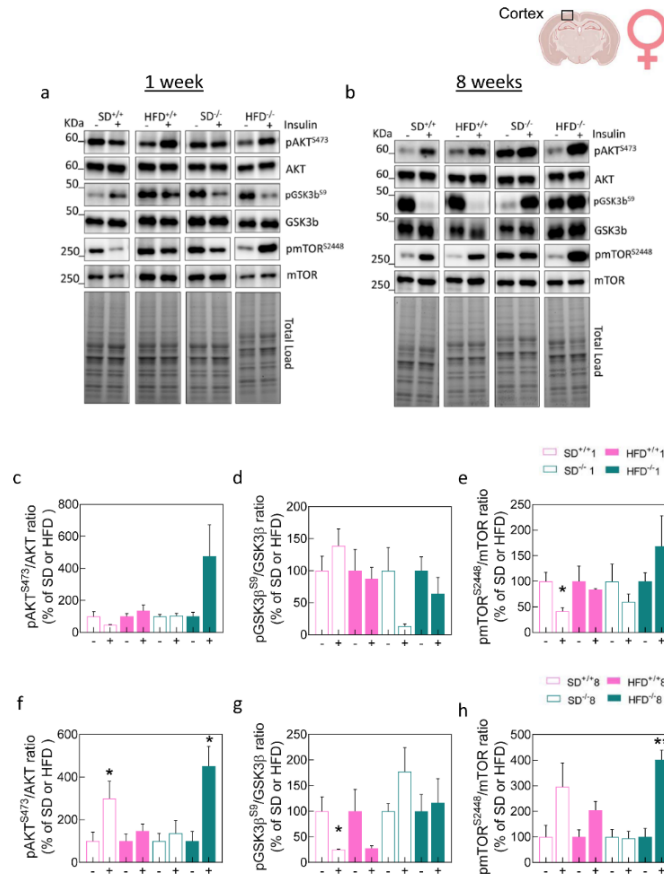


FIGURE 16. Activation of insulin signalling following insulin intranasal administration in female C57Bl/6j and BVR-A^{-/-} mice. (a-b) Representative western blot images at 1 and 8 weeks of SD and HFD, respectively. Densitometric evaluation of (c) AKT activation (evaluated as pAKT^{S473}/AKT ratio), (d) GSK3β inhibition (evaluated as pGSK3β^{S9}/GSK3β ratio), (e) mTOR activation (evaluated as pmTOR^{S2448}/mTOR ratio) at the end of 1 week of diet. (f) AKT activation (evaluated as pAKT^{S473}/AKT ratio), (g) GSK3β inhibition (evaluated as pGSK3β^{S9}/GSK3β ratio), (h) mTOR activation (evaluated as pmTOR^{S2448}/mTOR ratio) at the end of 8 weeks of diet. All densitometric values were normalized for total protein load and are given as the percentage of sets of SD or HFD mice not treated with insulin as 100%. Data presented as mean ± SEM. *Student t* test: * p < 0.05, **p < 0.001. (-) vehicle; (+): intranasal insulin.

4.4 Loss of BVR-A impairs brain insulin signalling in the frontal cortex of male mice fed with HFD

Approach used to investigate alterations of brain insulin pathway in male mice has been used for evaluating brain insulin signalling in WT and BVR-A^{-/-} C57Bl/6j male mice as well.

Our results show that male HFD^{+/+} mice are characterized by a significant decrease of IRS1 global activation after 8 weeks of diet mainly driven by pIRS1^{S636} increase (Figure 17c). In details, lack of BVR-A is associated with increased IRS1 inhibition (pIRS1^{S636} levels) in SD^{-/-} vs SD^{+/+} (Figure 17d). A similar trend is observed in SD^{+/+}8 vs SD^{+/+}1 (Figure 17d). Conversely, we found that IRS1 activation is significant increase in SD^{+/+}8 vs SD^{+/+}1, while lack of BVR-A prevented a such increase in knock-out mice (Figure 17e). As a net effect, reduced global IRS1 activation in SD^{-/-} mice occur. Similar observation can be found in HFD^{-/-} mice, thus suggesting that loss of BVR-A triggers the development of brain insulin resistance.

Downstream from IRS1 we found no changes for pPTEN^{S380} in HFD^{+/+}8 vs HFD^{+/+}1. Reduced levels of pPTEN^{S380} in SD^{+/+} vs SD^{-/-} mice after 1 week of diet and HFD^{+/+} vs HFD^{-/-} mice after 8 weeks of diet were observed (Figure 17f), suggesting that loss of BVR-A might favour PTEN activation.

In addition, our results show that male HFD^{+/+} mice are characterized by the aberrant activation of the AKT/mTOR axis after 8 weeks of diet (Figures 17g and 17i). A similar pattern can be observed both in HFD^{-/-}1 vs HFD^{+/+}1 suggesting that loss of BVR-A is associated with the hyper-activation of AKT/mTOR axis and likely accelerate this process. Indeed, 1 week of HFD in knock-out mice is enough to promote similar effects of 8 weeks of HFD in WT mice. Considering that AKT hyper-activation occur despite IRS1 inhibition, it is conceivable to hypothesize that AKT hyper-activation is

mediated by a different mechanism than the insulin signalling activation. One potential explanation can be that mTOR hyper-activation is responsible for AKT phosphorylation as reported in [177].

Our findings also show a significant increase of GSK3 β inhibition (pGSK3 β ^{S9}) in HFD^{+/+} mice after 8 weeks of diet (Figure 17h). This increase might be due to an mTOR-mediated feedback mechanism as reported for AKT. Remarkably, the role for BVR-A is highlighted in SD^{-/-} and in HFD^{-/-} mice where lack of BVR-A prevents an increase of GSK3 β inhibition despite AKT hyper-activation (Figure 17h).

Concerning pP70S6K^{T389}, we found no changes in HFD^{+/+} mice. Reduced levels of pP70S6K^{T389} in SD^{+/+} vs SD^{-/-} mice after 1 week of diet and HFD^{+/+} vs HFD^{-/-} mice after 8 weeks of diet were observed (Figure 17j), indicating that lack of BVR-A forestalls mTOR-mediated P70S6K phosphorylation.

At last, our data described an increase of pS6^{S235/S236} levels in HFD^{+/+} after 8 weeks of diet, though no change in pP70S6K^{T389}. Increased S6 phosphorylation in SD^{-/-} vs SD^{+/+} and HFD^{-/-} vs HFD^{+/+} mice after 1 week of diet (Figure 17k), implies that S6 protein could be correlated to an increase in the activation of other kinases such as ERK1/2, PKA, RSK, PKC, PKG, and DAPK [174] (Table 4).

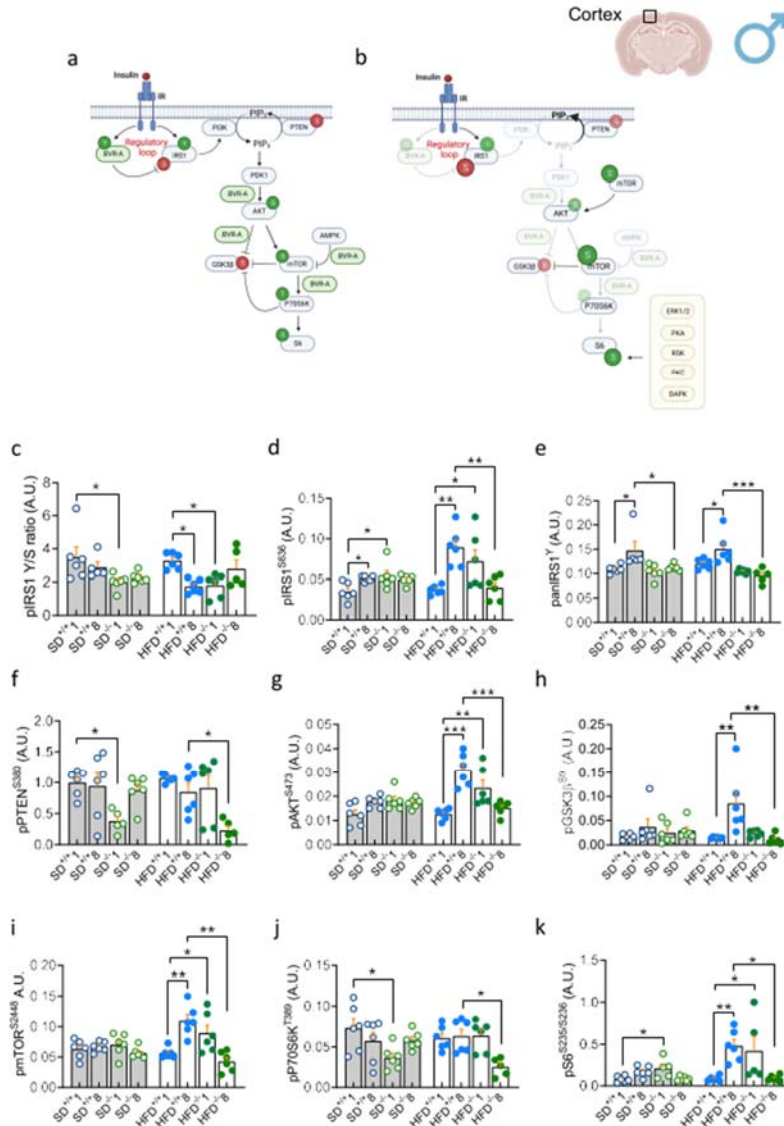


FIGURE 17. Evaluation of the levels of multiple targets of the insulin cascade in male C57Bl/6j and BVR-A^{-/-} mice. (a) Schematic representation of the insulin signalling under physiological conditions, and (b) in the absence of BVR-A protein. Arrows: activation; lines: inhibition; green circles: phosphorylation sites associated with protein activation; red circles: inhibitory phosphorylation sites. (c-k) Levels of proteins of the insulin signalling evaluated in frontal cortex isolated from C57Bl/6j and BVR-A^{-/-} mice fed with standard (SD) and high fat diets (HFD). Data presented as mean ± SEM. One-way ANOVA with Bonferroni test: * p < 0.05, **p < 0.001. SD^{+/+}: WT mice fed with standard diet; HFD^{+/+}: WT mice fed with standard diet; SD^{-/-}: BVR-A knock-out mice fed with standard diet; HFD^{-/-}: BVR-A knock-out mice fed with standard diet.

TABLE 4. Summary representation of dynamic changes of proteins involved in the insulin pathway. Arrows: ↑ indicates an increase, ↓ indicates a decrease. ≠ indicates no changes. Highlighted in red changes observed in WT mice fed with HFD. Highlighted in green similar changes observed in BVR-A^{-/-} mice, to support lack of BVR-A-mediated alterations.

			Age effect	Early Loss	Persistent Loss	Early Loss + diet	Persistent Loss + diet
		HFD ^{+/+8}	SD ^{+/+8}	SD ^{-/-1}	SD ^{-/-8}	HFD ^{-/-1}	HFD ^{-/-8}
inhibited	pIRS1 ^{S636}	↑	↑	↑	≠	↓	↓
activated	panIRS1 ^Y	↑	↑	≠	↓	≠	↓
	IRS1 Y/S	↓	≠	↓	≠	↓	≠
inhibited	pPTEN ^{S380}	≠	≠	↓	≠	≠	↓
activated	pAKT ^{S473}	↑	≠	≠	≠	↑	↓
inhibited	pGSK3β ^{S9}	↑	≠	≠	≠	≠	↓
activated	pmTOR ^{S2448}	↑	≠	≠	≠	↑	↓
activated	pP70S6K ^{T389}	≠	≠	↓	≠	≠	↓
activated	pS6 ^{S235/S236}	↑	≠	↑	≠	↑	↓

In support of our hypothesis about the pivotal role for BVR-A in regulating insulin signalling, we found that intranasal insulin administration promotes an increased activation of AKT and mTOR in SD^{+/+1} mice (Figure 18c and 18e), while an increased phosphorylation of AKT and of GSK3β in SD^{+/+8} mice (Figure 18f and 18g), as a part of physiological response. Conversely, insulin administration did not produce any effect in HFD-treated mice (Figures 18c, d and 18f, g), thus suggesting that activation of the signalling is impaired. In addition, intranasal insulin administration promoted an aberrant activation of the signalling in both SD^{-/-} and HFD^{-/-} mice, in which the hyper-activation of mTOR represent one of the main features (Figures 18e and 18h). Hyper-activation of mTOR in response to insulin is associated with the abnormal phosphorylation of both AKT and GSK3β, thus

supporting our hypothesis that lack of BVR-A triggers mTOR hyper-activation and related feedback mechanisms in response to insulin.

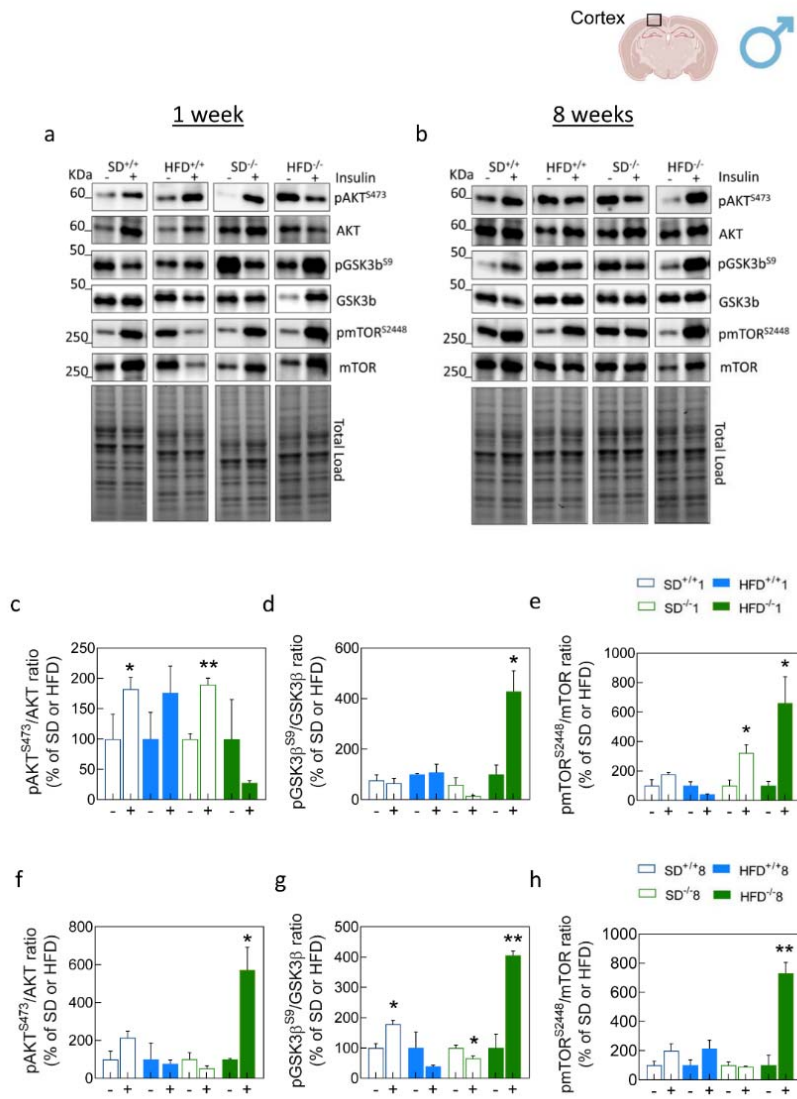


FIGURE 18. Activation of insulin signalling following insulin intranasal administration in male C57Bl/6j and BVR-A^{-/-} mice. (a-b) Representative western blot images at 1 and 8 weeks of SD and HFD, respectively. Densitometric evaluation of (c) AKT activation (evaluated as pAKT^{S473}/AKT ratio), (d) GSK3β inhibition (evaluated as pGSK3β^{S9}/GSK3β ratio), (e) mTOR activation (evaluated as pmTOR^{S2448}/mTOR ratio) at the end of 1 week of diet. (f) AKT activation (evaluated as pAKT^{S473}/AKT ratio), (g) GSK3β inhibition (evaluated as pGSK3β^{S9}/GSK3β ratio), (h) mTOR activation (evaluated as pmTOR^{S2448}/mTOR ratio) at the end of 8 weeks of diet. All densitometric values were normalized for total protein load and are given as the percentage of sets of SD or HFD mice not treated with insulin as 100%. Data presented as mean ± SEM. *Student t* test: * $p < 0.05$, ** $p < 0.001$. (-) vehicle; (+): intranasal insulin.

4.5 Brain insulin signalling shows mild alterations in the hippocampus of female mice fed with HFD

Alterations of brain insulin signalling were evaluated in the hippocampus female mice. Our results show that the global activation of IRS1 does not change in HFD^{+/+} female mice (Figure 19c). In details, lack of BVR-A is associated with significant decreased IRS1 inhibition (pIRS1^{S636} levels) in HFD^{-/-} vs HFD^{+/+} after 8 weeks of diet (Figure 19d), while no changes in SD mice were observed. IRS1 activation (panIRS1^Y) is significant increase in HFD^{+/+}8 vs HFD^{+/+}1 (Figure 19e), while the lack of BVR-A prevents a such phenomenon. Overall, reduced IRS1 S636 phosphorylation overweigh IRS1 Y phosphorylation activation, thus resulting in IRS1 hyper-activation in HFD^{-/-} mice.

We found reduced pPTEN^{S380} levels in HFD^{+/+}8 vs HFD^{+/+}1 (Figure 19f). No changes in SD mice group. Reduced levels of pPTEN^{S380} in SD^{+/+} vs SD^{-/-} mice and HFD^{-/-} vs HFD^{+/+} mice after 1 week of diet (Figure 19f) were observed, suggesting that loss of BVR-A might favour PTEN activation.

In addition, no changes for pAKT^{S473} occur in female HFD^{+/+} mice. Rather, a significant reduction of pAKT^{S473} both in HFD^{+/+}1 vs HFD^{-/-}1 and HFD^{+/+}8 vs HFD^{-/-}8 (Figure 19g) was observed, suggesting that lack of BVR-A prevents AKT phosphorylation (as described in female cortical samples).

Furthermore, downstream from AKT we found no changes for GSK3 β inhibition (pGSK3 β ^{S9}) in both HFD^{+/+} and SD^{+/+} mice after 8weeks of diet, in agreement with pAKT^{S473} levels (Figure 19h). Conversely, a significant decrease of pGSK3 β ^{S9} levels can be observe in SD^{-/-} and HFD^{-/-} mice (Figure 19h). These data lead to the hypothesis that the loss of BVR-A prevents the activation of AKT, and consequently GSK3 β inhibition is reduced.

In relation to mTOR, we observed no changes of pmTOR^{S2448} levels in HFD^{+/+} mice after 8 weeks of diet (Figure 19i), while a significant decrease of pmTOR^{S2448} levels in HFD^{-/-} mice was observed (Figure 19i).

pP70S6K^{T389} levels are not affected in HFD^{+/+} mice, although lack of BVR-A is associated with reduced P70S6K phosphorylation (Figure 19j) as reported also in the other brain regions evaluated in the current study.

Finally, we observed an increase of pS6^{S235/S236} levels in HFD^{+/+} after 8 weeks of diet, though no change in pP70S6K^{T389} (Figure 19k). Conversely, persistent lack of BVR-A is associated with lower levels of pS6^{S235/S236} in the hippocampus after 8 weeks of diet (Figure 19k), (Table 5).

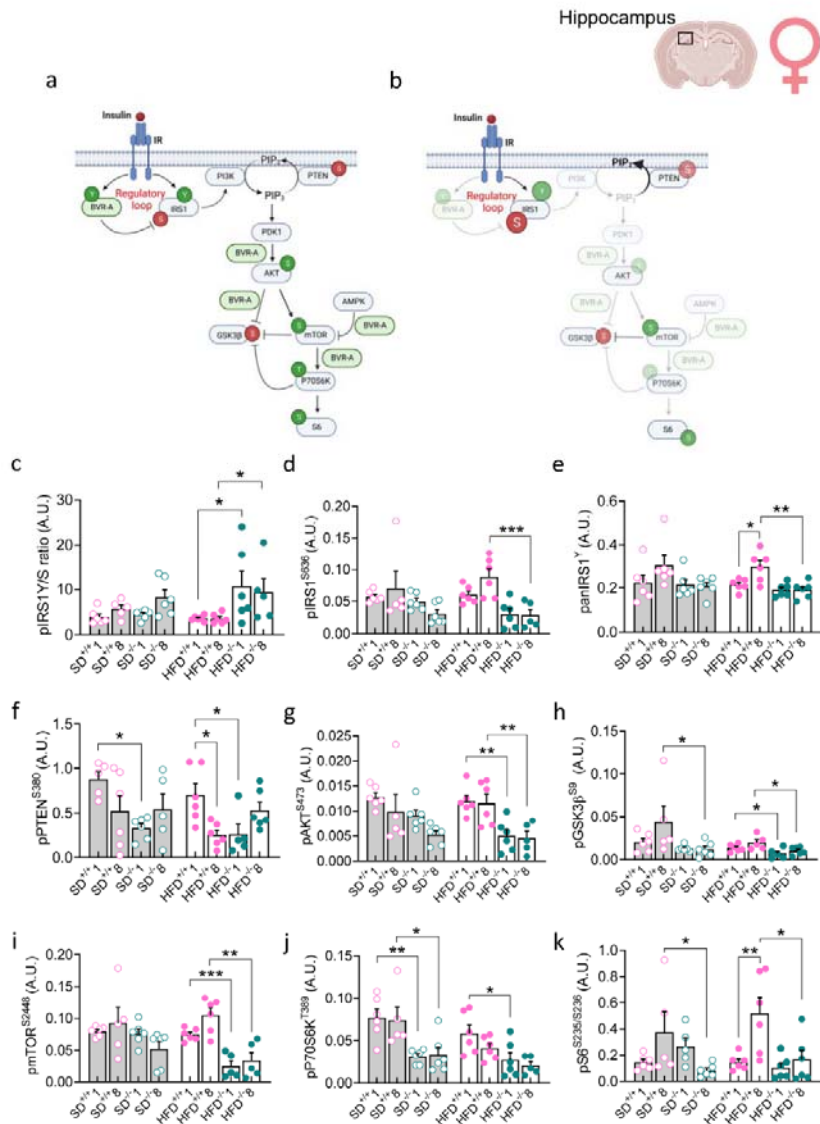


FIGURE 19. Evaluation of the levels of multiple targets of the insulin cascade in female C57Bl/6j and BVR-A^{-/-} mice. (a) Schematic representation of the insulin signalling under physiological conditions, and (b) in the absence of BVR-A protein. Arrows: activation; lines: inhibition; green circles: phosphorylation sites associated with protein activation; red circles: inhibitory phosphorylation sites. (c-k) Levels of proteins of the insulin signalling evaluated in hippocampus isolated from C57Bl/6j and BVR-A^{-/-} mice fed with standard (SD) and high fat diets (HFD). Data presented as mean ± SEM. One-way ANOVA with Bonferroni test: * p < 0.05, **p < 0.001. SD^{+/+}: WT mice fed with standard diet; HFD^{+/+}: WT mice fed with standard diet; SD^{-/-}: BVR-A knock-out mice fed with standard diet; HFD^{-/-}: BVR-A knock-out mice fed with standard diet.

TABLE 5. Summary representation of dynamic changes of proteins involved in the insulin pathway. Arrows: ↑ indicates an increase, ↓ indicates a decrease. ≠ indicates no changes. Highlighted in red changes observed in WT mice fed with HFD. Highlighted in green similar changes observed in BVR-A^{-/-} mice, to support lack of BVR-A-mediated alterations.

			Age effect	Early Loss	Persistent Loss	Early Loss + diet	Persistent Loss + diet
		HFD ^{+/+} 8	SD ^{+/+} 8	SD ^{-/-} 1	SD ^{-/-} 8	HFD ^{-/-} 1	HFD ^{-/-} 8
inhibited	pIRS1 ^{S636}	≠	≠	≠	≠	≠	↓
activated	panIRS1 ^Y	↑	≠	≠	≠	≠	↓
	IRS1 Y/S	≠	≠	≠	≠	↑	↑
inhibited	pPTEN ^{S380}	↓	≠	↓	≠	↓	≠
activated	pAKT ^{S473}	≠	≠	≠	≠	↓	↓
inhibited	pGSK3β ^{S9}	≠	≠	≠	↓	↓	↓
activated	pmTOR ^{S2448}	≠	≠	≠	≠	↓	↓
activated	pP70S6K ^{T389}	≠	≠	↓	↓	↓	≠
activated	pS6 ^{S235/S236}	↑	≠	≠	↓	≠	↑

Intranasal insulin administration promotes an increased activation of AKT along with its downstream targets GSK3β and of mTOR. This is also evident in HFD^{+/+} mice (Figure 20c, d,e and 20f, g, h) and might be explained by the fact that no major changes for BVR-A or insulin signalling proteins in the hippocampus of female mice were observed following HFD. Moreover, we observed an over-activation of AKT in HFD^{-/-} mice, that resemble to an abnormal response.

Together, our results suggest that hippocampus is more resilient than frontal cortex towards the effects mediated by the HFD.

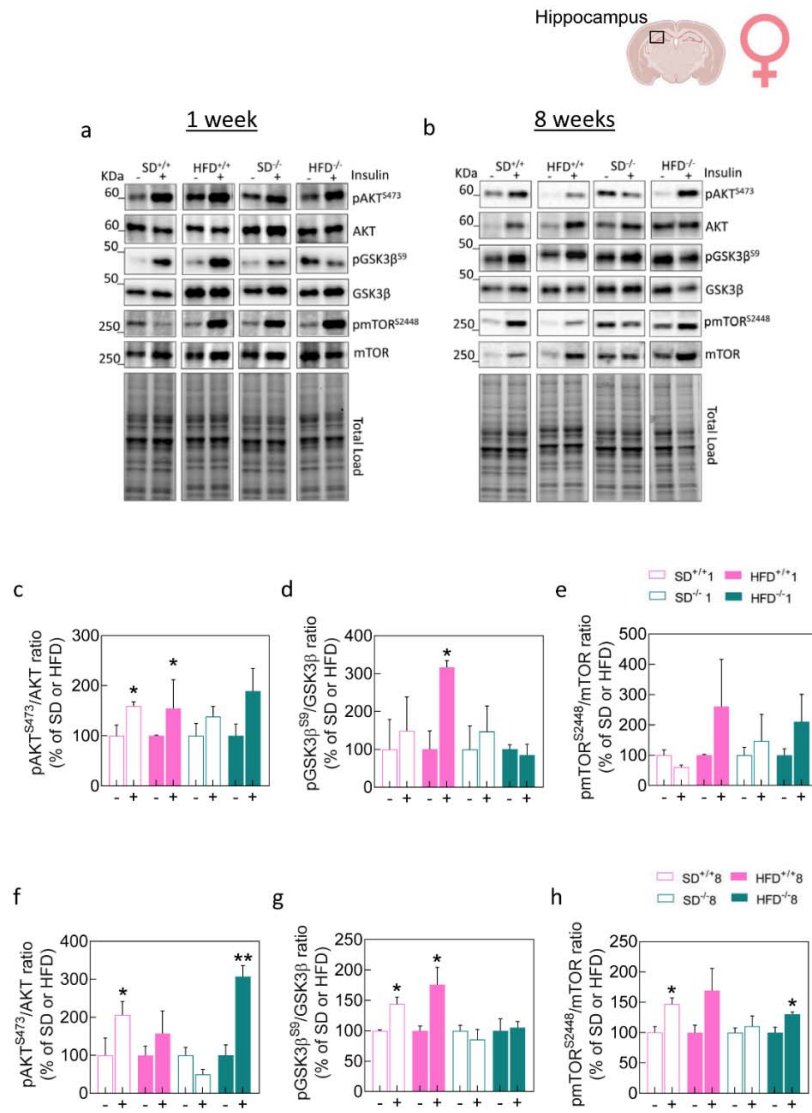


FIGURE 20. Activation of insulin signalling following insulin intranasal administration in female C57Bl/6j and BVR-A^{-/-} mice. (a-b) Representative western blot images at 1 and 8 weeks of SD and HFD, respectively. Densitometric evaluation of (c) AKT activation (evaluated as pAKT^{S473}/AKT ratio), (d) GSK3β inhibition (evaluated as pGSK3β^{S9}/GSK3β ratio), (e) mTOR activation (evaluated as pmTOR^{S2448}/mTOR ratio) at the end of 1 week of diet. (f) AKT activation (evaluated as pAKT^{S473}/AKT ratio), (g) GSK3β inhibition (evaluated as pGSK3β^{S9}/GSK3β ratio), (h) mTOR activation (evaluated as pmTOR^{S2448}/mTOR ratio) at the end of 8 weeks of diet. All densitometric values were normalized for total protein load and are given as the percentage of sets of SD or HFD mice not treated with insulin as 100%. Data presented as mean ± SEM. *Student t* test: * p < 0.05, **p < 0.001. (-) vehicle; (+):intranasal insulin.

4.6 Loss of BVR-A impairs brain insulin signalling in the hippocampus of male mice fed with HFD

Alterations of brain insulin signalling were evaluated in the hippocampus of male mice. Our results show that male HFD^{+/+} mice are characterized by a significant decrease of IRS1 global activation after 8 weeks of diet mainly driven by pIRS1^{S636} increase (Figure 21c). In details, lack of BVR-A is associated with increased IRS1 inhibition (pIRS1^{S636} levels) in HFD^{+/+}8 vs HFD^{+/+}1 and in HFD^{-/-}1 vs HFD^{+/+}1 (Figure 21d). A similar trend is observed in SD^{-/-}1 vs SD^{+/+}1 (Figure 21d). Instead, we found that IRS1 activation does not change. Consequently, reduced global IRS1 activation in HFD^{-/-} mice occur (Figure 21e).

Downstream from IRS1 we found no changes for pPTEN^{S380} in HFD^{+/+} after 8 weeks of diet. Reduced levels of pPTEN^{S380} in SD^{+/+} vs SD^{-/-} mice after 1 week of diet (Figure 21f) were found, suggesting that loss of BVR-A might favour PTEN activation.

Our findings also show that HFD^{+/+} male mice are characterized by a significant increase of AKT active form (pAKT^{S473}) (Figure 21g), that is further exacerbated in HFD^{-/-} mice after 8 weeks of diet. Interestingly, no changes for AKT in HFD^{-/-} mice after 1 week of diet or in SD^{-/-} mice have been observed. This agrees with the current hypothesis that lack of BVR-A impairs AKT activation during the early phases of the processes leading to bIR, whereas persistent BVR-A reduction under stressful conditions, i.e., HFD, promotes the activation of other molecular mechanisms responsible for AKT hyper-phosphorylation.

Downstream from AKT no changes for pGSK3 β ^{S9} levels were found (Figure 21h).

Intriguingly, one of the mechanisms that might be responsible for AKT hyper-phosphorylation is the aberrant mTOR activation. In fact, increased p mTOR^{S2448} levels in HFD^{+/+} mice and in HFD^{-/-} mice were found (Figure 21i).

Similarly to the other brain regions, reduced levels of pP70S6K^{T389} in SD^{-/-} after 1 week of diet were found (Figure 21j), strengthening the hypothesis that loss of BVR-A impairs mTOR-mediated phosphorylation of P70S6K. Data on HFD corroborate this hypothesis, since no changes for pP70S6K^{T389} can be observed despite mTOR hyper-activation.

Last but not least, we observed an increase of pS6^{S235/S236} levels in HFD^{+/+} mice after 8 weeks of diet, though no change in pP70S6K^{T389} (Figure 21k). Increased S6 phosphorylation can be found also in SD^{-/-} vs SD^{+/+} and HFD^{-/-} vs HFD^{+/+} mice after 1 week of diet (Figure 21k) despite no significant increase of pP70S6K^{T389}, (Table 6).

Data obtained from the evaluation of the insulin signalling in the hippocampus, seem to have the same trend found in the frontal cortex, except few alterations that appears to be less pronounced. Hence, considering that hippocampus is more resilient with respect to frontal cortex towards the effects of the HFD, we propose that a longer diet would be need to promote effects with a similar extent.

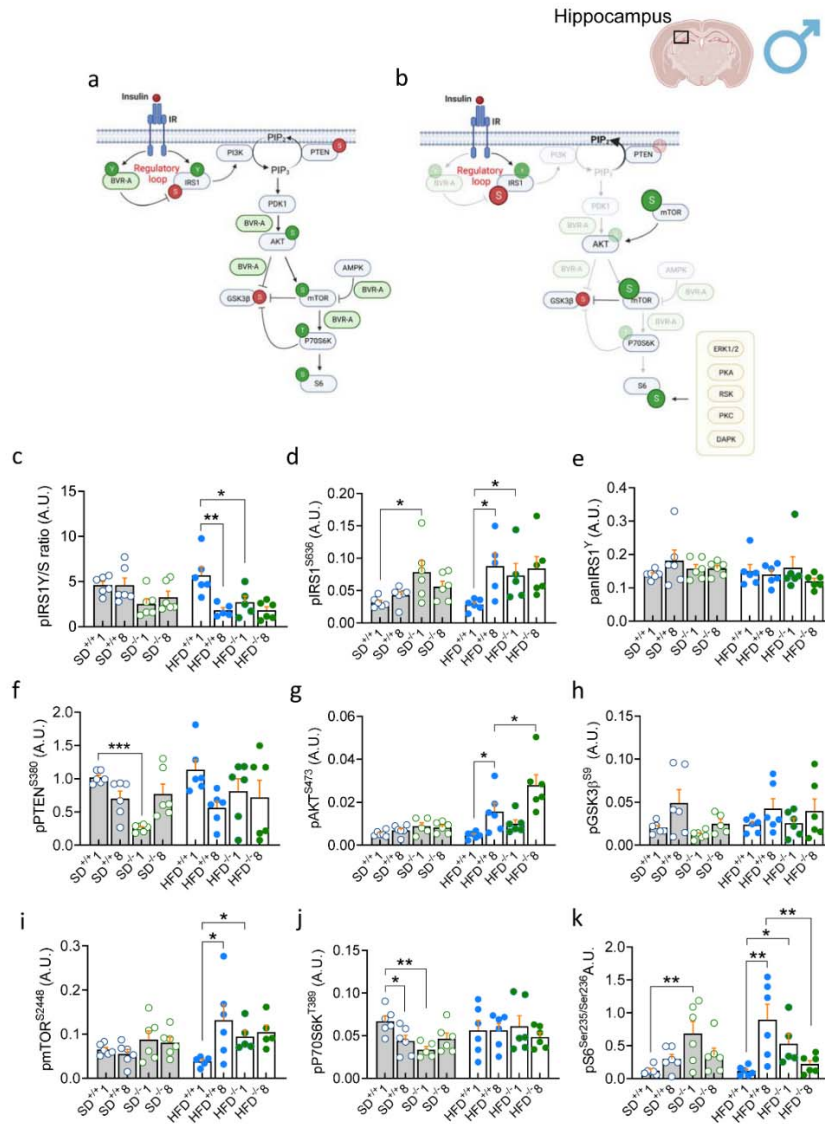


FIGURE 21. Evaluation of the levels of multiple targets of the insulin cascade in male C57Bl/6j and BVR-A^{-/-} mice. (a) Schematic representation of the insulin signalling under physiological conditions, and (b) in the absence of BVR-A protein. Arrows: activation; lines: inhibition; green circles: phosphorylation sites associated with protein activation; red circles: inhibitory phosphorylation sites. (c-i) Levels of proteins of the insulin signalling evaluated in hippocampus isolated from C57Bl/6j and BVR-A^{-/-} mice fed with standard (SD) and high fat diets (HFD). (j) Circulating insulin levels in plasma samples collected after the sacrifice in non-fasted mice. Data presented as mean \pm SEM. One-way ANOVA with Bonferroni test: * $p < 0.05$, ** $p < 0.001$, *** $p < 0.0001$. SD^{+/+}: WT mice fed with standard diet; HFD^{+/+}: WT mice fed with standard diet; SD^{-/-}: BVR-A knock-out mice fed with standard diet; HFD^{-/-}: BVR-A knock-out mice fed with standard diet.

TABLE 6. Summary representation of dynamic changes of proteins involved in the insulin pathway. Arrows: ↑ indicates an increase, ↓ indicates a decrease. ≠ indicates no changes. Highlighted in red changes observed in WT mice fed with HFD. Highlighted in green similar changes observed in BVR-A^{-/-} mice, to support lack of BVR-A-mediated alterations.

			Age effect	Early Loss	Persistent Loss	Early Loss + diet	Persistent Loss + diet
		HFD ^{+/+} 8	SD ^{+/+} 8	SD ^{-/-} 1	SD ^{-/-} 8	HFD ^{-/-} 1	HFD ^{-/-} 8
inhibited	pIRS1 ^{S636}	↑	≠	↑	≠	↑	≠
activated	panIRS1 ^Y	≠	≠	≠	≠	≠	≠
	IRS1 ^{Y/S}	↓	≠	≠	≠	↓	≠
inhibited	pPTEN ^{S380}	≠	≠	↓	≠	≠	≠
activated	pAKT ^{S473}	↑	≠	≠	≠	≠	↑
inhibited	pGSK3β ^{S9}	≠	≠	≠	≠	≠	≠
activated	pmTOR ^{S2448}	↑	≠	≠	≠	↑	≠
activated	pP70S6K ^{T389}	≠	↓	↓	≠	≠	≠
activated	pS6 ^{S235/S236}	↑	≠	↑	≠	↑	↓

We found that intranasal insulin administration promotes an increased activation of AKT that reflects on downstream targets, i.e., GSK3β and mTOR, in SD^{+/+} mice (Figures 22c ,d, e and 22f, g, h). No changes were observed in HFD^{+/+} group, except the hyper-activation of mTOR in HFD^{+/+} mice after 8 weeks of diet (Figure 22h). A similar pattern in HFD^{-/-} mice can be found, suggesting that loss of BVR-A impairs the signalling activation by triggering mTOR aberrant activation. In addition, we observed that the intranasal insulin leads to the over-inhibition of GSK3β in SD^{-/-} and HFD^{-/-} mice after 1 week of diet (figure 22d), that seems to be an anomalous response.

In conclusion, lack of BVR-A in the hippocampus of male mice promotes an abnormal response to insulin, as previously observed in the cortex of male and female, thus representing a shared mechanism.

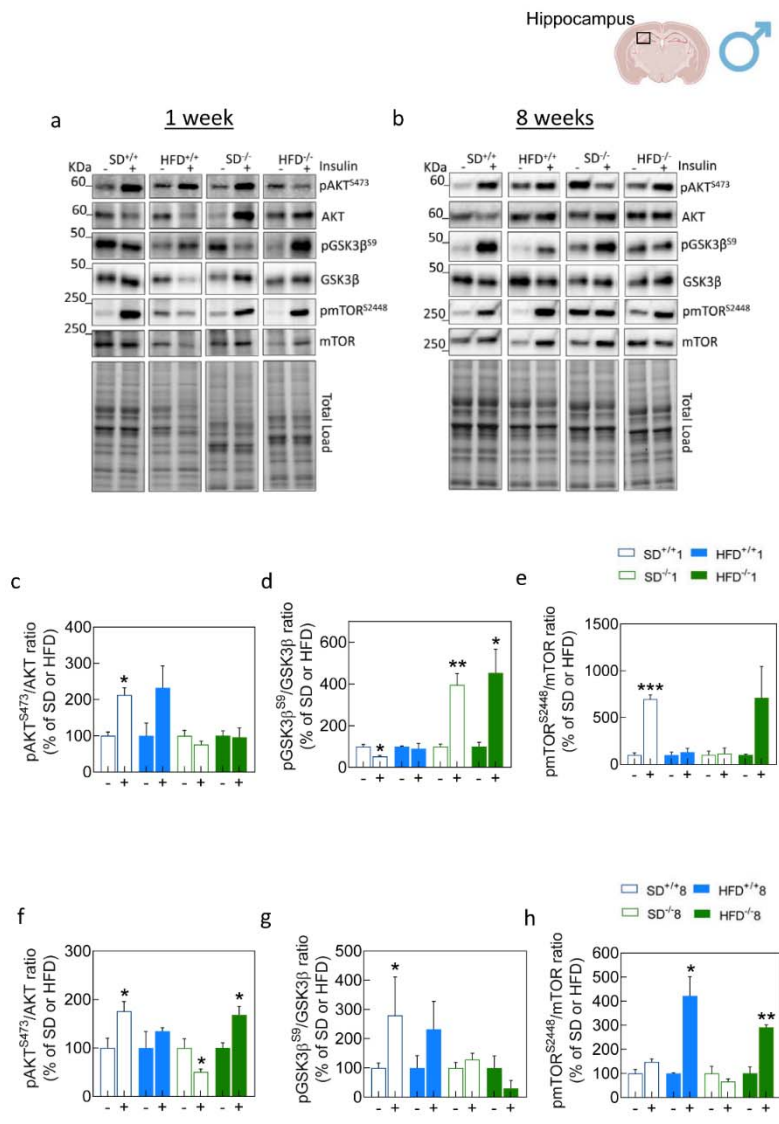


FIGURE 22. Activation of insulin signalling following insulin intranasal administration in male C57Bl/6j and BVR-A^{-/-} mice. (a-b) Representative western blot images at 1 and 8 weeks of SD and HFD, respectively. Densitometric evaluation of (c) AKT activation (evaluated as pAKT^{S473}/AKT ratio), (d) GSK3β inhibition (evaluated as pGSK3β^{S9}/GSK3β ratio), (e) mTOR activation (evaluated as pmTOR^{S2448}/mTOR ratio) at the end of 1 week of diet. (f) AKT activation (evaluated as pAKT^{S473}/AKT ratio), (g) GSK3β inhibition (evaluated as pGSK3β^{S9}/GSK3β ratio), (h) mTOR activation (evaluated as pmTOR^{S2448}/mTOR ratio) at the end of 8 weeks of diet. All densitometric values were normalized for total protein load and are given as the percentage of sets of SD or HFD mice not treated with insulin as 100%. Data presented as mean ± SEM. *Student t* test: * p < 0.05, **p < 0.001. (-) vehicle; (+):intranasal insulin.

4.7 Loss of BVR-A in the liver alters insulin signalling and worse glucose metabolism in female mice fed with HFD

In order to test the hypothesis that reduced BVR-A protein levels represent an early event in the development of insulin resistance and that this is a mechanism shared by different tissues/organs, we evaluated changes of insulin signalling in the liver. We completed the analyses for female mice but not for male. Furthermore, we were not able to perform the evaluation of panIRS1^Y, and thus we show here only the results collected by the multiplex approach.

Our data demonstrate that HFD group is characterized by no significant changes of IRS1 inhibition. We found a significant reduction of pIRS1^{S636} levels SD^{+/+} after 8 weeks of diet (figure 23c), and also in SD^{-/-} mice after 1 week of diet (figure 23c). Reduced pIRS1^{S636} levels persist in SD^{-/-} mice even after 8 weeks of diet (Figure 23c). Hence, loss of BVR-A is not associated with a consistent IRS1 inhibition in the liver, while it sustain IRS1 activation under the HFD regimen.

Downstream from IRS1, we found that female HFD^{+/+} and SD^{+/+} mice are characterized by a significant decrease of PTEN inhibition (pPTEN^{S380}) after 8 week of diet respectively (figure 23d). Similarly, loss of BVR-A leads to reduced pPTEN^{S380} levels in SD^{-/-}1 vs SD^{+/+}1. Conversely, PTEN inhibition in increased with the persistent reduction of BVR-A both in SD^{-/-}8 vs SD^{+/+}8 and in HFD^{-/-}8 vs HFD^{+/+}8 (Figure 23d).

AKT active form (pAKT^{S473}) is decreased in HFD^{+/+} and SD^{+/+} after 8 weeks of diet (figure 23e). Furthermore, a decrease of pAKT^{S473} levels in SD^{-/-} mice after 1 week of diet, was observed and persisted also after 8 weeks SD^{-/-} and in HFD^{-/-} groups (figure 23e).

We found that pGSK3 β ^{S9} levels are not different in HFD^{+/+} mice when comparing 8 weeks vs 1 week (Figure 23f). A significant reduction for pGSK3 β ^{S9} was observed in SD^{-/-} mice after 1 week of diet (Figure 23f).

Regarding mTOR, our findings show reduced pmTOR^{S2448} levels in HFD^{+/+}8 vs HFD^{+/+}1 (figure 23g), as well as in SD^{+/+}8 vs SD^{+/+}1 (figure 23g) and in SD^{-/-}1 vs SD^{+/+}1 (figure 23g).

pP70S6K^{T389} levels follow mTOR activation. A trend to a reduction can be observed in HFD^{+/+} mice, although it does not reach a statistical significance. Moreover, reduced pP70S6K^{T389} were found in SD^{+/+}8 vs SD^{+/+}1 and in SD^{-/-} mice after 1 week of diet (Figure 23h).

Finally, we evaluated pS6^{S235/S236} levels. No significant change was detected in HFD mice. We noted that pS6^{S235/S236} levels are reduced in SD^{-/-} after 1 week of diet (Figure 23i).

Results about insulin signalling were implemented by measures of circulating insulin levels in plasma samples collected after the sacrifice in non-fasted mice.

Our data show no changes for circulating insulin in HFD^{+/+} mice (Figure 23j). Conversely, a significant increase in SD^{+/+} was observed (Figure 23j), suggesting that HFD impairs insulin production/clearance in female mice. Interestingly, insulin levels do not increase neither in SD^{-/-} mice (Figure 23j), while a rise is observed in HFD^{-/-} after 8 weeks of diet (Figure 23j). Hence, in light of the glucometabolic alterations reported in Figure 12c, it is conceivable to hypothesize that lack of BVR-A greatly alters insulin signalling and insulin sensitivity in the liver.

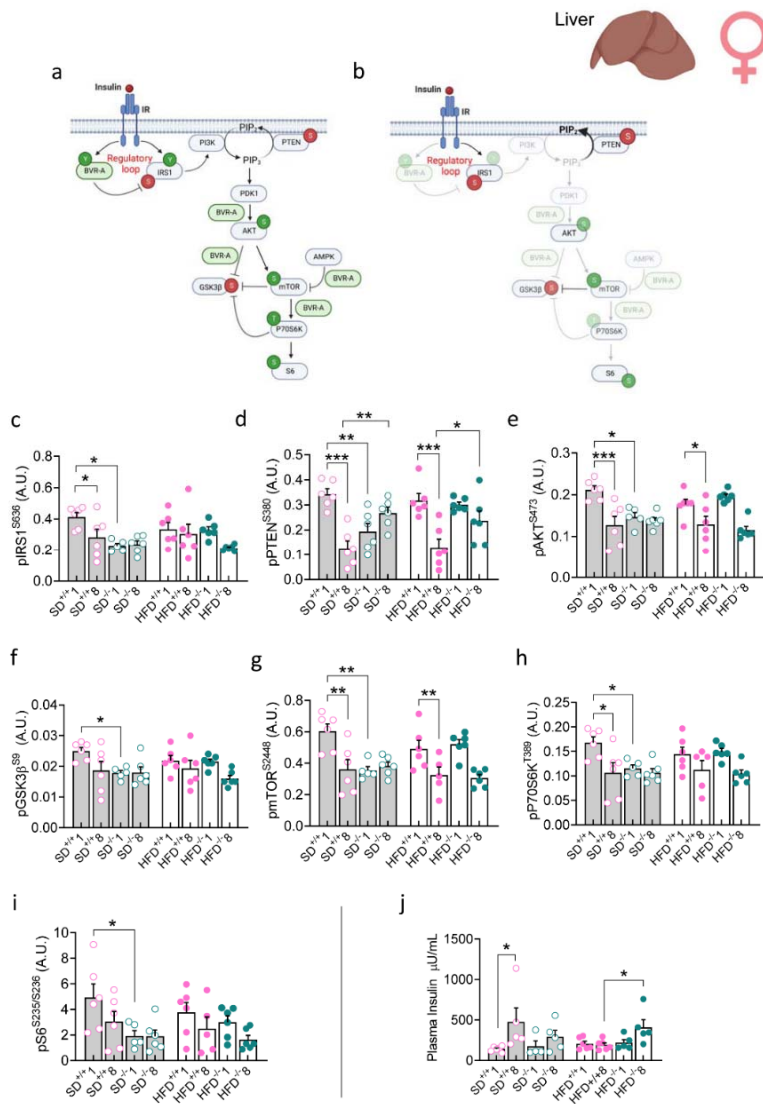


FIGURE 23. Evaluation of the levels of multiple targets of the insulin cascade in female C57Bl/6j and BVR-A^{-/-} mice. (a) Schematic representation of the insulin signalling under physiological conditions, and (b) in the absence of BVR-A protein. Arrows: activation; lines: inhibition; green circles: phosphorylation sites associated with protein activation; red circles: inhibitory phosphorylation sites. (c-i) Levels of proteins of the insulin signalling evaluated liver isolated from C57Bl/6j and BVR-A^{-/-} mice fed with standard (SD) and high fat diets (HFD). (j) Circulating insulin levels in plasma samples collected after the sacrifice in non-fasted mice. Data presented as mean ± SEM. One-way ANOVA with Bonferroni test: * p < 0.05, **p < 0.001, ***p < 0.0001. SD^{+/+}: WT mice fed with standard diet; HFD^{+/+}: WT mice fed with standard diet; SD^{-/-}: BVR-A knock-out mice fed with standard diet; HFD^{-/-}: BVR-A knock-out mice fed with standard diet.

			Age effect	Early Loss	Persistent Loss	Early Loss + diet	Persistent Loss + diet
		HFD ^{+/+8}	SD ^{+/+8}	SD ^{-/-1}	SD ^{-/-8}	HFD ^{-/-1}	HFD ^{-/-8}
inhibited	pIRS1^{S636}	≠	↓	↓	≠	≠	≠
inhibited	pPTEN^{S380}	↓	↓	↓	↑	≠	↑
activated	pAKT^{S473}	↓	↓	↓	≠	≠	≠
inhibited	pGSK3β^{S9}	≠	≠	↓	≠	≠	≠
activated	pmTOR^{S2448}	↓	↓	↓	≠	≠	≠
activated	pP70S6K^{T389}	≠	↓	↓	≠	≠	≠
activated	pS6^{S235/S236}	≠	≠	↓	≠	≠	≠

TABLE 7. Summary representation of dynamic changes of proteins involved in the insulin pathway. Arrows: ↑ indicates an increase, ↓ indicates a decrease. ≠ indicates no changes. Highlighted in red changes observed in WT mice fed with HFD. Highlighted in green similar changes observed in BVR-A^{-/-} mice, to support lack of BVR-A-mediated alterations.

4.8 Sex-associated differences in cognitive tasks after HFD can be observed and are associated with the impairment of brain insulin signalling

Based on the sex differences observed in WT and BVR-A^{-/-} C57Bl/6j mice received either a SD or an HFD for 1 or 8 weeks (Figure 11), we wanted to explore whether these differences reflected on cognitive function. The Y-maze and NOR tests were performed at the end of dietary treatment to assess short-term (spatial, as reference and working memories) and long-term (object recognition) memories, respectively.

First, we tested short-term memory by evaluating spontaneous alternation in the Y-maze test that allow identifying early-onset cognitive deficits. Our results show that female HFD^{+/+} mice are characterized by a significant increase of spontaneous alternation performance after 8 weeks of diet (Figure 24a). No significant changes in female SD^{+/+} mice, were observed (Figure 24a). Conversely, loss of BVR-A is associated with a consistent impairment of short-term memory in both HFD and SD groups.

Next, NOR test is administered to female mice and it allows the evaluation of the mice's ability to explore a novel object, as a sign of good recognition performance. NOR data are collected by measuring two index [discrimination (DI) and preference (PI) index]. Our findings show that DI and PI are not different in HFD^{+/+} mice when comparing 8 weeks vs 1 week (Figure 24b, c). Conversely, a significant increase in both DI and PI measures in SD^{+/+}8 vs SD^{+/+}1, was observed (Figure 24b, c), thus suggesting that HFD regimen greatly impairs the physiological improvement associated with growth and development. Similar outcomes were collected in female BVR-A^{-/-} mice, (Figure 24b, c), supporting the role for BVR-A in the observed alterations.

The same behavioural tests were performed on male mice. Our data indicates that male HFD^{+/+} and SD^{+/+} mice are characterized by no changes of spontaneous alternation measures after 8 weeks of diet (Figure 24d). However, in the absence of BVR-A a significant reduction in SD^{+/+}1 vs SD^{-/-}1 can be observed (Figure 24d). Similar outcomes have been collected with NOR test. DI and PI measures are significantly reduced in SD^{-/-}1 vs SD^{+/+}1 (Figure 24e, f), suggesting that reduced BVR-A is associated with worse cognitive performance also in male.

Intriguingly, despite no significant changes in HFD^{+/+} male mice, where the most significant alterations of BVR-A protein levels and brain insulin signalling were observed, our correlation analyses show positive and significant association between BVR-A levels and outcomes of memory tasks.

A significant correlation between BVR-A levels evaluated in the frontal cortex and both DI and PI were found (Figures 24g, h). No association exist with BVR-A protein levels measured in hippocampus (Figure 24i, j). In other words, HFD^{+/+} mice showing lower BVR-A protein levels in the frontal cortex are those that perform worse in NOR test.

Overall, these data suggest that loss of BVR-A affects cognitive functions in agreement with previous reports.

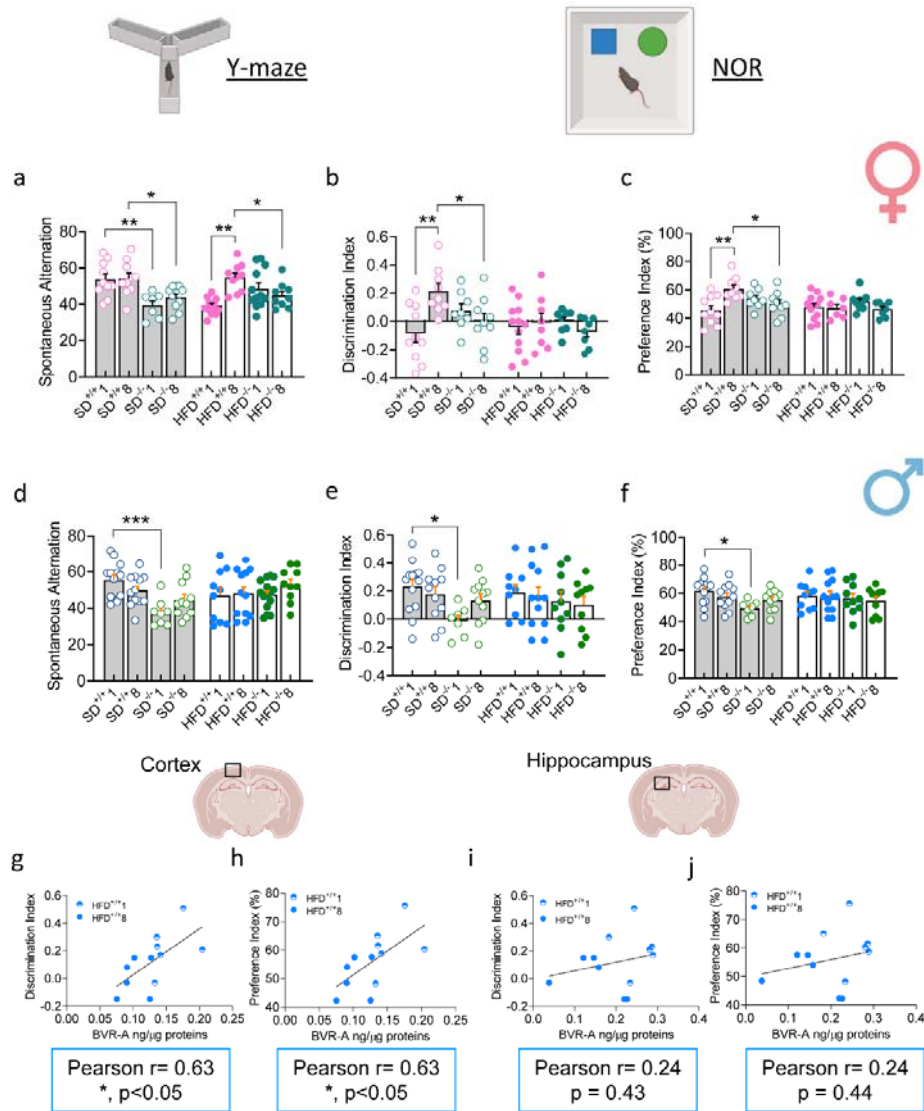


FIGURE 24. Defects in cognitive and memory functions in female and male HFD-fed mice associated with loss of BVR-A. (a and d) Measurement of spontaneous alternation by Y-maze test in female and male mice, respectively. (b and c) Evaluation of the mice's ability to explore a novel object by NOR test in female mice and (e and f) in male mice. Data presented as mean \pm SEM. One-way ANOVA with Bonferroni test: * $p < 0.05$, ** $p < 0.001$, *** $p < 0.0001$. SD^{+/+}: WT mice fed with standard diet; HFD^{+/+}: WT mice fed with standard diet; SD^{-/-}: BVR-A knock-out mice fed with standard diet; HFD^{-/-}: BVR-A knock-out mice fed with standard diet. Significant correlations found between BVR-A levels and NOR test evaluated in the (g and h) frontal cortex and in the (i and j) hippocampus of male mice (Pearson's coefficient).

4.9 HFD is not associated with increased oxidative stress levels in both male and female mice

Oxidative stress (OS) is one of the main factors contributing to cellular alterations, since it promotes disorders of glucose and lipid metabolism and was found to foster the development of brain insulin resistance [80].

Therefore, we were interested in assessing whether loss of BVR-A and the alterations of insulin signalling observed in both female and male mice, were associated with increased OS. To this aim, we evaluated: (i) Protein carbonyls (PC) levels, that are one of the most abundant indices of protein oxidation, and (ii) the amount of 3-nitrotyrosine (3-NT), obtained by protein modification of tyrosine residues in the presence of peroxynitrite [93].

We were able to evaluate OS markers only in SD^{+/+} and HFD^{+/+}, while the analyses for SD^{-/-} and HFD^{-/-} are still ongoing.

Our results show no significant changes in both frontal cortex and hippocampal samples from female mice (Figure 25a, b).

In male mice, we observed a significant increase of PC levels both SD^{+/+}8 vs SD^{+/+}1 and HFD^{+/+}8 vs HFD^{+/+}1 (Figure 25c) along with a significant increase of 3-NT levels in SD^{+/+}8 vs SD^{+/+}1 (Figure 25c), in the frontal cortex. No changes were observed in the hippocampus (Figure 25d).

These data suggest that loss of BVR-A and alterations of brain insulin signalling occur before an augmentation of OS levels under metabolic disorders, thus strengthening our hypothesis about BVR-A as an early marker for bIR.

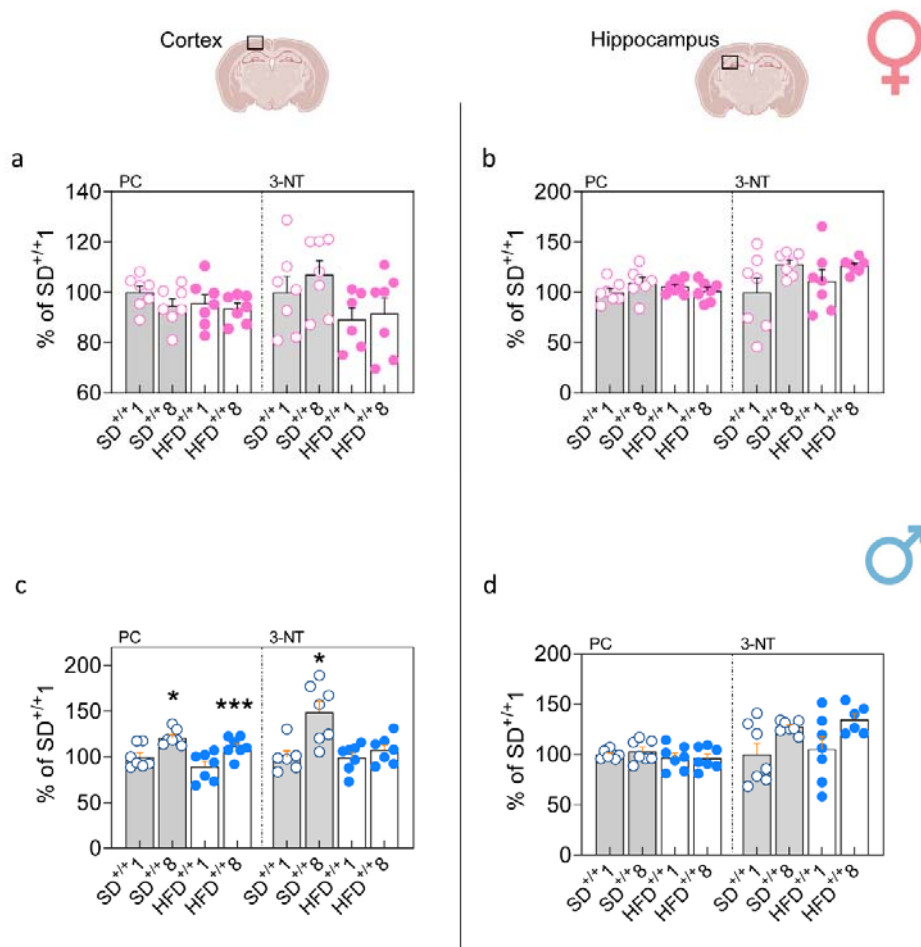


FIGURE 25. Oxidative stress markers levels in C57Bl/6j female and male mice. PC and 3-NT levels were evaluated in (a) the frontal cortex and in (b) the hippocampus of female mice at 1 and 8 weeks of diet. PC and 3-NT levels were evaluated in (c) the frontal cortex and in (d) the hippocampus of male mice at 1 and 8 weeks of diet. Data were expressed as the percentage of SD^{+/+}1 set as 100%. Data are shown as mean ± SEM. One-way ANOVA with Bonferroni test: * p < 0.05, **p < 0.001, ***p < 0.0001. SD^{+/+}: WT mice fed with standard diet; HFD^{+/+}: WT mice fed with standard diet.

5. DISCUSSION AND CONCLUSION

HFD in C57Bl/6j mice is a well-established experimental model of obesity and insulin resistance, almost completely resembling the hallmarks of metabolic syndrome identified in humans [178]. It also impacts on brain function and affects synaptic plasticity, learning, and memory through molecular mechanisms that are still poorly understood [179]. Interestingly, reduced BVR-A protein levels was observed both in neurodegenerative and metabolic disorders and was associated with alterations of insulin signalling that resemble early alterations before overt insulin resistance development [107]. These lines of evidence would suggest that alterations of BVR-A are worth of investigations as potential marker anticipating insulin resistance onset.

In this study, we addressed a fundamental question concerning the BVR-A protein, particularly its role as a central regulator in the insulin signalling pathway. Specifically, we investigated whether BVR-A levels change in response to a HFD and whether these changes serve as an early indicator of insulin resistance development. Considering that we did not completed the analyses on liver samples, we will mainly refer to bIR.

Our findings shed new light on this subject by revealing significant alterations in BVRA protein levels in response to HFD, with notable distinctions based on gender and brain region. What sets our study apart is the comparison we make between WT mice fed an HFD and knock-out mice lacking the BVR-A subjected to the same dietary regimen as the WT group. This approach enabled us to distinguish between changes solely attributable to genotype (observed in $SD^{-/-}$ mice) and those resulting from a combined effect of genotype and diet (observed in $HFD^{-/-}$ mice).

Incorporating these various groups into our experimental protocol provided a unique advantage. It allowed us to determine whether the alterations observed in WT mice following 8 weeks of HFD (HFD^{+/+}) represent early events or occur later in the progression towards bIR. We propose that changes in insulin signalling, occurring before a consistent increase in IRS1 inhibition (a marker of insulin resistance), are early events. Conversely, alterations accompanied by a significant inhibition of IRS1 are characteristic features of established bIR. Furthermore, if similar changes are observed in knock-out mice after 1 or 8 weeks of the diet, it suggests whether these alterations are associated with early or persistent loss of BVR-A, respectively.

In addition, the diet protocol we used, does not make mice obese since the diet is administered for a short time. This represents another advantage to address the aim of our project since we wanted to identify early changes in the sequelae of the events leading to bIR by trying to avoid confounding factors like obesity and related alterations.

Overall, our results indicate that evaluating BVRA may be valuable in understanding the molecular processes involved in insulin signalling alterations and the development of insulin resistance.

The first striking finding of our work relies with the observation that male mice are more susceptible than female mice to the effects of HFD on the brain. Indeed, while HFD promotes similar alterations of peripheral glucose metabolism after both 1 and 8 weeks of diet, when we looked at the brain the situation is quite different. HFD^{+/+} male mice are characterized by reduced BVR-A protein levels both in the frontal cortex and in the hippocampus, while HFD^{+/+} female only in the frontal cortex. These changes are accompanied by alterations of insulin signalling that might be explained

considering BVR-A changes, and demonstrating the existence of 2 phases in the process leading to bIR:

- An early phase in which loss of BVR-A is associated with IRS1 activation, mainly driven by reduced IRS1 inhibition (reduced S636 phosphorylation), rather than increased IRS1 Y phosphorylation.
- A late phase in which reduced BVR-A levels are associated with increased IRS1 inhibition and thus insulin resistance.

Changes observed upstream in the signalling pathway are consistent with the proposed role for BVR-A to be part of a regulatory loop along with IR and IRS1 [24, 107]. Moreover, these changes are accompanied by alterations observed downstream in the pathway that agree with the role for BVR-A to function as scaffold protein [24, 107].

If we look at the results collected in the frontal cortex of HFD^{+/+} male mice it is evident that loss of BVR-A parallels increased IRS1 inhibition along with the hyper-activation of AKT/mTOR axis and the over-inhibition of GSK3 β , that closely resemble to what have been observed in AD brain [167, 168]. These observations clearly recapitulate a condition of bIR. Similar observations in HFD^{-/-} mice after 1 week of diet can be observed, suggesting that loss of BVR-A is a key event in the process and accelerate the development of bIR. Indeed, 1 week of HFD in knock-out mice is enough to promote similar alterations observed after 8 weeks of HFD in WT mice. Moreover, we believe that the observed hyper-activation of AKT and the following over-inhibition of GSK3 β result from feedback mechanisms independent from BVR-A role. In fact, as previously demonstrated loss of BVR-A impairs AKT activation and GSK3 β inhibition [123]. On the other hand, loss of BVR-A leads to mTOR hyperactivation [180], that might be responsible for the increased phosphorylation of AKT and GSK3 β in a

feedback loop [165]. These results suggest that HFD leads to bIR in male mice and that loss of BVR-A greatly contribute to the observed alterations. This concept is further strengthened by the observation that intranasal insulin stimulates the activation of the signalling in SD^{+/+} mice, but not in HFD^{+/+} mice. Intranasal insulin triggers the mTOR hyper-activation HFD^{+/+} mice after 8 weeks of diet. Remarkably, both SD^{-/-} and HFD^{-/-} mice treated with intranasal insulin show an aberrant activation of the signalling in which mTOR hyper-activation seems to be a common feature, further supporting the idea that loss of BVR-A favours the aberrant activation of the insulin signalling by leading to mTOR hyper-activation. These data are consistent with data observed in MCI and AD brains [146, 147].

mTOR hyper-activation does not reflect on an increased activation of one of its conical targets, i.e., P70S6K, in HFD^{+/+} male and similar observations have been collected in HFD^{-/-} mice. This is something interesting and might suggest we identified a new point in which BVR-A could be involved and that deserves further investigations.

Interestingly, if we look at the results collected in the frontal cortex of HFD^{+/+} female mice, the situation is slightly different. In this case, reduced BVR-A protein levels are not associated with a frank inhibition of IRS1 (no changes in the IRS1 Y/S ratio), thus suggesting that bIR has not developed, yet. Despite of that, downstream in the pathway, the hyper-activation of the AKT/mTOR axis is evident, with no significant changes for GSK3 β S9 phosphorylation. As explained in the result section, lack of BVR-A in female mice promotes different effects on mTOR. It appears that mTOR hyper-activation along with over-inhibition of GSK3 β , can be observed in SD^{-/-} mice after 1 week of diet, further supporting the hypothesis that the simple loss of BVR-A might be enough to favour mTOR hyper-activation in female

mice. Within this picture, we can propose that increased pmTOR^{S2448} levels in HFD^{+/+} might be an early response to HFD driven by reduced BVR-A protein levels. As explained for male mice, mTOR hyperactivation might be responsible for a feedback phosphorylation of AKT. This hypothesis is also supported by the observation that PTEN is more activated (less inhibited) in HFD^{+/+} female mice, and thus activation of AKT must result from a different mechanism. Furthermore, AKT hyper-activation is not associated with increased GSK3 β inhibition in HFD^{+/+} female mice, in agreement with the scaffold role for BVR-A [24]. Notwithstanding with that, persistent lack of BVR-A in female mice both in SD^{-/-} and HFD^{-/-} is associated with reduced AKT/mTOR activation that is something in agreement with previous lines of evidence [167]. Our interpretation of these results is that the activation of brain insulin signalling is impaired in frontal cortex of female mice fed with HFD. The observed alterations are early events occurring before a frank IRS1 inhibition. Lack of BVR-A seems to be implicated in the observed alterations considering that similar results have been collected in knock-out mice. This scenario could be interpreted as a condition of insulin resistance considering that intranasal insulin administration in HFD^{+/+} female mice do not promote the activation of AKT, neither those of AKT downstream targets. Similar results can be observed in knock-out mice, thus suggesting that lack of BVR-A greatly affect the response to insulin even in the absence of an over IRS1 inhibition. Strikingly, we observed that HFD^{-/-} female mice show an aberrant activation of AKT/mTOR after 8 weeks of diet, as observed in male, supporting the hypothesis that loss of BVR-A promotes mTOR hyper-activation in response to insulin.

Also in female mice, mTOR hyper-activation does not reflect on an increased activation of P70S6K, supporting our hypothesis that BVR-A could

be involved in the physiological mTOR-mediated phosphorylation of P70S6K.

Sex-differences observed in the frontal cortex can be also noticed in the hippocampus. However, it seems that the alterations of the signalling occur later in the hippocampus than the frontal cortex, particularly in female mice. Indeed, HFD^{+/+} female mice do not show reduced BVR-A protein levels in the hippocampus, neither an increased inhibition of IRS1 or the aberrant activation of the AKT/mTOR axis. In these mice, intranasal insulin administration promotes a significant activation of AKT and downstream targets both in SD^{+/+} and HFD^{+/+}, suggesting that the signalling is still preserved from alterations.

This hypothesis is further corroborated by measures of cognitive functions. The frontal cortex has been associated with working memory, attention, and executive control [181], and recent data from Kar and DiCarlo (2021) [182] place the frontal cortex at the top of the hierarchy of ventral stream visual areas involved in object recognition. Indeed, they show that frontal cortex inputs improve both behavioural performance and neural encoding for objects when recognition is difficult. Our results agree with this paradigm, since we observed that major molecular alterations occur in the frontal cortex and are associated with worse outcome in NOR, both in female and male mice.

Overall, our results suggest that loss of BVR-A is among the first events that can be observed during the development of bIR. Reduced BVR-A protein levels produce different effects on insulin signalling considering that BVR-A is a crucial player at different levels both upstream and downstream in the pathway. Based on BVR-A alterations, two phases in the development of bIR can be identified: an early phase in which loss of BVR-A is not

associated with IRS1 inhibition and a late phase in which persistent loss of BVR-A is associated with IRS1 inhibition. The novelty of our study relies with the fact that during the early phase the signalling does not respond properly to insulin, thus suggesting that we are already in a condition of bIR. Findings presented in the current project also resemble what we previously observed in the brain from a mouse model of Alzheimer's disease [24, 183], showing two age-associated phases: an early phase characterized by reduced BVR-A protein levels and activation together with the hyper-activation of the IR/IRS1 axis; and a late phase where the persistent impairment of BVRA is associated with inhibition of IRS1 and the onset of brain insulin resistance [24, 183]. Indeed, we proposed that the hyper-activation of IRS1 represents a signal triggering the activation of feed-back mechanisms aimed to turn-off IRS1 hyper-activity and thus leading to brain insulin resistance [24, 183]. The existence of these two phases is supported by *in vitro* studies showing that insulin treatment (100 μ M) increased glucose uptake in the short period (after 15-30 min) [117], while insulin led to insulin resistance development after 2 hours [24, 183], in HEK cells knocked-down for BVR-A.

Another aim of our study, was to clarify whether loss of BVR-A mediates the development of insulin resistance only in the brain or it is a shared molecular mechanism among tissues. This would be of great interest in searching for new potential biomarkers candidates to identify people at risk to develop metabolic disorders, i.e., obesity and diabetes.

Findings from animal models of obesity showed that hepatic or adipocyte-specific deletion of BVRA hampers insulin cascade and is associated with impaired glucose metabolism [184-187]. In these mice, high-fat diet regimen leads to hyper-insulinemia but reduced activation of the AKT and MAPK pathways both in the liver and in the adipocytes [184-187]. Similarly,

reduced BVRA protein levels prompted the development of brain insulin resistance in animal models of aging or neurodegenerative diseases [24, 101, 188]. Conversely, improving BVRA functions ameliorated the insulin signalling activation, by fostering the IR/AKT/GSK3 β axis, which results in increased glucose uptake in diabetic mice [184] and in the brain [148, 189]. Results collected in animal models of metabolic disorders were further strengthened by our group in humans. Recent studies from our group have shown that a consistent reduction of BVRA protein levels is present in individuals with obesity and type-2 diabetes (T2D) [25, 190, 191]. Reduction in BVRA protein levels was linked to abnormal activation of the IR/IRS1/AKT/GSK3 β /GLUT4 pathway, which was related to poor glucometabolic control, as well as the presence of metabolic syndrome, liver steatosis, and inflammation of visceral adipose tissue in individuals with obesity and T2D [25, 190-192].

In our study, we have evaluated liver samples exclusively from female mice, with ongoing analyses of samples from male mice. Our results clearly show that BVR-A protein levels are reduced in the liver following the HFD. However, when we examined liver insulin signalling, we found that changes observed in HFD^{+/+}, are similar to those observed in SD^{-/-} vs SD^{+/+}, but also in SD^{+/+} mice as function of age (1 vs 8 weeks). The sole differences that discriminate changes in SD^{+/+} mice as function of age, and the alterations observed in HFD^{+/+} and SD^{-/-} are represented by BVR-A levels and circulating insulin. Notably, SD^{+/+} mice show increased insulin levels with age that appears to be part of the physiological process associated with growth [193]. This phenomenon is not observed in SD^{-/-} mice, suggesting that reduced IRS1 inhibition in these mice, might represent a “protective” mechanism to counteract the failure of insulin to increase. In some way, this

mechanism seems successful in $SD^{-/-}$, given that no alterations in IPGTT were observed. The absence of BVR-A likely promotes the activation of different mechanisms than insulin signalling, ultimately favouring glucose uptake and metabolism in the liver. Studies in our lab are ongoing to decipher such mechanisms. Conversely, loss of BVR-A is associated with no changes in circulating insulin along with impaired IPGTT in $HFD^{+/+}$ mice. In this case, loss of BVR-A is insufficient to prevent the worsening of glucose metabolism, suggesting that HFD outweigh the effects of reduced BVR-A. From this intricate picture, it emerges that reduced BVR-A protein levels are among the first molecular events that might be identified in the development of insulin resistance. As observed in the brain, loss of BVR-A precedes IRS1 inhibition. Finally, we acknowledge that $HFD^{-/-}$ mice exhibit similar changes to those observed in $HFD^{+/+}$ mice, except for higher circulating insulin levels, which may suggest impaired insulin clearance.

Liver participates in insulin clearance, that is decreased in conditions of insulin resistance [194-196]. Moreover, insulin clearance is associated to obesity and hepatic fat accumulation [197, 198]. The mechanisms that regulate hepatic insulin clearance are still unknown. Insulin clearance is not a static process since lower clearance rates are observed in postprandial compared to fasting state, and it is influenced by several factors, like nutrient intake [199] and some hormones [200, 201]. Interestingly, increased BMI along with increased circulating insulin in $HFD^{-/-}$ mice was observed, thus suggesting that persistent loss of BVR-A might contribute to liver functions and fat accumulation.

Results collected in liver are in line with our previous findings in both obese and T2D subjects in which we observed consistently reduced BVRA levels in peripheral blood mononuclear cell (PBMC) under basal conditions (following

overnight fasting), with respect to matched controls [25, 190, 191]. In obese subjects showing reduced insulin sensitivity with respect to controls, decreased BVRA levels were associated with a basal hyper-activation of IRS1 and to a less extent of AKT and AS160 [25] – this pathway is known to promote GLUT4 translocation on the plasma membrane to increase glucose uptake, among the others [32]. Intriguingly, IRS1 hyper-activation in PBMC isolated from obese individuals mainly results from reduced inhibitory phosphorylation [25]. Hence, reduced BVRA levels in obese subjects likely represent a compensatory mechanism to foster insulin signalling activation in the context of reduced insulin sensitivity.

Together, these results suggest that peripheral insulin concentrations depend not only by the pancreas (as secretory organ) but also by the liver (insulin modulator), and mostly important sex-differences exist and needs to be taken into consideration.

6. REFERENCES

1. Breijyeh, Z. and R. Karaman, *Comprehensive Review on Alzheimer's Disease: Causes and Treatment*. *Molecules*, 2020. **25**(24).
2. De-Paula, V.J., et al., *Alzheimer's disease*. *Subcell Biochem*, 2012. **65**: p. 329-52.
3. Chen, G.F., et al., *Amyloid beta: structure, biology and structure-based therapeutic development*. *Acta Pharmacol Sin*, 2017. **38**(9): p. 1205-1235.
4. Braak, H. and E. Braak, *Neuropathological staging of Alzheimer-related changes*. *Acta Neuropathol*, 1991. **82**(4): p. 239-59.
5. Serrano-Pozo, A., et al., *Neuropathological alterations in Alzheimer disease*. *Cold Spring Harb Perspect Med*, 2011. **1**(1): p. a006189.
6. Singh, S.K., et al., *Overview of Alzheimer's Disease and Some Therapeutic Approaches Targeting Abeta by Using Several Synthetic and Herbal Compounds*. *Oxid Med Cell Longev*, 2016. **2016**: p. 7361613.
7. Tarawneh, R., et al., *Diagnostic and Prognostic Utility of the Synaptic Marker Neurogranin in Alzheimer Disease*. *JAMA Neurol*, 2016. **73**(5): p. 561-71.
8. Mantzavinos, V. and A. Alexiou, *Biomarkers for Alzheimer's Disease Diagnosis*. *Curr Alzheimer Res*, 2017. **14**(11): p. 1149-1154.
9. Van Cauwenberghe, C., C. Van Broeckhoven, and K. Sleegers, *The genetic landscape of Alzheimer disease: clinical implications and perspectives*. *Genet Med*, 2016. **18**(5): p. 421-30.
10. Corder, E.H., et al., *Gene dose of apolipoprotein E type 4 allele and the risk of Alzheimer's disease in late onset families*. *Science*, 1993. **261**(5123): p. 921-3.
11. Saunders, A.M., et al., *Apolipoprotein E epsilon 4 allele distributions in late-onset Alzheimer's disease and in other amyloid-forming diseases*. *Lancet*, 1993. **342**(8873): p. 710-1.
12. Farrer, L.A., et al., *Effects of age, sex, and ethnicity on the association between apolipoprotein E genotype and Alzheimer disease. A meta-analysis. APOE and Alzheimer Disease Meta Analysis Consortium*. *JAMA*, 1997. **278**(16): p. 1349-56.
13. Alzheimer's, A., *2014 Alzheimer's disease facts and figures*. *Alzheimers Dement*, 2014. **10**(2): p. e47-92.
14. *2023 Alzheimer's disease facts and figures*. *Alzheimers Dement*, 2023. **19**(4): p. 1598-1695.
15. Scheltens, P., et al., *Alzheimer's disease*. *Lancet*, 2021. **397**(10284): p. 1577-1590.
16. Sullivan, J.L., et al., *Collaborative capacity and patient-centered care in the Veterans' Health Administration Community Living Centers*. *Int J Care Coord*, 2019. **22**(2): p. 90-99.
17. McKhann, G.M., et al., *The diagnosis of dementia due to Alzheimer's disease: recommendations from the National Institute on Aging-Alzheimer's Association workgroups on diagnostic guidelines for Alzheimer's disease*. *Alzheimers Dement*, 2011. **7**(3): p. 263-9.
18. Sperling, R.A., et al., *Toward defining the preclinical stages of Alzheimer's disease: recommendations from the National Institute on Aging-Alzheimer's Association*

- workgroups on diagnostic guidelines for Alzheimer's disease. *Alzheimers Dement*, 2011. **7**(3): p. 280-92.
19. Dubois, B., et al., *Preclinical Alzheimer's disease: Definition, natural history, and diagnostic criteria*. *Alzheimers Dement*, 2016. **12**(3): p. 292-323.
 20. Kumar, A., et al., *Alzheimer Disease*, in *StatPearls*. 2023: Treasure Island (FL).
 21. Wattmo, C., L. Minthon, and A.K. Wallin, *Mild versus moderate stages of Alzheimer's disease: three-year outcomes in a routine clinical setting of cholinesterase inhibitor therapy*. *Alzheimers Res Ther*, 2016. **8**: p. 7.
 22. Apostolova, L.G., *Alzheimer Disease*. Continuum (Minneap Minn), 2016. **22**(2 Dementia): p. 419-34.
 23. Livingston, G., et al., *Dementia prevention, intervention, and care: 2020 report of the Lancet Commission*. *Lancet*, 2020. **396**(10248): p. 413-446.
 24. Barone, E., et al., *Impairment of biliverdin reductase-A promotes brain insulin resistance in Alzheimer disease: A new paradigm*. *Free Radic Biol Med*, 2016. **91**: p. 127-42.
 25. Cimini, F.A., et al., *Reduced biliverdin reductase-A levels are associated with early alterations of insulin signaling in obesity*. *Biochim Biophys Acta Mol Basis Dis*, 2019. **1865**(6): p. 1490-1501.
 26. Sanger, F., *Chemistry of insulin*. *Br Med Bull*, 1960. **16**: p. 183-8.
 27. Poutout, V., et al., *Regulation of the insulin gene by glucose and fatty acids*. *J Nutr*, 2006. **136**(4): p. 873-6.
 28. Lee, J. and P.F. Pilch, *The insulin receptor: structure, function, and signaling*. *Am J Physiol*, 1994. **266**(2 Pt 1): p. C319-34.
 29. Wang, J., et al., *Regulation of insulin preRNA splicing by glucose*. *Proc Natl Acad Sci U S A*, 1997. **94**(9): p. 4360-5.
 30. Andrali, S.S., et al., *Glucose regulation of insulin gene expression in pancreatic beta-cells*. *Biochem J*, 2008. **415**(1): p. 1-10.
 31. Hutton, J.C., *Insulin secretory granule biogenesis and the proinsulin-processing endopeptidases*. *Diabetologia*, 1994. **37 Suppl 2**: p. S48-56.
 32. Haeusler, R.A., T.E. McGraw, and D. Accili, *Biochemical and cellular properties of insulin receptor signalling*. *Nat Rev Mol Cell Biol*, 2018. **19**(1): p. 31-44.
 33. Dimitriadis, G., et al., *Insulin effects in muscle and adipose tissue*. *Diabetes Res Clin Pract*, 2011. **93 Suppl 1**: p. S52-9.
 34. Hom, F.G., C.J. Goodner, and M.A. Berrie, *A [³H]2-deoxyglucose method for comparing rates of glucose metabolism and insulin responses among rat tissues in vivo. Validation of the model and the absence of an insulin effect on brain*. *Diabetes*, 1984. **33**(2): p. 141-52.
 35. Hasselbalch, S.G., et al., *No effect of insulin on glucose blood-brain barrier transport and cerebral metabolism in humans*. *Diabetes*, 1999. **48**(10): p. 1915-21.
 36. Havrankova, J., et al., *Identification of insulin in rat brain*. *Proc Natl Acad Sci U S A*, 1978. **75**(11): p. 5737-41.
 37. Ramnanan, C.J., et al., *Interaction between the central and peripheral effects of insulin in controlling hepatic glucose metabolism in the conscious dog*. *Diabetes*, 2013. **62**(1): p. 74-84.
 38. Rhea, E.M. and W.A. Banks, *Role of the Blood-Brain Barrier in Central Nervous System Insulin Resistance*. *Front Neurosci*, 2019. **13**: p. 521.

39. Benedict, C., et al., *Intranasal insulin to improve memory function in humans*. Neuroendocrinology, 2007. **86**(2): p. 136-42.
40. Taouis, M. and I. Torres-Aleman, *Editorial: Insulin and The Brain*. Front Endocrinol (Lausanne), 2019. **10**: p. 299.
41. Craft, S. and G.S. Watson, *Insulin and neurodegenerative disease: shared and specific mechanisms*. Lancet Neurol, 2004. **3**(3): p. 169-78.
42. Petersen, M.C. and G.I. Shulman, *Mechanisms of Insulin Action and Insulin Resistance*. Physiol Rev, 2018. **98**(4): p. 2133-2223.
43. Andersen, A.S., F.C. Wiberg, and T. Kjeldsen, *Localization of specific amino acids contributing to insulin specificity of the insulin receptor*. Ann N Y Acad Sci, 1995. **766**: p. 466-8.
44. Whittaker, J. and L. Whittaker, *Characterization of the functional insulin binding epitopes of the full-length insulin receptor*. J Biol Chem, 2005. **280**(22): p. 20932-6.
45. Seino, S., et al., *Structure of the human insulin receptor gene and characterization of its promoter*. Proc Natl Acad Sci U S A, 1989. **86**(1): p. 114-8.
46. Seino, S. and G.I. Bell, *Alternative splicing of human insulin receptor messenger RNA*. Biochem Biophys Res Commun, 1989. **159**(1): p. 312-6.
47. Knudsen, L., P. De Meyts, and V.V. Kiselyov, *Insight into the molecular basis for the kinetic differences between the two insulin receptor isoforms*. Biochem J, 2011. **440**(3): p. 397-403.
48. Belfiore, A., et al., *Insulin receptor isoforms and insulin receptor/insulin-like growth factor receptor hybrids in physiology and disease*. Endocr Rev, 2009. **30**(6): p. 586-623.
49. Taniguchi, C.M., B. Emanuelli, and C.R. Kahn, *Critical nodes in signalling pathways: insights into insulin action*. Nat Rev Mol Cell Biol, 2006. **7**(2): p. 85-96.
50. Czech, M.P., *The nature and regulation of the insulin receptor: structure and function*. Annu Rev Physiol, 1985. **47**: p. 357-81.
51. Le Marchand-Brustel, Y., *Molecular mechanisms of insulin action in normal and insulin-resistant states*. Exp Clin Endocrinol Diabetes, 1999. **107**(2): p. 126-32.
52. Hubbard, S.R., *The insulin receptor: both a prototypical and atypical receptor tyrosine kinase*. Cold Spring Harb Perspect Biol, 2013. **5**(3): p. a008946.
53. Riehle, C. and E.D. Abel, *Insulin Signaling and Heart Failure*. Circ Res, 2016. **118**(7): p. 1151-69.
54. Grillo, C.A., et al., *Insulin-stimulated translocation of GLUT4 to the plasma membrane in rat hippocampus is PI3-kinase dependent*. Brain Res, 2009. **1296**: p. 35-45.
55. Condorelli, F., et al., *Caspase cleavage enhances the apoptosis-inducing effects of BAD*. Mol Cell Biol, 2001. **21**(9): p. 3025-36.
56. Halestrap, A.P., et al., *Mitochondria and cell death*. Biochem Soc Trans, 2000. **28**(2): p. 170-7.
57. Sedzikowska, A. and L. Szablewski, *Insulin and Insulin Resistance in Alzheimer's Disease*. Int J Mol Sci, 2021. **22**(18).
58. Kleinert, M., et al., *Animal models of obesity and diabetes mellitus*. Nat Rev Endocrinol, 2018. **14**(3): p. 140-162.

59. Tanti, J.F. and J. Jager, *Cellular mechanisms of insulin resistance: role of stress-regulated serine kinases and insulin receptor substrates (IRS) serine phosphorylation*. *Curr Opin Pharmacol*, 2009. **9**(6): p. 753-62.
60. Guo, S., *Insulin signaling, resistance, and the metabolic syndrome: insights from mouse models into disease mechanisms*. *J Endocrinol*, 2014. **220**(2): p. T1-T23.
61. Reaven, G.M., *The insulin resistance syndrome: definition and dietary approaches to treatment*. *Annu Rev Nutr*, 2005. **25**: p. 391-406.
62. Blazquez, E., et al., *Insulin in the brain: its pathophysiological implications for States related with central insulin resistance, type 2 diabetes and Alzheimer's disease*. *Front Endocrinol (Lausanne)*, 2014. **5**: p. 161.
63. Ferreira, L.S.S., et al., *Insulin Resistance in Alzheimer's Disease*. *Front Neurosci*, 2018. **12**: p. 830.
64. Cholerton, B., L.D. Baker, and S. Craft, *Insulin, cognition, and dementia*. *Eur J Pharmacol*, 2013. **719**(1-3): p. 170-179.
65. Verdile, G., S.J. Fuller, and R.N. Martins, *The role of type 2 diabetes in neurodegeneration*. *Neurobiol Dis*, 2015. **84**: p. 22-38.
66. Burillo, J., et al., *Insulin Resistance and Diabetes Mellitus in Alzheimer's Disease*. *Cells*, 2021. **10**(5).
67. Niswender, K.D., et al., *Insulin activation of phosphatidylinositol 3-kinase in the hypothalamic arcuate nucleus: a key mediator of insulin-induced anorexia*. *Diabetes*, 2003. **52**(2): p. 227-31.
68. Steen, E., et al., *Impaired insulin and insulin-like growth factor expression and signaling mechanisms in Alzheimer's disease--is this type 3 diabetes?* *J Alzheimers Dis*, 2005. **7**(1): p. 63-80.
69. Rivera, E.J., et al., *Insulin and insulin-like growth factor expression and function deteriorate with progression of Alzheimer's disease: link to brain reductions in acetylcholine*. *J Alzheimers Dis*, 2005. **8**(3): p. 247-68.
70. Talbot, K. and H.Y. Wang, *The nature, significance, and glucagon-like peptide-1 analog treatment of brain insulin resistance in Alzheimer's disease*. *Alzheimers Dement*, 2014. **10**(1 Suppl): p. S12-25.
71. Moloney, A.M., et al., *Defects in IGF-1 receptor, insulin receptor and IRS-1/2 in Alzheimer's disease indicate possible resistance to IGF-1 and insulin signalling*. *Neurobiol Aging*, 2010. **31**(2): p. 224-43.
72. Liu, Y., et al., *Deficient brain insulin signalling pathway in Alzheimer's disease and diabetes*. *J Pathol*, 2011. **225**(1): p. 54-62.
73. Bomfim, T.R., et al., *An anti-diabetes agent protects the mouse brain from defective insulin signaling caused by Alzheimer's disease-associated Abeta oligomers*. *J Clin Invest*, 2012. **122**(4): p. 1339-53.
74. Talbot, K., et al., *Demonstrated brain insulin resistance in Alzheimer's disease patients is associated with IGF-1 resistance, IRS-1 dysregulation, and cognitive decline*. *J Clin Invest*, 2012. **122**(4): p. 1316-38.
75. Lopes, J.P., C.R. Oliveira, and P. Agostinho, *Role of cyclin-dependent kinase 5 in the neurodegenerative process triggered by amyloid-Beta and prion peptides: implications for Alzheimer's disease and prion-related encephalopathies*. *Cell Mol Neurobiol*, 2007. **27**(7): p. 943-57.

76. Weingarten, M.D., et al., *A protein factor essential for microtubule assembly*. Proc Natl Acad Sci U S A, 1975. **72**(5): p. 1858-62.
77. Sergeant, N., et al., *Biochemistry of Tau in Alzheimer's disease and related neurological disorders*. Expert Rev Proteomics, 2008. **5**(2): p. 207-24.
78. Schubert, M., et al., *Insulin receptor substrate-2 deficiency impairs brain growth and promotes tau phosphorylation*. J Neurosci, 2003. **23**(18): p. 7084-92.
79. Balaraman, Y., et al., *Glycogen synthase kinase 3beta and Alzheimer's disease: pathophysiological and therapeutic significance*. Cell Mol Life Sci, 2006. **63**(11): p. 1226-35.
80. Barone, E., et al., *The interplay among oxidative stress, brain insulin resistance and AMPK dysfunction contribute to neurodegeneration in type 2 diabetes and Alzheimer disease*. Free Radic Biol Med, 2021. **176**: p. 16-33.
81. Goldstein, B.J., K. Mahadev, and X. Wu, *Redox paradox: insulin action is facilitated by insulin-stimulated reactive oxygen species with multiple potential signaling targets*. Diabetes, 2005. **54**(2): p. 311-21.
82. Storzhevykh, T.P., et al., *Mitochondrial respiratory chain is involved in insulin-stimulated hydrogen peroxide production and plays an integral role in insulin receptor autophosphorylation in neurons*. BMC Neurosci, 2007. **8**: p. 84.
83. Sultana, R. and D.A. Butterfield, *Role of oxidative stress in the progression of Alzheimer's disease*. J Alzheimers Dis, 2010. **19**(1): p. 341-53.
84. Castilla-Cortazar, I., et al., *Hepatoprotection and neuroprotection induced by low doses of IGF-II in aging rats*. J Transl Med, 2011. **9**: p. 103.
85. Maiese, K., Z.Z. Chong, and Y.C. Shang, *Mechanistic insights into diabetes mellitus and oxidative stress*. Curr Med Chem, 2007. **14**(16): p. 1729-38.
86. Carvalho, C., et al., *Metabolic alterations induced by sucrose intake and Alzheimer's disease promote similar brain mitochondrial abnormalities*. Diabetes, 2012. **61**(5): p. 1234-42.
87. Butterfield, D.A., M.L. Bader Lange, and R. Sultana, *Involvements of the lipid peroxidation product, HNE, in the pathogenesis and progression of Alzheimer's disease*. Biochim Biophys Acta, 2010. **1801**(8): p. 924-9.
88. Butterfield, D.A., *Oxidative stress in neurodegenerative disorders*. Antioxid Redox Signal, 2006. **8**(11-12): p. 1971-3.
89. Markesbery, W.R. and M.A. Lovell, *Four-hydroxynonenal, a product of lipid peroxidation, is increased in the brain in Alzheimer's disease*. Neurobiol Aging, 1998. **19**(1): p. 33-6.
90. Reed, T.T., et al., *Proteomic identification of HNE-bound proteins in early Alzheimer disease: Insights into the role of lipid peroxidation in the progression of AD*. Brain Res, 2009. **1274**: p. 66-76.
91. Levine, R.L., *Carbonyl modified proteins in cellular regulation, aging, and disease*. Free Radic Biol Med, 2002. **32**(9): p. 790-6.
92. Suzuki, Y.J., M. Carini, and D.A. Butterfield, *Protein carbonylation*. Antioxid Redox Signal, 2010. **12**(3): p. 323-5.
93. Butterfield, D.A., et al., *Elevated levels of 3-nitrotyrosine in brain from subjects with amnesic mild cognitive impairment: implications for the role of nitration in the progression of Alzheimer's disease*. Brain Res, 2007. **1148**: p. 243-8.

94. Wang, W., et al., *Mitochondria dysfunction in the pathogenesis of Alzheimer's disease: recent advances*. Mol Neurodegener, 2020. **15**(1): p. 30.
95. Moreira, P.I., *Alzheimer's disease and diabetes: an integrative view of the role of mitochondria, oxidative stress, and insulin*. J Alzheimers Dis, 2012. **30 Suppl 2**: p. S199-215.
96. Reddy, V.P., et al., *Oxidative stress in diabetes and Alzheimer's disease*. J Alzheimers Dis, 2009. **16**(4): p. 763-74.
97. Gerbitz, K.D., K. Gempel, and D. Brdiczka, *Mitochondria and diabetes. Genetic, biochemical, and clinical implications of the cellular energy circuit*. Diabetes, 1996. **45**(2): p. 113-26.
98. Moreira, P.I., et al., *Brain mitochondrial dysfunction as a link between Alzheimer's disease and diabetes*. J Neurol Sci, 2007. **257**(1-2): p. 206-14.
99. de la Monte, S.M., *Insulin resistance and Alzheimer's disease*. BMB Rep, 2009. **42**(8): p. 475-81.
100. Neumann, K.F., et al., *Insulin resistance and Alzheimer's disease: molecular links & clinical implications*. Curr Alzheimer Res, 2008. **5**(5): p. 438-47.
101. Lanzillotta, C., et al., *Insulin resistance, oxidative stress and mitochondrial defects in Ts65dn mice brain: A harmful synergistic path in down syndrome*. Free Radic Biol Med, 2021. **165**: p. 152-170.
102. Singleton, J.W. and L. Laster, *Biliverdin reductase of guinea pig liver*. J Biol Chem, 1965. **240**(12): p. 4780-9.
103. Kutty, R.K. and M.D. Maines, *Purification and characterization of biliverdin reductase from rat liver*. J Biol Chem, 1981. **256**(8): p. 3956-62.
104. Maines, M.D. and G.M. Trakshel, *Purification and characterization of human biliverdin reductase*. Arch Biochem Biophys, 1993. **300**(1): p. 320-6.
105. Wegiel, B. and L.E. Otterbein, *Go green: the anti-inflammatory effects of biliverdin reductase*. Front Pharmacol, 2012. **3**: p. 47.
106. Barone, E., et al., *The Janus face of the heme oxygenase/biliverdin reductase system in Alzheimer disease: it's time for reconciliation*. Neurobiol Dis, 2014. **62**: p. 144-59.
107. Cimini, F.A., et al., *Role of Biliverdin Reductase A in the Regulation of Insulin Signaling in Metabolic and Neurodegenerative Diseases: An Update*. Int J Mol Sci, 2022. **23**(10).
108. Han, R., J. Liang, and B. Zhou, *Glucose Metabolic Dysfunction in Neurodegenerative Diseases-New Mechanistic Insights and the Potential of Hypoxia as a Prospective Therapy Targeting Metabolic Reprogramming*. Int J Mol Sci, 2021. **22**(11).
109. Zhang, X., N. Alshakhshir, and L. Zhao, *Glycolytic Metabolism, Brain Resilience, and Alzheimer's Disease*. Front Neurosci, 2021. **15**: p. 662242.
110. Maines, M.D., *Overview of heme degradation pathway*. Curr Protoc Toxicol, 2001. **Chapter 9**: p. Unit 9 1.
111. Vasavda, C., et al., *Bilirubin Links Heme Metabolism to Neuroprotection by Scavenging Superoxide*. Cell Chem Biol, 2019. **26**(10): p. 1450-1460 e7.
112. Canesin, G., et al., *Heme-Derived Metabolic Signals Dictate Immune Responses*. Front Immunol, 2020. **11**: p. 66.
113. Gibbs, P.E., T. Miralem, and M.D. Maines, *Biliverdin reductase: a target for cancer therapy?* Front Pharmacol, 2015. **6**: p. 119.

114. O'Brien, L., et al., *Biliverdin reductase isozymes in metabolism*. Trends Endocrinol Metab, 2015. **26**(4): p. 212-20.
115. Hunter, T. and J.A. Cooper, *Protein-tyrosine kinases*. Annu Rev Biochem, 1985. **54**: p. 897-930.
116. Pawson, T. and J.D. Scott, *Protein phosphorylation in signaling--50 years and counting*. Trends Biochem Sci, 2005. **30**(6): p. 286-90.
117. Lerner-Marmarosh, N., et al., *Human biliverdin reductase: a member of the insulin receptor substrate family with serine/threonine/tyrosine kinase activity*. Proc Natl Acad Sci U S A, 2005. **102**(20): p. 7109-14.
118. Gibbs, P.E., et al., *Human biliverdin reductase-based peptides activate and inhibit glucose uptake through direct interaction with the kinase domain of insulin receptor*. FASEB J, 2014. **28**(6): p. 2478-91.
119. Lucke-Wold, B.P., et al., *Common mechanisms of Alzheimer's disease and ischemic stroke: the role of protein kinase C in the progression of age-related neurodegeneration*. J Alzheimers Dis, 2015. **43**(3): p. 711-24.
120. Ahmad, Z., M. Salim, and M.D. Maines, *Human biliverdin reductase is a leucine zipper-like DNA-binding protein and functions in transcriptional activation of heme oxygenase-1 by oxidative stress*. J Biol Chem, 2002. **277**(11): p. 9226-32.
121. Kawamoto, S., et al., *Heme oxygenase-1 induction enhances cell survival and restores contractility to unvascularized three-dimensional adult cardiomyocyte grafts implanted in vivo*. Tissue Eng Part A, 2011. **17**(11-12): p. 1605-14.
122. Kapitulnik, J. and M.D. Maines, *Pleiotropic functions of biliverdin reductase: cellular signaling and generation of cytoprotective and cytotoxic bilirubin*. Trends Pharmacol Sci, 2009. **30**(3): p. 129-37.
123. Sharma, N., et al., *Loss of biliverdin reductase-A favors Tau hyper-phosphorylation in Alzheimer's disease*. Neurobiol Dis, 2019. **125**: p. 176-189.
124. Lerner-Marmarosh, N., et al., *Human biliverdin reductase is an ERK activator; hBVR is an ERK nuclear transporter and is required for MAPK signaling*. Proc Natl Acad Sci U S A, 2008. **105**(19): p. 6870-5.
125. Gibbs, P.E., et al., *Formation of ternary complex of human biliverdin reductase-protein kinase Cdelta-ERK2 protein is essential for ERK2-mediated activation of Elk1 protein, nuclear factor-kappaB, and inducible nitric-oxidase synthase (iNOS)*. J Biol Chem, 2012. **287**(2): p. 1066-79.
126. Rich-Edwards, J.W., et al., *Sex and Gender Differences Research Design for Basic, Clinical, and Population Studies: Essentials for Investigators*. Endocr Rev, 2018. **39**(4): p. 424-439.
127. Tramunt, B., et al., *Sex differences in metabolic regulation and diabetes susceptibility*. Diabetologia, 2020. **63**(3): p. 453-461.
128. Mauvais-Jarvis, F., *Role of Sex Steroids in beta Cell Function, Growth, and Survival*. Trends Endocrinol Metab, 2016. **27**(12): p. 844-855.
129. Yang, J.T., et al., *Sex Differences in Neuropathology and Cognitive Behavior in APP/PS1/tau Triple-Transgenic Mouse Model of Alzheimer's Disease*. Neurosci Bull, 2018. **34**(5): p. 736-746.
130. Vina, J. and A. Lloret, *Why women have more Alzheimer's disease than men: gender and mitochondrial toxicity of amyloid-beta peptide*. J Alzheimers Dis, 2010. **20 Suppl 2**: p. S527-33.

131. Alzheimer's, A., *2013 Alzheimer's disease facts and figures*. *Alzheimers Dement*, 2013. **9**(2): p. 208-45.
132. Zhang, Z., *Gender differentials in cognitive impairment and decline of the oldest old in China*. *J Gerontol B Psychol Sci Soc Sci*, 2006. **61**(2): p. S107-15.
133. Markowska, A.L., *Sex dimorphisms in the rate of age-related decline in spatial memory: relevance to alterations in the estrous cycle*. *J Neurosci*, 1999. **19**(18): p. 8122-33.
134. Frick, K.M., et al., *Reference memory, anxiety and estrous cyclicity in C57BL/6NIA mice are affected by age and sex*. *Neuroscience*, 2000. **95**(1): p. 293-307.
135. Benice, T.S., et al., *Sex-differences in age-related cognitive decline in C57BL/6J mice associated with increased brain microtubule-associated protein 2 and synaptophysin immunoreactivity*. *Neuroscience*, 2006. **137**(2): p. 413-23.
136. Zhao, L., et al., *Sex differences in metabolic aging of the brain: insights into female susceptibility to Alzheimer's disease*. *Neurobiol Aging*, 2016. **42**: p. 69-79.
137. Li, R. and M. Singh, *Sex differences in cognitive impairment and Alzheimer's disease*. *Front Neuroendocrinol*, 2014. **35**(3): p. 385-403.
138. Long, J., et al., *New evidence of mitochondria dysfunction in the female Alzheimer's disease brain: deficiency of estrogen receptor-beta*. *J Alzheimers Dis*, 2012. **30**(3): p. 545-58.
139. Mukai, H., et al., *Modulation of synaptic plasticity by brain estrogen in the hippocampus*. *Biochim Biophys Acta*, 2010. **1800**(10): p. 1030-44.
140. Hojo, Y., et al., *Hippocampal synthesis of sex steroids and corticosteroids: essential for modulation of synaptic plasticity*. *Front Endocrinol (Lausanne)*, 2011. **2**: p. 43.
141. Fester, L., et al., *Estrogen-regulated synaptogenesis in the hippocampus: sexual dimorphism in vivo but not in vitro*. *J Steroid Biochem Mol Biol*, 2012. **131**(1-2): p. 24-9.
142. Kramar, E.A., et al., *BDNF upregulation rescues synaptic plasticity in middle-aged ovariectomized rats*. *Neurobiol Aging*, 2012. **33**(4): p. 708-19.
143. Ooishi, Y., et al., *Modulation of synaptic plasticity in the hippocampus by hippocampus-derived estrogen and androgen*. *J Steroid Biochem Mol Biol*, 2012. **131**(1-2): p. 37-51.
144. Anastasio, T.J., *Exploring the contribution of estrogen to amyloid-Beta regulation: a novel multifactorial computational modeling approach*. *Front Pharmacol*, 2013. **4**: p. 16.
145. Jiao, S.S., et al., *Sex Dimorphism Profile of Alzheimer's Disease-Type Pathologies in an APP/PS1 Mouse Model*. *Neurotox Res*, 2016. **29**(2): p. 256-66.
146. Barone, E., et al., *Biliverdin reductase--a protein levels and activity in the brains of subjects with Alzheimer disease and mild cognitive impairment*. *Biochim Biophys Acta*, 2011. **1812**(4): p. 480-7.
147. Tramutola, A., et al., *Alteration of mTOR signaling occurs early in the progression of Alzheimer disease (AD): analysis of brain from subjects with pre-clinical AD, amnesic mild cognitive impairment and late-stage AD*. *J Neurochem*, 2015. **133**(5): p. 739-49.
148. Barone, E., et al., *Biliverdin Reductase-A Mediates the Beneficial Effects of Intranasal Insulin in Alzheimer Disease*. *Mol Neurobiol*, 2019. **56**(4): p. 2922-2943.

149. de Git, K.C. and R.A. Adan, *Leptin resistance in diet-induced obesity: the role of hypothalamic inflammation*. *Obes Rev*, 2015. **16**(3): p. 207-24.
150. Petrov, D., et al., *High-fat diet-induced deregulation of hippocampal insulin signaling and mitochondrial homeostasis deficiencies contribute to Alzheimer disease pathology in rodents*. *Biochim Biophys Acta*, 2015. **1852**(9): p. 1687-99.
151. Boitard, C., et al., *Impairment of hippocampal-dependent memory induced by juvenile high-fat diet intake is associated with enhanced hippocampal inflammation in rats*. *Brain Behav Immun*, 2014. **40**: p. 9-17.
152. Gargiulo, S., et al., *Evaluation of growth patterns and body composition in C57Bl/6J mice using dual energy X-ray absorptiometry*. *Biomed Res Int*, 2014. **2014**: p. 253067.
153. Ennaceur, A., *One-trial object recognition in rats and mice: methodological and theoretical issues*. *Behav Brain Res*, 2010. **215**(2): p. 244-54.
154. Antunes, M. and G. Biala, *The novel object recognition memory: neurobiology, test procedure, and its modifications*. *Cogn Process*, 2012. **13**(2): p. 93-110.
155. Hiramatsu, M., et al., *Cilostazol prevents amyloid beta peptide(25-35)-induced memory impairment and oxidative stress in mice*. *Br J Pharmacol*, 2010. **161**(8): p. 1899-912.
156. Ibi, D., et al., *Combined effect of neonatal immune activation and mutant DISC1 on phenotypic changes in adulthood*. *Behav Brain Res*, 2010. **206**(1): p. 32-7.
157. Kraeuter, A.K., P.C. Guest, and Z. Sarnyai, *The Y-Maze for Assessment of Spatial Working and Reference Memory in Mice*. *Methods Mol Biol*, 2019. **1916**: p. 105-111.
158. Spinelli, M., et al., *Brain insulin resistance impairs hippocampal synaptic plasticity and memory by increasing GluA1 palmitoylation through FoxO3a*. *Nat Commun*, 2017. **8**(1): p. 2009.
159. Matsubara, Y., et al., *Organ and brain crosstalk: The liver-brain axis in gastrointestinal, liver, and pancreatic diseases*. *Neuropharmacology*, 2022. **205**: p. 108915.
160. Perluigi, M., et al., *Aberrant crosstalk between insulin signaling and mTOR in young Down syndrome individuals revealed by neuronal-derived extracellular vesicles*. *Alzheimers Dement*, 2022. **18**(8): p. 1498-1510.
161. Fructuoso, M., et al., *Increased levels of inflammatory plasma markers and obesity risk in a mouse model of Down syndrome*. *Free Radic Biol Med*, 2018. **114**: p. 122-130.
162. Rose, M., et al., *Modulation of insulin signaling pathway genes by ozone inhalation and the role of glucocorticoids: A multi-tissue analysis*. *Toxicol Appl Pharmacol*, 2023. **469**: p. 116526.
163. Hafsi, S., et al., *Gene alterations in the PI3K/PTEN/AKT pathway as a mechanism of drug-resistance (review)*. *Int J Oncol*, 2012. **40**(3): p. 639-44.
164. Miralem, T., et al., *Interaction of human biliverdin reductase with Akt/protein kinase B and phosphatidylinositol-dependent kinase 1 regulates glycogen synthase kinase 3 activity: a novel mechanism of Akt activation*. *FASEB J*, 2016. **30**(8): p. 2926-44.
165. Hermida, M.A., J. Dinesh Kumar, and N.R. Leslie, *GSK3 and its interactions with the PI3K/AKT/mTOR signalling network*. *Adv Biol Regul*, 2017. **65**: p. 5-15.

166. Chong, Z.Z., F. Li, and K. Maiese, *Oxidative stress in the brain: novel cellular targets that govern survival during neurodegenerative disease*. Prog Neurobiol, 2005. **75**(3): p. 207-46.
167. Di Domenico, F., et al., *mTOR in Down syndrome: Role in Ass and tau neuropathology and transition to Alzheimer disease-like dementia*. Free Radic Biol Med, 2018. **114**: p. 94-101.
168. Jaworski, T., E. Banach-Kasper, and K. Gralec, *GSK-3beta at the Intersection of Neuronal Plasticity and Neurodegeneration*. Neural Plast, 2019. **2019**: p. 4209475.
169. Zhang, H.H., et al., *S6K1 regulates GSK3 under conditions of mTOR-dependent feedback inhibition of Akt*. Mol Cell, 2006. **24**(2): p. 185-97.
170. Wang, H., et al., *Convergence of the mammalian target of rapamycin complex 1- and glycogen synthase kinase 3-beta-signaling pathways regulates the innate inflammatory response*. J Immunol, 2011. **186**(9): p. 5217-26.
171. Tavares, M.R., et al., *The S6K protein family in health and disease*. Life Sci, 2015. **131**: p. 1-10.
172. Artemenko, M., et al., *p70 S6 kinase as a therapeutic target in cancers: More than just an mTOR effector*. Cancer Lett, 2022. **535**: p. 215593.
173. Dann, S.G., A. Selvaraj, and G. Thomas, *mTOR Complex1-S6K1 signaling: at the crossroads of obesity, diabetes and cancer*. Trends Mol Med, 2007. **13**(6): p. 252-9.
174. Biever, A., E. Valjent, and E. Puighermanal, *Ribosomal Protein S6 Phosphorylation in the Nervous System: From Regulation to Function*. Front Mol Neurosci, 2015. **8**: p. 75.
175. Hammelrath, L., et al., *Morphological maturation of the mouse brain: An in vivo MRI and histology investigation*. Neuroimage, 2016. **125**: p. 144-152.
176. Semple, B.D., et al., *Brain development in rodents and humans: Identifying benchmarks of maturation and vulnerability to injury across species*. Prog Neurobiol, 2013. **106-107**: p. 1-16.
177. Memmott, R.M. and P.A. Dennis, *Akt-dependent and -independent mechanisms of mTOR regulation in cancer*. Cell Signal, 2009. **21**(5): p. 656-64.
178. Fisher-Wellman, K.H., et al., *A Direct Comparison of Metabolic Responses to High-Fat Diet in C57BL/6J and C57BL/6NJ Mice*. Diabetes, 2016. **65**(11): p. 3249-3261.
179. Liu, Z., et al., *High-fat diet induces hepatic insulin resistance and impairment of synaptic plasticity*. PLoS One, 2015. **10**(5): p. e0128274.
180. Lanzillotta, C., et al., *BVR-A Deficiency Leads to Autophagy Impairment through the Dysregulation of AMPK/mTOR Axis in the Brain-Implications for Neurodegeneration*. Antioxidants (Basel), 2020. **9**(8).
181. Miller, E.K. and J.D. Cohen, *An integrative theory of prefrontal cortex function*. Annu Rev Neurosci, 2001. **24**: p. 167-202.
182. Kar, K. and J.J. DiCarlo, *Fast Recurrent Processing via Ventrolateral Prefrontal Cortex Is Needed by the Primate Ventral Stream for Robust Core Visual Object Recognition*. Neuron, 2021. **109**(1): p. 164-176 e5.
183. Barone, E., et al., *Biliverdin Reductase-A Mediates the Beneficial Effects of Intranasal Insulin in Alzheimer Disease*. Mol Neurobiol, 2018.
184. Gibbs, P.E., et al., *Nanoparticle Delivered Human Biliverdin Reductase-Based Peptide Increases Glucose Uptake by Activating IRK/Akt/GSK3 Axis: The Peptide Is*

- Effective in the Cell and Wild-Type and Diabetic Ob/Ob Mice.* J Diabetes Res, 2016. **2016**: p. 4712053.
185. Hinds, T.D., Jr., et al., *Biliverdin Reductase A Attenuates Hepatic Steatosis by Inhibition of Glycogen Synthase Kinase (GSK) 3 β Phosphorylation of Serine 73 of Peroxisome Proliferator-activated Receptor (PPAR) α .* J Biol Chem, 2016. **291**(48): p. 25179-25191.
186. Stec, D.E., et al., *Biliverdin Reductase A (BVRA) Knockout in Adipocytes Induces Hypertrophy and Reduces Mitochondria in White Fat of Obese Mice.* Biomolecules, 2020. **10**(3).
187. Tramutola, A., et al., *Brain insulin resistance triggers early onset Alzheimer disease in Down syndrome.* Neurobiol Dis, 2020. **137**: p. 104772.
188. Triani, F., et al., *Biliverdin reductase-A impairment links brain insulin resistance with increased A β production in an animal model of aging: Implications for Alzheimer disease.* Biochim Biophys Acta Mol Basis Dis, 2018. **1864**(10): p. 3181-3194.
189. Tramutola, A., et al., *Intranasal Administration of KYCCSRK Peptide Rescues Brain Insulin Signaling Activation and Reduces Alzheimer's Disease-like Neuropathology in a Mouse Model for Down Syndrome.* Antioxidants (Basel), 2023. **12**(1).
190. Ceccarelli, V., et al., *Reduced Biliverdin Reductase-A Expression in Visceral Adipose Tissue is Associated with Adipocyte Dysfunction and NAFLD in Human Obesity.* Int J Mol Sci, 2020. **21**(23).
191. Cimini, F.A., et al., *Biliverdin reductase-A protein levels are reduced in type 2 diabetes and are associated with poor glycometabolic control.* Life Sci, 2021. **284**: p. 119913.
192. Palozza, P., et al., *The protective role of carotenoids against 7-keto-cholesterol formation in solution.* Mol Cell Biochem, 2008. **309**(1-2): p. 61-8.
193. Hannon, T.S., J. Janosky, and S.A. Arslanian, *Longitudinal study of physiologic insulin resistance and metabolic changes of puberty.* Pediatr Res, 2006. **60**(6): p. 759-63.
194. Gaggini, M., et al., *Non-alcoholic fatty liver disease (NAFLD) and its connection with insulin resistance, dyslipidemia, atherosclerosis and coronary heart disease.* Nutrients, 2013. **5**(5): p. 1544-60.
195. Smith, G.I., et al., *Influence of adiposity, insulin resistance, and intrahepatic triglyceride content on insulin kinetics.* J Clin Invest, 2020. **130**(6): p. 3305-3314.
196. Polidori, D.C., et al., *Hepatic and Extrahepatic Insulin Clearance Are Differentially Regulated: Results From a Novel Model-Based Analysis of Intravenous Glucose Tolerance Data.* Diabetes, 2016. **65**(6): p. 1556-64.
197. Gastaldelli, A., et al., *Relationship between hepatic/visceral fat and hepatic insulin resistance in nondiabetic and type 2 diabetic subjects.* Gastroenterology, 2007. **133**(2): p. 496-506.
198. Bril, F., et al., *Metabolic and histological implications of intrahepatic triglyceride content in nonalcoholic fatty liver disease.* Hepatology, 2017. **65**(4): p. 1132-1144.
199. Lundsgaard, A.M., et al., *Opposite Regulation of Insulin Sensitivity by Dietary Lipid Versus Carbohydrate Excess.* Diabetes, 2017. **66**(10): p. 2583-2595.

200. Ahren, B., K. Thomaseth, and G. Pacini, *Reduced insulin clearance contributes to the increased insulin levels after administration of glucagon-like peptide 1 in mice*. *Diabetologia*, 2005. **48**(10): p. 2140-6.
201. Tura, A., et al., *Increased insulin clearance in mice with double deletion of glucagon-like peptide-1 and glucose-dependent insulinotropic polypeptide receptors*. *Am J Physiol Regul Integr Comp Physiol*, 2018. **314**(5): p. R639-R646.

7. APPENDIX

Appendix A

Article

Dynamic Changes of BVRA Protein Levels Occur in Response to Insulin: A Pilot Study in Humans

Flavia Agata Cimini ¹, Antonella Tramutola ², Ilaria Barchetta ¹, Valentina Ceccarelli ¹, Elena Gangitano ¹, Simona Lanzillotta ², Chiara Lanzillotta ², Maria Gisella Cavallo ¹ and Eugenio Barone ^{2,*}

¹ Department of Experimental Medicine, Sapienza University of Rome, 00185 Rome, Italy

² Department of Biochemical Sciences "A. Rossi-Fanelli", Sapienza University of Rome, 00185 Rome, Italy

* Correspondence: eugenio.barone@uniroma1.it

Abstract: Biliverdin reductase-A (BVRA) is involved in the regulation of insulin signaling and the maintenance of glucose homeostasis. Previous research showed that BVRA alterations are associated with the aberrant activation of insulin signaling in dysmetabolic conditions. However, whether BVRA protein levels change dynamically within the cells in response to insulin and/or glucose remains an open question. To this aim, we evaluated changes of intracellular BVRA levels in peripheral blood mononuclear cells (PBMC) collected during the oral glucose tolerance test (OGTT) in a group of subjects with different levels of insulin sensitivity. Furthermore, we looked for significant correlations with clinical measures. Our data show that BVRA levels change dynamically during the OGTT in response to insulin, and greater BVRA variations occur in those subjects with lower insulin sensitivity. Changes of BVRA significantly correlate with indexes of increased insulin resistance and insulin secretion (HOMA-IR, HOMA- β , and insulinogenic index). At the multivariate regression analysis, the insulinogenic index independently predicted increased BVRA area under curve (AUC) during the OGTT. This pilot study showed, for the first time, that intracellular BVRA protein levels change in response to insulin during OGTT and are greater in subjects with lower insulin sensitivity, supporting the role of BVR-A in the dynamic regulation of the insulin signaling pathway.

Keywords: biliverdin reductase-A; insulin signaling; metabolism; obesity; diabetes



Citation: Cimini, F.A.; Tramutola, A.; Barchetta, I.; Ceccarelli, V.; Gangitano, E.; Lanzillotta, S.; Lanzillotta, C.; Cavallo, M.G.; Barone, E. Dynamic Changes of BVRA Protein Levels Occur in Response to Insulin: A Pilot Study in Humans. *Int. J. Mol. Sci.* **2023**, *24*, 7282. <https://doi.org/10.3390/ijms24087282>

Academic Editor: Dumitru Constantin-Teodosiu

Received: 29 March 2023

Revised: 12 April 2023

Accepted: 13 April 2023

Published: 14 April 2023



Copyright: © 2023 by the authors. Licensee MDPI, Basel, Switzerland. This article is an open access article distributed under the terms and conditions of the Creative Commons Attribution (CC BY) license (<https://creativecommons.org/licenses/by/4.0/>).

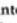
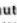
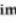



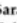
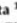
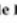

1. Introduction

Biliverdin reductase-A (BVRA), mainly known as the enzyme responsible for bilirubin production in the degradation pathway of heme, has recently drawn attention for its role in regulating insulin signaling and participating in the maintenance of metabolic homeostasis [1]. BVRA is endowed with a dual-specificity serine/threonine/tyrosine (Ser/Thr/Tyr) kinase activity [2,3], a scaffold protein function [3–9], and transcription functions [10] directly involved in the regulation of the cell redox metabolism and of the complex insulin signaling pathway at different levels. Alterations of BVRA protein levels influence many metabolic processes, such as glucose uptake, regulation of lipid and protein metabolism, cell proliferation, differentiation, and death [4–6,11–16].

Insulin responses are promoted through the phosphorylation (activation) of the insulin receptor substrates-1 and -2 (IRS1 and IRS2) complexes. Such activation is achieved following the binding of insulin to the extracellular domain of the IR, which autophosphorylates on tyrosine (Tyr) residues. Such phosphorylation is required for the activation of IR kinase activity, that in turn promotes IRS1 phosphorylation. The coupling between IR and IRS1 is crucial for the induction of the intracellular cascade. Like IRS1, BVRA is a direct target of IR [11], which phosphorylates both BVRA and IRS1 on specific Tyr residues thus resulting in their activation [11]. Then, as part of a regulatory loop, BVRA phosphorylates IRS1 on inhibitory Ser residues (e.g., Ser307) to avoid IRS1 aberrant activation in response to IR [11]. Once activated, IRS1 works as a scaffold protein, driving the activation of the two main

Article

Intranasal Administration of KYCCSRK Peptide Rescues Brain Insulin Signaling Activation and Reduces Alzheimer's Disease-like Neuropathology in a Mouse Model for Down Syndrome

Antonella Tramutola ¹ , Simona Lanzillotta ¹ , Giuseppe Aceto ^{2,3} , Sara Pagnotta ¹, Gabriele Ruffolo ^{4,5} , Pierangelo Cifelli ⁶, Federico Marini ⁷ , Cristian Ripoli ^{2,3} , Eleonora Palma ^{4,5} , Claudio Grassi ^{2,3} , Fabio Di Domenico ¹ , Marzia Perluigi ¹ and Eugenio Barone ^{1,*} 

¹ Department of Biochemical Sciences "A. Rossi-Fanelli", Sapienza University of Rome, Piazzale A. Moro 5, 00185 Roma, Italy

² Department of Neuroscience, Università Cattolica del Sacro Cuore, 00168 Roma, Italy

³ Fondazione Policlinico Universitario A. Gemelli, Istituto di Ricovero e Cura a Carattere Scientifico, 00168 Roma, Italy

⁴ Department of Physiology and Pharmacology, Istituto Pasteur-Fondazione Cenci Bolognietti, University of Rome Sapienza, 00185 Rome, Italy

⁵ IRCCS San Raffaele Roma, 00163 Rome, Italy

⁶ Department of Applied Clinical and Biotechnological Sciences, University of L'Aquila, 67100 L'Aquila, Italy

⁷ Department of Chemistry, Sapienza University of Rome, Piazzale A. Moro 5, 00185 Roma, Italy

* Correspondence: eugenio.barone@uniroma1.it



Citation: Tramutola, A.; Lanzillotta, S.; Aceto, G.; Pagnotta, S.; Ruffolo, G.; Cifelli, P.; Marini, F.; Ripoli, C.; Palma, E.; Grassi, C.; et al. Intranasal Administration of KYCCSRK Peptide Rescues Brain Insulin Signaling Activation and Reduces Alzheimer's Disease-like Neuropathology in a Mouse Model for Down Syndrome. *Antioxidants* **2023**, *12*, 111. <https://doi.org/10.3390/antiox12010111>

Academic Editor: Stanley Omaye

Received: 19 December 2022

Revised: 29 December 2022

Accepted: 30 December 2022

Published: 2 January 2023



Copyright: © 2023 by the authors. Licensee MDPI, Basel, Switzerland. This article is an open access article distributed under the terms and conditions of the Creative Commons Attribution (CC BY) license (<https://creativecommons.org/licenses/by/4.0/>).

Abstract: Down syndrome (DS) is the most frequent genetic cause of intellectual disability and is strongly associated with Alzheimer's disease (AD). Brain insulin resistance greatly contributes to AD development in the general population and previous studies from our group showed an early accumulation of insulin resistance markers in DS brain, already in childhood, and even before AD onset. Here we tested the effects promoted in Ts2Cje mice by the intranasal administration of the KYCCSRK peptide known to foster insulin signaling activation by directly interacting and activating the insulin receptor (IR) and the AKT protein. Therefore, the KYCCSRK peptide might represent a promising molecule to overcome insulin resistance. Our results show that KYCCSRK rescued insulin signaling activation, increased mitochondrial complexes levels (OXPHOS) and reduced oxidative stress levels in the brain of Ts2Cje mice. Moreover, we uncovered novel characteristics of the KYCCSRK peptide, including its efficacy in reducing DYRK1A (triplicated in DS) and BACE1 protein levels, which resulted in reduced AD-like neuropathology in Ts2Cje mice. Finally, the peptide elicited neuroprotective effects by ameliorating synaptic plasticity mechanisms that are altered in DS due to the imbalance between inhibitory vs. excitatory currents. Overall, our results represent a step forward in searching for new molecules useful to reduce intellectual disability and counteract AD development in DS.

Keywords: Alzheimer's disease; brain insulin resistance; Down syndrome; DYRK1A; intellectual disability

1. Introduction

Down syndrome (DS) is the most frequent genetic cause of intellectual disability and is strongly associated with Alzheimer's disease (AD) [1]. It is a multifaceted disorder with over 80 clinically defined phenotypes including those affecting the central nervous system, heart, gastrointestinal tract, skeleton, and immune system [2]. Phenotypes associated with trisomy 21 vary in both incidence and severity, leading to a vast array of phenotypic combinations [3]. Prevalence of overweight can reach 70% in subjects with DS leading